HIGH FAT DIET INDUCES RETINAL MICROVASCULAR INFLAMMATION AND

DEGENERATION: ROLE OF TXNIP-NLRP3 INFLAMMASOME AXIS

by

ISLAM N. MOHAMED

(Under the Direction of AZZA B. EL-REMESSY)

ABSTRACT

Diabetic retinopathy (DR) is a leading cause of blindness in US adults. DR starts with an early vaso-regressive stage of non-proliferative diabetic retinopathy (NPDR), which progresses into proliferative diabetic retinopathy (PDR). Over one-third of U.S. adults are obese. Obesity is now considered a disease state, rather than a mere risk stage for developing metabolic syndrome. Clinical and experimental evidence signifies glycemia, hypertension, and obesity as independent risk factors for developing retinopathy and retinal microvascular abnormalities in non-diabetic populations or on top of type 1 or 2 diabetes. It also emphasizes caspase-1/IL-β activation as a major pathophysiological component. However, data from experimental models are lacking and little is known about the upstream molecular mechanisms involved. Therefore, the overall goal of current studies is to model the detrimental effects of obesity and hypertension on instigating early stage retinal microvascular lesions. In the first study, HFD-induced obesity or hypertension showed similar effects on early retinal microvascular lesions, thioredoxin interacting protein (TXNIP) expression, oxidative and inflammatory stress. However, HFD selectively increased TXNIP-NLRP3 (NOD-like receptor protein) interaction, inflammasome activation and cleaved caspase-1 and IL-1β expression. Moreover, retinal vasculature and surrounding macroglial tissue

were prominent sites for HFD-induced TXNIP up-regulation. In the second study, TXNIP deletion in TXNIP knockout (TKO) mice mitigated HFD-induced retinal NLRP3 inflammasome activation, adhesion molecule upregulation, leukostasis and blood retinal barrier (BRB) breakdown on the short term, and acellular capillaries formation and microvascular abnormalities on the long term. TXNIP-NLRP3-inflammasome activation in human retinal endothelial (HRE) cells was confirmed in-vitro in response to saturated fatty acid "palmitate"; a direct activator of the NLRP3-inflammasome. TXNIP was also required for palmitate-induced adhesion molecule upregulation in HRE cells and TXNIP-NLRP3 inflammasome axis mediated the process in an autotocrine positive feedback loop fashion. Furthermore, circulating leukocytes from HFD wild-type (WT) mice and obese subjects resulted in increased leukostasis and endothelial cell death in culture in a TXNIP dependent manner. In summary, our findings highlight the early detrimental effects of HFD-induced obesity on the development of retinal microvascular lesions. TXNIP-NLRP3 inflammasome axis provides novel therapeutic targets for earlier intervention or prevention of obesity and pre-diabetes microvascular complications.

INDEX WORDS:

Oxidative stress, inflammation, metabolic syndrome, obesity, high fat diet, hypertension, inflammasome, leukostasis, retinal acellular capillaries, thioredoxin interacting protein, NOD-like receptor protein, caspase-1 & IL-1 β .

HIGH FAT DIET INDUCES RETINAL MICROVASCULAR INFLAMMATION AND DEGENERATION: ROLE OF TXNIP-NLRP3 INFLAMMASOME AXIS

by

ISLAM N. MOHAMED B.PHARM, AIN SHAMS UNIVERSITY, EGYPT, 2005 MS, STATE UNIVERSITY OF NEW YORK AT BUFFALO, NY, USA, 2010

A DISSERTATION Submitted to the Graduate Faculty of The University of Georgia in Partial Fulfillment of the Requirements for the Degree

DOCTOR OF PHILOSOPHY
ATHENS, GEORGIA

2014

© 2014

Islam N. Mohamed

All Rights Reserved

HIGH FAT DIET INDUCES RETINAL MICROVASCULAR INFLAMMATION AND DEGENERATION: ROLE OF TXNIP-NLRP3 INFLAMMASOME AXIS

by

ISLAM N. MOHAMED

Major Professor: Azza B. El-Remessy, PhD, RPh, FAHA

Committee: Susan C Fagan, Pharm.D., BCPS, FCCP

Lakshman Segar, Ph.D.

Adviye Ergul, MD, PhD, FAHA Ruth B. Caldwell, PhD, FARVO

Electronic Version Approved:

Julie Coffield Interim Dean of the Graduate School The University of Georgia July 2014.

DEDICATION

All praise is due to Allah (SWT), the most graceful and the most merciful.

First, I would like to dedicate this PhD dissertation to the soul of my beloved Mother: *Shadia Abou Seada B.Pharm, MS*. The one who brought me up as a Pharmacist and made me the man who I am today. Who passed away in the middle of this PhD journey and sacrificed enjoying my company in the last few years of her life, in order for me to achieve this goal.

To my beloved father: *Nabil Badr*, *PhD*., whom I owe everything and who is the one who made the PhD a standard inspiration to achieve in my life.

To my brother: *Ahmed Nabil Badr (Engineer)* and Sister: *Ingy Nabil Badr B.Pharm.* who always believed in me and supported me in such journey.

To my in-laws: General. Mamdouh Abdelkader and Mrs. Salwa Shoreim, for their continuous sacrifices and support.

Last but never least: to my soul mate and beloved wife: *Randa Mohamed*, *B. Pharm*. and my cherished daughters: *Habiba & Malak Mohamed*, whom are the outmost blessings of my life, and whom I couldn't achieve anything without their unconditional love and support.

ACKNOWLEDGEMENTS

First and foremost, I can never be thankful enough to my Mentor: Dr. Azza El-Remessy. Great mentors inspire and shape lives by teaching how to become a better person and take your skills to the next level. Dr. El-Remessy, your finger prints will stay with me for life.

I am also grateful for all my advisory committee members:

Dr. Susan Fagan, Dr. Adviye Ergul, Dr. Lakshman Segar and Dr. Ruth Caldwell for their irreplaceable mentorship, guidance and insights.

I would like to thank each and every person from our Retinopathy lab:

Mrs. Su Matragoon: for all her sincere help and being a second mother for all of us.

Dr. Mohammed Abdelsaid: your efficiency and productivity is always an inspiration.

Dr. Barbara Mysona: for being always there for us and our best support system personally and professionally.

Dr. Ahmed Shanab: for inspiring us how to do science with the touch of art.

Sally El-Shaer: your dedication is a role model to follow.

Mrs. Megan Bartasis: for keeping things in "order" all the time.

For all CET fellow students, postdocs and staff: you will always be like family to me.

I was so fortunate to be part of the CET.

Thank you.

TABLE OF CONTENTS

						Page
ACKNOWLED	OGEMENTS					v
LIST OF FIGU	RES					viii
CHAPTER						
1 REVIE	W OF CURRENT LITER	ATURE A	ND R	ATIONALE		1
]	References					19
2 PROBL	EM STATEMENT,	GAP	IN :	KNOWLEDGE	AND	CENTRAL
НҮРОТ	HESIS					35
2	2.1 Problem statement and	l gap in kn	owled	ge		35
,	2.2 Central hypothesis					36
<u>,</u>	2.3.1 Specific aim 1					36
<u>,</u>	2.3.1 Specific aim 2					38
<u>,</u>	2.4 Significance					39
,	2.5 References					41
3 THIOR	EDOXIN INTERACTIN	G PROTE	EIN IS	S REQUIRED FO	OR END	OTHELIAL
NLRP3	-INFLAMMASOME AC	TIVATIO	N ANI	D CELL DEATH	IN A RA	AT MODEL
OF HIG	H FAT DIET					45
	3.1 Abstract					46
	3.2 Introduction					47
,	3.3 Materials and Methods	s				48

	3.4 Results53
	3.5 Discussion
	3.6 References 62
4	HIGH FAT DIET-INDUCED OBESITY DRIVES LEUKOSTASIS, BARRIER
	DYSFUNCTION AND MICROVASCULAR DEGENERATION THROUGH
	TXNIP-NLRP3 INFLAMMASOME ACTIVATION88
	4.1 Abstract89
	4.2 Introduction90
	4.3 Materials and Methods92
	4.4 Results
	4.5 Discussion
	4.6 References 109
5	INTEGRATED DISCUSSION
	5.1 References
ΔI	PPENDICES 152

LIST OF FIGURES AND TABLES

P	a	g	e

Figure 1.1: Convergence of sterile inflammation and microbial infection on pattern recognition
receptor (PRRs)
Figure 1.2: Major classes of PRRs and their subcellular localization
Figure 1.3: Major upstream activators of TXNIP expression
Figure 1.4: Depicted role of TXNIP as a direct activator of NLRP3-inflammasome31
Figure 1.5: NLRP3-inflammasome activation in various cell types of the retinal NVU33
Figure 2.1: Outlining diagram of the central hypothesis
Figure 3.1: HFD causes retinal microvascular degeneration, oxidative and inflammatory stress.65
Figure 3.2: HFD induces retinal TXNIP expression and NLRP3 inflammasome activation67
Figure 3.3: Gene expression levels of TXNIP and other inflammasome members; NLRP3,
NLRP1 and NLRC4 in HFD69
Figure 3.4: HFD induces TXNIP-NLRP3 interaction associated with retinal inflammasome
activation71
Figure 3.5 HFD-induced TXNIP expression co-localizes within retinal microvasculature73
Figure 3.6 TXNIP is required for palmitate-induced NLRP3-inflammasome activation in HRE
cells75
Figure 3.7 TXNIP is required for palmitate-induced IL-1β maturation in HRE cells78
Figure 3.8 TXNIP is required for palmitate-induced apoptosis and cell death in HRE cells80

Supp. fig. 3.1 Representative images for number of acellular capillaries (arrows) identified in
tryptic-digest of retinas stained with PASH staining82
Supp. fig. 3.2 Dose-response proinflammatory effects of palmitate in human retinal endothelial
(HRE) cells84
Supp. fig. 3.3 Representative images of HRE cell viability in response to palmitate86
Figure 4.1 HFD results in weight gain, impaired glucose tolerance and dyslipidemia in both WT
and TKO mice112
Figure 4.2 Deletion of TXNIP abrogates HFD-induced retinal NLRP3-inflammasome
activation114
Figure 4.3 Overexpression of TXNIP activates NLRP3-inflammasome in human ECs116
Figure 4.4 Deletion of TXNIP prevents HFD-induced retinal microvascular inflammation and
leukostasis
Figure 4.5 Silencing TXNIP or inhibiting IL-1 Receptor prevents adhesion molecule expression
in human ECs. 120
Figure 4.6 Deletion of TXNIP in leukocytes prevents leukostasis and endothelial cell death122
Figure 4.7 HFD induces retinal BRB breakdown and microvascular degeneration via TXNIP124
Figure 4.8 HFD induces retinal microvascular changes in WT but not in TKO mice126
Figure 5.1 Summary of the overall findings
Supp. Fig.4.1 Optimization experiments for overexpression of TXNIP in human EC128
Table 4.1 Summary of the FPBG levels of all animal groups throughout the study at 8, 12 and 18-
weeks
Table 4.2 Summary of the physical and metabolic parameters of lean and obese subjects enrolled
for PBMC isolation

CHAPTER 1

REVIEW OF CURRENT LITERATURE AND RATIONALE

1.1 Overview of diabetes mellitus and its vascular complications.

Diabetes mellitus is a devastating metabolic disorder that arises mainly due to either the absence of the major hormone responsible for glucose uptake and utilization by different body organs; "Insulin" in type 1 diabetes mellitus (type 1 DM), or the decreased reaction of these target tissues to the anabolic effects of insulin; also known as "Insulin resistance" in type 2 diabetes mellitus (type 2 DM). In 2012, 29.1 million Americans or 9.3% of the population had diabetes compared to 25.8 million and 8.3% in 2010; 90-95% of them are type 2 DM [1, 2]. Diabetes is a lifetime disorder that carries most of its burden in its associated macro and microvascular complications. Diabetes is a leading risk factor in precipitating cardiovascular diseases including atherosclerosis, ischemic heart diseases and stroke. In addition, diabetes is also known for its ravaging effects on different microvascular beds, most notably; retinal microvasculature, glomeruli and the peripheral microvasculature, producing what is clinically defined as diabetic retinopathy, nephropathy and neuropathy [1, 2]. Major clinical studies including: United Kingdom Prospective Diabetes Study (UKPDS) [3, 4], Action to Control Cardiovascular Risk in Diabetes (ACCORD), Action in Diabetes and Vascular Disease (ADVANCE) study [5-12] and Diabetes Control and Complications Trial (DCCT) [13, 14] have established the importance of tight and early glycemic and metabolic control as a major factor for reducing microvascular complications in both type 1 or type 2 diabetes. However, diabetes

has a complex metabolic nature especially in the vast majority of type 2 diabetic patients. Type 2 DM does not only involve impaired glucose tolerance and higher blood glucose and plasma HbA1C levels, but also a dysregulation of carbohydrate, lipid & protein metabolism. Therefore, the question whether these other metabolic disorders can contribute to diabetes-induced complications and the molecular mechanisms involved remains incompletely understood. Since retina vasculature is the main target for our proposed studies, the next section will illustrate the impact of diabetes on retina microvascular complications.

1.2 Overview of Diabetic retinopathy.

1.2.1 Clinical features of DR.

Diabetic retinopathy (DR) is the leading cause of blindness in US adults 20-75 years of age. According to the last statistical updates, in the period between 2004-2008, the estimated crude prevalence rates for retinopathy in patients 40 years and older known to have DM were 28.5-40.3% and almost 1 of every 12 persons with DM in this age group has advanced visionthreatening retinopathy [1, 2],[15]. DR is a progressive neurovascular disease that is categorized based on the proliferative status of the retinal vasculature into an early initial vaso-regressive stage; clinically defined as non-proliferative diabetic retinopathy (NPDR), followed by a vasoproliferative response or proliferative diabetic retinopathy (PDR). Clinically, NPDR is characterized by distinct neurovascular degenerative changes which are believed to form the basis for subsequent ischemia and neovascularization later in the disease such as: capillary nonperfusion and degeneration (evident as non-perfused areas in fluorescein-infusion retinal angiograms), retinal microaneurysms, flame-hemorrhages and exudates, which is associated with increased retinal thickness/edema in addition to neuronal dysfunction observed as changes in contrast sensitivity, electroretinogram (ERG) and nerve fiber layer thickness in diabetic patients. Advanced PDR stages are mainly due to the vasoproliferative neovascular events that take place

in the long standing diabetic retina and can directly result in vision impairment and loss in severe cases. Week and leaky new vessels are associated with vitreous hemorrhage, development of a fibrovascular membrane in the vitreous that might evolve into tractional retinal detachment in addition to the development of macular edema [16-19].

1.2.2 Experimental features of DR.

Experimental modeling is only successful so far in reproducing some of the major early NPDR neurovascular features in diabetic animal models, whereas, studying late features of PDR including pre-retinal pathological neovascularization and macular edema could not be achieved due to the absence of a macula in most laboratory animals and rodents. Increased retinal microvascular permeability as result of the blood retinal barrier (BRB) breakdown and retinal microvascular degeneration, manifested as increased formation of non-perfused acellular capillaries, are among the hallmarks of NPDR changes that has been reproducibly observed in almost all animal models tested. Other neurovascular features including increased death of retinal neuroglia and ganglion cells were reported in diabetic rodent models, while microaneurysms have been detected in diabetic dogs, cats, and primates, but not reproducibly in diabetic rodents [17, 20, 21].

1.3 Obesity, metabolic syndrome and development of pre-diabetic retinopathy.

Over one-third of U.S. adults (nearly 79 millions) are obese, which doubles to around 70% if totally combined with the overweight incidence [22-24]. Obesity is now considered an established disease state, rather than a mere risk stage for developing dyslipidemia, insulin resistance, culminating into the complex metabolic syndrome disorder, type 2 diabetes and cardiovascular complications [23,25]. Increased caloric intake and consumption of saturated/trans-fat and cholesterol are the standing reasons behind these alarming epidemic rates. Several population studies have established each of glycemia, hypertension or obesity as an

independent risk factor for developing retinopathy and retinal microvascular abnormalities in the general non-diabetic population [26-29] or in addition to type 1 or type 2 diabetes [30]. Various components of the metabolic syndrome were associated with increased retinal microvascular abnormalities. A larger waist circumference was associated with wider venular diameter and retinopathy lesions, a higher blood pressure level was associated with focal arteriolar narrowing, arteriovenous nicking, enhanced arteriolar wall reflex and narrower arteriolar diameter and a higher triglyceride level was associated with enhanced arteriolar wall reflex [31, 32]. It has now become evident that these retinal vascular changes might be markers of the early preclinical stages of these metabolic disorders and might predict the onset of clinical disease [30]. Obesity is well characterized by increased inflammation and oxidative stress [33-35]. Systemic low grade inflammation, oxidative stress and its associated endothelial dysfunction/activation has been suggested as the most plausible reasons for such clinical observations [35-37]. However, data from experimental models are lacking and little is known about the exact molecular mechanisms involved in instigating these retinal microvascular insults.

1.4 Sterile inflammation, a driving force in development of retinopathy.

1.4.1 Sterile inflammation, danger signals and pattern recognition receptors.

According to the type of initial insult, inflammation can be generally classified as two main categories: microbial inflammation and sterile inflammation. Inflammation that occurs in response to a chemical, biochemical or metabolic insult, trauma or injury in absence of any microorganism is classically defined as sterile inflammation [38-41]. In microbial inflammation, pro-inflammatory insults that are directly sensed by the innate immune cells can be collectively called pathogen-associated molecular patterns (PAMPs) [42, 43]. PAMPs encompass a major class of conserved structural moieties that are either a metabolic byproduct or cellular fragments of microorganisms. As for sterile inflammation, pro-inflammatory non-infectious materials that

result from tissue damage or endogenous molecules released during cellular injury have been known as damage-associated molecular patterns (DAMPs) [43, 44]. Sterile inflammation has been implicated as one of the largest roots of many metabolic, cardiovascular and neurodegenerative diseases. Monosodium urate crystals (MSU), cholesterol crystals engulfed by circulating macrophages/foam cells and β-amyloid plaques are among the most renowned DAMPs responsible for; gout, atherosclerosis and Alzheimer's disease, respectively [40]. As depicted in Fig.1.1, similar to microbial inflammation, sterile inflammation involves the same cellular machinery and receptors which are believed to be responsive to both PAMPs and DAMPs. These receptors are responsible for the subsequent induction of pro-inflammatory responses, which are collectively termed pattern recognition receptors (PRRs). Five major classes of PRRs have been identified to date. As illustrated in Fig.1.2, PRR can be generally classified based on their cellular location or major structural features into: 1) transmembranal Toll-like receptors (TLRs); located at the cell surface or in endosomes, 2) transmembranal Ctype lectin receptors (CLRs); characterized with a carbohydrate-binding domain, 3) cytosolic nucleotide-binding oligomerization domain like receptors or NOD-like receptor proteins (NLRs/NLRPs), 4) intracellular retinoic acid-inducible gene-1 (RIG-1)-like receptors (RLRs); which are primarily involved in antiviral responses; and 5) the absent in melanoma 2 (AIM2)like receptors, which are characterized by the presence of a pyrin domain and a DNA-binding HIN domain involved in the detection of intracellular microbial DNA. Upon their activation with their cognate ligands (PAMPs and/or DAMPs), these receptors mediate the subsequent proinflammatory response by activating the major pro-inflammatory and pro-apoptotic pathways, including the nuclear factor kappa- B (NFkB) and mitogen activated protein (MAP) kinases, the major instigators for the pro-inflammatory defensive/detrimental response (for a full review, see references [40, 43, 45, 46]).

1.4.2 NLRP3-inflammasome, the prominent PRR.

Unlike the many other PRRs, NLRs have not been restricted to a specific ligand or a typical cognate molecular pattern (PAMP or DAMP) [45, 46]. However, among all the PRRs, the NLR family has been one the most extensively studied PRRs due to its major role in activating the inflammasome; the large multi-protein complex involved in instigating inflammation. NLRs are generally composed of three separate domains: 1) the N-terminal domain: which contains a pyrin domain, a caspase recruitment domain, or a baculovirus inhibitory repeat domain and has been used as a structural sub-classification for the NLR family. 2) The central NBD or NACHT (nucleotide-binding domain or NAIP, CIITA, HET-E and TP1) domain, which is responsible for dNTPase activity and oligomerization in the presence of nucleotides, primarily ATP. 3) A Leucine rich repeat domain (LRRs) at the C terminus of NLR proteins [47]. Upon activation by different PAMPs (whole pathogens or bacterial pore-forming toxins) or DAMPs (extracellular ATP, Glucose, MSU, Amyloid-β, Silica or Asbestos) [48]& [49], the NLR protein oligomerizes with the ASC (apoptosis-associated speck like) adaptor protein which then recruits procaspase-1, allowing its autocleavage and activation. Activated caspase-1 enzyme in turn cleaves upregulated premature proinflammatory cytokines: interleukin-1 (IL-1) and interleukin-18 (IL-18) and causes their release [50, 51]. Several NLRs have the capability to activate the inflammasome in vitro, including: NLRP1, NLRP2, NLRP3, NLRP6, NLRP12, NLRC4 and NOD-2, however, the physiological characterization of inflammasome activation has been established only for a handful of prominent NLRPs, including; NLRP1, NLRP3, NLRC4 and NAIP5 [47]. Of which, NLRP3 inflammasome has been highlighted as one of the most established multi-protein complexes responsible for instigating metabolic, cardiovascular and neurodegenerative diseaseassociated inflammation [48, 52-57].

1.4.3 Caspase-1/IL-1 β axis: landmarks of sterile inflammation in DR.

Sterile inflammation has been increasingly recognized as a major player in initiating or sustaining neuro- and vascular degeneration and retinal dysfunction in metabolic disorders such as diabetes or mechanical strain such as glaucoma or traumatic injury [58, 59]. Caspase-1 activation (also known as Interleukin-1\beta (IL-1\beta) converting enzyme) and increased IL-1\beta levels are well-documented landmarks of sterile inflammation in retinal chronic inflammatory conditions like diabetic retinopathy with a crucial proinflammatory role in mediating retinal endothelial cell dysfunction and microvascular degeneration. Clinically, increased IL-1β levels have been early reported in both the aqueous and vitreous humors and plasma samples of patients with diabetic retinopathy versus control subjects, and were positively correlated with severity or the progression from mild or moderate non proliferative diabetic retinopathy (NPDR) into proliferative diabetic retinopathy (PDR) [60-62]. Experimentally, caspase-1 activation in the retina was reported as early as 2 months after onset of streptozotocin (STZ)-induced diabetes, which was persistently higher until 8 months of diabetes and significantly correlated with the severity of diabetes as indicated by percentage of glycated hemoglobin [63]. Moreover, intravitreal administration if IL-1β resulted in massive increases in the number of degenerated retinal acellular capillaries and apoptotic capillary cells labeled with terminal deoxynucleotidyl transferase dUTP nick end labeling (TUNEL) in isolated retinal microvasculature in non-diabetic wistar rats [64] and pharmacological inhibition of caspase-1 using minocycline (an antimicrobial drug) or deletion of IL-1receptor suppressed IL-1β dependent increases in degenerated acellular capillaries formation in the retinas of diabetic mice [65].

1.4.4 Caspase-1/IL-1 β axis in the retinal neurovascular unit.

The neurovascular unit (NVU) is a term that is commonly used to describe the elaborate structure of the multicellular interface of endothelial cells, pericytes, glial cells (astrocytes and Müller cells) and neurons, which serves as the functional building unit of the brain and the retina. The NVU is formed as a result of the immaculate arrangement of small blood capillaries or microvascular tissue composed of endothelial cells immediately ensheathed by pericytes, which are in turn surrounded with the astrocytes alongside with the end feet processes of Müller glial cells (specialized glia that exist only in the retina) and neurons. This spatial and proximal arrangement of these different but highly related cell types facilitates their direct and mutual interaction, necessary for maintaining CNS/retina homeostasis in terms of nutritional support, housekeeping and formation of the blood brain or retinal barrier which protects the CNS against edema or any circulating metabolic or biochemical hazards in the blood stream. Several studies have implicated both endothelial cells and Müller cells as the major possible sources of retinal caspase-1/IL-1\beta activation in experimental models of hyperglycemia. Experimental evidence showed increased caspase-1 activation and IL-1β production in cultured bovine retinal endothelial cells and retinal Müller cell line rMC-1 (a glia-like cell type) in response to high glucose levels [63, 65-67]. Another study suggested the retinal endothelial tissue to be the initial source of increased IL-1\beta production in response to hyperglycemia, after which, increasing levels of IL-1β are sustained via its own auto stimulation in endothelial tissue and macroglia (Müller cells and astrocytes). This scenario was based on the difference in the readily-induced caspase-1/IL-1\beta activation response to high glucose levels in cultured bovine retinal endothelial cells that was absent in cultured rat Müller cells, astrocytes and microglia [68]. In the same study, the early increase of IL-1\beta levels in isolated rat retinal vascular tissue in vivo was maintained and coincided with increased markers of glial activation at later time points of hyperglycemia [68]. Prior evidence also indicated the upregulation of IL-1 β production in retinal microglial cells directly caused panretinal apoptosis in a rat model of STZ-induced diabetes [69]. In a model of oxygen-induced retinopathy (OIR), upregulation of IL-1 β in retinal microglia cells was linked to apoptosis of cultured microvascular endothelial cells under hypoxic conditions and vaso-obliteration/vaso-regression effects indirectly via induction of Semaphorin-3A from retinal ganglion cells in OIR [70]. Yet, little is known about the upstream molecular signaling involved in the activation of the retinal NLRP3 inflammasome responsible for the caspase-1/IL-1 β axis or in endothelial cells, macroglia or Müller cells and/or other retinal cell types in models of diabetic retinopathy or other retinal pathologies. More importantly, the question whether this axis can directly contribute to early stage pre-diabetic retinopathy remained unexplored.

1.5 Thioredoxin interacting protein (TXNIP): a possible link between oxidative stress and sterile inflammation.

1.5.1 Thioredoxin system.

The thioredoxin system is a ubiquitous thiol-reducing system that consists of cytoplasmic thioredoxin (Trx), nicotinamide adenine dinucleotide phosphate-oxidase (NADPH) and homodimeric seleno-protein thioredoxin reductase [71]. Trx is a multifunctional protein that acts as a protein disulfide reductase and participates in redox-dependent processes, including protein folding, regulation of apoptosis and antioxidant protection from oxidative stress [72]. Trx has 2 isoforms, cytosolic/nuclear (Trx-1) and mitochondrial (Trx-2) [73]. The activity and expression of Trx is regulated by thioredoxin-interacting protein (TXNIP), which tightly controls cellular redox-state [74]. TXNIP is also known as vitamin D₃ upregulated protein-1 (VDUP-1) and thioredoxin binding protein-2 (TBP-2). TXNIP belongs to the α-arrestin family so it may serve as adaptor and scaffold protein with several interacting domains to activate various signaling pathways (reviewed in [75]).

1.5.2 Redox dependent functions of TXNIP.

Traditionally, TXNIP has been known for its redox dependent signaling which involves the suppression of the anti-oxidant defense mechanism and increased unopposed levels of cellular reactive oxygen species (ROS) by limiting the availability of free sulfhydryl (thiol) group of Trx [76, 77]. Trx also exerts anti-apoptotic effects by binding and inhibiting the pro-apoptotic protein apoptosis signal-regulating kinase (ASK-1). Thus, under stress conditions, Trx can dissociate from ASK-1 and gain kinase activity to activate c-jun-N-terminal kinase (JNK) and p38 MAPK signaling pathway leading to apoptosis. TXNIP is a stress sensor and its expression can be induced to a various number of exogenous and endogenous stimuli including inflammation, metabolic stress, changes in calcium levels, as well as changes in oxygen levels [78-83]. In addition to modulating cellular redox state, TXNIP plays a critical role in stress-induced cellular apoptosis as it binds reduced-Trx and inhibits its activity resulting in activation of the pro-apoptotic protein ASK-1 pathways [84, 85].

1.5.3 Redox independent functions of TXNIP.

On the other hand, TXNIP has been also identified as a member of the alpha arrestin protein family, highlighting the other major roles of TXNIP as a scaffolding protein in a redox-dependent and independent ways [86]. TXNIP shuttling and targeting of proteins into different subcellular compartments including the plasma membrane, mitochondria and the nucleus provided a new paradigm in TXNIP signaling inside and outside the neurovascular unit (reviewed in [87, 88]). In the retinal neurovascular unit, redox dependent signaling cascades that include changes in activation of tyrosine receptor activity due to oxidative inhibition of the redox-sensitive phospho-tyrosine phosphatases (PTP) have been reported. In particular, silencing or genetic deletion of TXNIP expression impaired vascular endothelial growth factor receptor-2 (VEGFR2) signaling, with major implications in angiogenesis and ischemic retinopathy

pathophysiology [89, 90]. TXNIP can also mediate the translocation of Trx-1 to the plasma membrane under increased ROS levels, which was found to be also essential for VEGFR2 signaling in endothelial cells [91]. In addition, TXNIP can shuttle from the nucleus to bind the mitochondrial Trx-2 and mediate the internalization of glucose transporter GLUT1 from the plasma membrane to inhibit glucose uptake in response to increased ROS and high glucose levels in cultured beta cells and hepatocytes, respectively [92, 93]. As illustrated in Fig.1.3, an essential role of enhanced TXNIP in induction of inflammation and proinflammatory cytokine expression has been demonstrated in models of diabetic retinopathy and retinal neurotoxicity in vivo and in cultured cells [78, 79, 85, 94-96].

1.5.4 Pro-inflammatory role of TXNIP.

The contribution of TXNIP to inflammatory cytokine production was first demonstrated at the transcription level. Forced expression of TXNIP in isolated microvascular endothelial cells resulted in nuclear translocation and direct activation of the canonical NFκB pathway [79]. Knocking down TXNIP expression completely abolishes NF-κB binding to the cyclooxygenase-2 (Cox2) promoter, suggesting that TXNIP induces inflammatory gene expression by increasing transcription factor accessibility to gene promoters. The same study demonstrated evidence that the mechanism involves remodeling of histone H3 via activation of p38 MAPK. Later, studies demonstrated that TXNIP induces the expression of other proinflammatory cytokines and enzymes including IL-1β, ICAM-1, TNF-α, VEGF-A and Cox2, [79, 85, 94].

1.6 TXNIP and NLRP3 inflammasome activation: facts and controversy

The role of TXNIP as a redox sensitive switch that links increased cellular ROS levels and induction of the proinflammatory gene expression has been extended beyond the transcriptional factor level. Recent advances suggest the direct protein-protein interaction of TXNIP with the NLRP3-inflammasome, one of the executional machineries responsible for the

maturation and release of mature pro-inflammatory cytokines IL-1β and IL-18. Nevertheless, the emerging role of TXNIP as a direct activator of the NLRP3-inflammasome has been quiet controversial. In February 2010, Zhou R et al [48] was the first to identify TXNIP as a direct activator of the NLRP3 inflammasome in an ROS dependent manner. In this study, different NLRP3-inflammasome activators including monosodium urate crystals, ATP and silica were able to induce increases in cellular ROS levels in cultured macrophages, allowing the dissociation of TXNIP from Trx and its increased binding to the inflammasome receptor, NLRP3. TXNIP inhibition or deletion using TXNIP knockout (TKO) mice and their isolated macrophages and pancreatic islet tissue had impaired immunogenic response in terms of neutrophil flux and IL-1β production, in response to intraperitoneal injections of urate crystals in vivo, and increased ROS and glucose levels in vitro, respectively. However, these observations were challenged by another report in the same year in October 2010, which indicated that they could not replicate the same results utilizing isolated macrophages from TXNIP knockout (TKO) mice. These negative results came in line with a previous report in 2008 from mice lacking Gp91phox subunit of NADPH oxidase cytochrome b (one of the major sources for superoxide anion production in macrophages) [97]. Another report in early 2011 has also claimed that TXNIP contribution to the increase of IL-1\beta production in cultured adipocytes was mainly through the induction of the IL-1β expression in response to increased glucose levels rather than the direct activation of the NLRP3-inflammasome. This was based on their observation that TXNIP knockdown using siRNA did not affect caspase-1 activity under regular or increased glucose levels [98].

Despite the initial rise in controversy, published literature support the role of TXNIP as one of the direct activators for the NLRP3-inflammasome as illustrated in Fig.1.4. In cultured macrophages, Zhou R et al [99] reported that ROS-induced activation of the NLRP3-

inflammasome was associated with increased localization of TXNIP into the mitochondria. Another report showed that increased ROS levels in the mitochondria resulted in oxidation of Trx, liberation of TXNIP and increased its interaction with NLRP3 that was associated with a conformational change in the NLRP3 protein pyrin domain, as predicted by molecular modeling [100]. Increased S-nitrosylation of NLRP3 in macrophages of TXNIP knockout (TKO) mice compared to wild-type controls was suggested to be responsible for the associated decrease in IL-1β production, as a result of increased levels of nitric oxide and inducible nitric oxide synthase (iNOS), in a model of LPS-induced endotoxic shock [101]. Furthermore, TXNIPmediated activation of the NLRP3 inflammasome has been extensively supported in other nonimmune cell types, rather than macrophages only. In lung endothelial cells, NADPH-derived ROS promoted the activation of the direct association between TXNIP and NLRP3 and hence, NLRP3-inflammasome activation [102]. In pancreatic beta cells, TXNIP has been proposed as an effective link that couples endoplasmic reticulum stress (ER-stress) and inflammation via NLRP3-inflammasome activation. Terminal levels of ER-stress known as the unfolded protein response can induce rapid increases in TXNIP expression as a result of the increased activity of the PERK (dsRNA-activated protein kinase-like ER kinase) and IRE1 (inositol-requiring 1) pathways, which in turn can increase TXNIP mRNA stability by reducing levels of a TXNIP destabilizing microRNA, miR-17 [103]. Finally, pharmacological inhibition of TXNIP utilizing pleiotropic agents like: quercetin (a natural antioxidant of flavonoid origin), allopurinol (a uric acid synthesis inhibitor), hemin (an inducer for the anti-oxidant protein heme oxygenase-1) or rosuvastatin (a lipid lowering drug of the 3-hydroxy-3-methyl-glutaryl-CoA reductase inhibitor class) have been reported to inhibit the TXNIP-NLRP3-IL-1\beta axis and ameliorate the proinflammatory insult in different disease models of high fructose diet-induced hypothalamic

insulin resistance [104], non-alcoholic fatty liver disease (NAFLD) [105], acute liver failure [106], and diabetic cardiomyopathy [107], respectively.

1.7 TXNIP-NLRP3 Inflammasome activation in the retinal NVU.

1.7.1 TXNIP-NLRP3-Inflammasome activation in Müller glial cells in hyperglycemic models.

In Müller cells, TXNIP-mediated NLRP3-inflammasome activation was further discussed in models of STZ-induced diabetes in vivo [108] and in cultured retinal Müller cell line rMC-1 under high glucose levels [109]. In the first study, hyperglycemia in STZ-induced diabetic rats resulted in upregulation of retinal TXNIP and IL-1\beta expression along with other proinflammatory gene expression including iNOS and the pattern recognition receptors TLR4 and P2X7R at 4 weeks of diabetes that was associated with increased expression of glial fibrillary acidic protein (GFAP), a marker of glial cell activation. Knockdown of TXNIP by intravitreal injection of promoter targeted siRNA was able to significantly reduce the IL-1β and GFAP up-regulation. In vitro, the authors tried to dissect the temporal regulation of hyperglycemia-induced pro-oxidative and pro-inflammatory response in cultured rMC-1 cells. They observed that despite the sustained upregulation of TXNIP expression in response to sustained high levels of glucose from 4 hours up to 5 days in culture, which is consistent with the role of TXNIP as a glucose responsive protein, the associated activation of the NLRP3inflammasome in terms of pro-IL-1β, NLRP3 inflammasome and procaspase-1 levels oscillates at 4 h and day 3 of high glucose exposure. The first early response at 4 h occurs in the absence of ROS release, while the second late response at day 3 occurs under ROS/oxidative stress. These events correlated with an early ER-stress response to the increased glucose metabolism and ATP generation, which is then followed by a later response of hypoxic like conditions, restriction of ATP and increased ROS production and induction of autophagic-apoptosis pathway and

inflammation. These observations suggested a relationship between high glucose response, oxidative and ER-Stress in which TXNIP could be an effective link with NLRP3 inflammasome activation [108]. The second study further dissected the role of purinergic signaling (purines are well-known DAMP activators for the PRR and NLRP3 inflammasome activation in cultured rMC-1 cells. The study showed that the high glucose-mediated response of increased caspase-1 activation in rMC-1cells is in part due to the autocrine stimulation of ATP-sensing P2 receptors and adenosine-sensing P1 receptors. This was supported by the ability of apyrase, which metabolizes extracellular ATP to AMP, or adenosine deaminase (ADA), which metabolizes extracellular adenosine to inosine, to attenuate the response. They further elaborated that the purinergic signaling involved is mainly due to the P1/P2 receptor-mediated cAMP response, rather than P2X7 ATP-gated ion channel receptors. Despite the increased P2X7 mRNA expression in response to high glucose levels (25 mM), neither P2X7 protein nor function was detected in rMC-1 cells. In addition, attenuation of caspase-1 activity under high glucose conditions was achieved by either suramin (a nonselective P2 antagonist), or A2 adenosine receptor antagonists, but not by antagonism of antagonism of P2X7 ATP-gated ion channel receptors. Lastly, the increase in caspase-1 activity was stimulated by high glucose levels or exogenous addition of ATP, 5'-N-ethylcarboxamido-adenosine, a nonselective P1 receptor agonist, forskolin, an adenylyl cyclase activator which increases intracellular levels of cAMP, or dipyridamole, which suppresses adenosine reuptake under control glucose levels (5 mM). The increased caspase-1 activity correlated with increased gene expression of caspase-1 and TXNIP. The authors proposed an intricate model where Müller cells exposed to high glucose upregulate NLRP3 via NFkB transcriptional signaling, TXNIP via MondoA/MLX transcriptional signaling, and cAMP/PKA-driven increase in the Ets-1 transcription factor, which positively modulates caspase-1 gene expression [109].

1.7.2 TXNIP- NLRP3-Inflammasome activation in Müller glial cells in neurotoxic models.

In another model of retinal neurotoxicity, our group findings also supported a contributing role for TXNIP-mediated NLRP3-inflammasome activation in retinal Müller cells facilitating neuroglial activation and death of retinal ganglion cells [78]. Intravitreal injections of N-methyl-D-Aspartate (NMDA) as a model of neuronal excitotoxicity resulted in a massive increase in retinal ganglion cell (RGC) death one day after injections, associated with increased oxidative stress, blood retinal barrier breakdown, Müller and glial cell activation and expression of pro-inflammatory mediators in wild type (WT) mice, but not in TXNIP knockout (TKO) mice. Immunolocalization studies highlighted Müller cells as a major source of the pro-inflammatory response, evidenced by increased GFAP immunoreactivity in Müller cell filaments which colocalized with that of IL-1β and TNFα in WT mice versus TKO mice in response to NMDA injections. Isolated primary Müller cell cultures from both WT and TKO mice confirmed that TXNIP deletion abrogated the NMDA-induced upregulation of NLRP3, cleaved caspase-1 and increased production of IL-1β and TNFα in culture media [78]. Such initial insults, were necessary for maintaining secondary events including increased microvascular degeneration indicated by the number of acellular capillaries formation, a hall mark of retinal ischemia. These effects were associated with increased death and dysfunctional activity of other neuronal cell types; bipolar and photoreceptor cells that occurred 2-3 weeks after initial NMDA injections, which helped to sustain and aggravate the primary insult of increased RGC cell death [78]. In line with these findings, NLRP3-inflammasome activation was also noted to be directly upregulated in astrocytes [110] and neurons including RGC [111] which are also critical

components of the neurovascular unit in other experimental models of glaucoma and transient ischemia reperfusion injury.

1.8 Inflammasome activation in other retina cell types.

Despite the fact that retinal pigmented epithelium (RPE) cells are not considered to be part of either the sensory retina or the typical neurovascular unit, it's worth mentioning that NLRP3-inflammasome activation is also attracting increasing attention as a crucial instigator of the proinflammatory response in other retinal diseases like retinal geographic atrophy associated with age-related macular degeneration (AMD). Sections from human ocular tissue from patients with geographic atrophy or neovascular AMD were positive for NLRP3 immunostaining when compared to tissues from age-matched controls [112]. Of note, RPE cells were found to express all inflammasome components including ASC, NLRP-3 and caspase-1. As an immediate sensor of many DAMPs, several metabolic components of the drusen lesions associated with AMD (extracellular accumulations of a lipoprotein-like material that build up between Bruch's membrane and the RPE) like: beta-amyloid (1-40 & 1-42), N-retinylidene-N-retinylethanolamine (A2E; an essential component for lipofuscin/drusen), Alu RNA transcripts due to deficiency of DICER1, a ribonuclease type III enzyme or due to IL-1α treatment, have been recently shown to activate the NLRP3-inflammasome proinflammatory response, where its inhibition was able to prevent RPE degeneration both in vivo and in cultured RPE cells in vitro [112-116]. Activation of the NLRP3 inflammasome occurs traditionally after "priming" which involves the upregulation of the inflammasome gene expression via various transcriptionally active signaling receptors followed by "activation" step leading to activation of caspase-1 and secretion of IL-18 and IL-1\beta. While published literature support the significance of IL-1\beta, little is known about the role of IL-18. The recent study by Ambati group showed the activation of NLRP3inflammasome and release of IL-18 resulting in RPE cell death and geographic atrophy of AMD [116]. Similar findings were observed in response to beta amyloid insult in RPE cells. [113]. Together, these findings demonstrate central role of NLRP3-inflammasome activation in RPE cells and in models of age-related macular degeneration. Fig.1.5 Summarizes and illustrates all discussed literature on NLRP3-inflammasome activation in various cell types of the NVU of the retina.

1.9 Summary and rationale for current studies

Taken together, in light of all discussed literature, this review lends further credit for the central role TXNIP-NLRP3 inflammasome activation plays a major role in mediating the proinflammatory response involved in the pathophysiology of different retinal diseases, and in specific, in the pathogenesis of DR. An increasing body of evidence proposes caspase-1/IL-1β activation as one of the cornerstone detrimental events in different subcellular components of the retinal neurovascular unit, most importantly, in endothelial and Müller glial cells. However, the upstream molecular pathways responsible for the activation of the NLRP3 inflammasome in endothelial cells remained unexplored, especially in the context of early pre-diabetic/metabolic syndrome retinopathy which is associated with multiple contributions of other metabolic disorders, rather than merely hyperglycemia. On the other hand, it is still unclear whether the same pathological landmarks of increased retinal leukostasis, blood retinal barrier dysfunction and accelerated acellular capillaries formation of established DR can also contribute to the development of pre-diabetic retinal microvascular manifestations observed in metabolic syndrome or obesity patients. Further, delineating the molecular pathways involved in TXNIP-NLRP3 inflammasome axis provides novel therapeutic targets for modulating the specific components of sterile inflammatory response; the largest root of many metabolic, cardiovascular and neurodegenerative diseases.

1.10 References

- 1. Centers for Disease Control and Prevention, U.D.o.H.a.H.S., *National Diabetes Statistics Report: Estimates of Diabetes and Its Burden in the United States*, 2014. . 2014.
- 2. Association, A.D., *Statistics About Diabetes*. 2014.
- 3. Intensive blood-glucose control with sulphonylureas or insulin compared with conventional treatment and risk of complications in patients with type 2 diabetes (UKPDS 33). UK Prospective Diabetes Study (UKPDS) Group. Lancet, 1998. **352**(9131): p. 837-53.
- 4. Effect of intensive blood-glucose control with metformin on complications in overweight patients with type 2 diabetes (UKPDS 34). UK Prospective Diabetes Study (UKPDS) Group. Lancet, 1998. **352**(9131): p. 854-65.
- 5. Gerstein, H.C., et al., Long-term effects of intensive glucose lowering on cardiovascular outcomes. N Engl J Med, 2011. **364**(9): p. 818-28.
- 6. Ismail-Beigi, F., et al., Effect of intensive treatment of hyperglycaemia on microvascular outcomes in type 2 diabetes: an analysis of the ACCORD randomised trial. Lancet, 2010. **376**(9739): p. 419-30.
- 7. O'Connor, P.J. and F. Ismail-Beigi, *Near-Normalization of Glucose and Microvascular Diabetes Complications: Data from ACCORD and ADVANCE.* Ther Adv Endocrinol Metab, 2011. **2**(1): p. 17-26.
- 8. Patel, A., et al., *Intensive blood glucose control and vascular outcomes in patients with type 2 diabetes.* N Engl J Med, 2008. **358**(24): p. 2560-72.
- 9. Liebson, P.R., *Diabetes Control and Cardiovascular Risk: ACCORD, ADVANCE, AVOID, and SANDS.* Prev Cardiol, 2008. **11**(4): p. 230-6.
- 10. Chew, E.Y., et al., Effects of medical therapies on retinopathy progression in type 2 diabetes. N Engl J Med, 2010. **363**(3): p. 233-44.
- 11. Gerstein, H.C., et al., *Diabetic retinopathy, its progression, and incident cardiovascular events in the ACCORD trial.* Diabetes Care, 2013. **36**(5): p. 1266-71.
- 12. Ginsberg, H.N., *The ACCORD (Action to Control Cardiovascular Risk in Diabetes) Lipid trial: what we learn from subgroup analyses.* Diabetes Care, 2011. **34 Suppl 2**: p. S107-8.
- 13. Gubitosi-Klug, R.A., *The diabetes control and complications trial/epidemiology of diabetes interventions and complications study at 30 years: summary and future directions.* Diabetes Care, 2014. **37**(1): p. 44-9.
- 14. Aiello, L.P., Diabetic retinopathy and other ocular findings in the diabetes control and complications trial/epidemiology of diabetes interventions and complications study. Diabetes Care, 2014. **37**(1): p. 17-23.
- 15. Kempen, J.H., et al., *The prevalence of diabetic retinopathy among adults in the United States*. Arch Ophthalmol, 2004. **122**(4): p. 552-63.
- 16. Frank, R.N., *Diabetic retinopathy*. N Engl J Med, 2004. **350**(1): p. 48-58.
- 17. Tang, J. and T.S. Kern, *Inflammation in diabetic retinopathy*. Prog Retin Eye Res, 2011. **30**(5): p. 343-58.
- 18. Nunes, S., et al., *Microaneurysm turnover is a biomarker for diabetic retinopathy progression to clinically significant macular edema: findings for type 2 diabetics with nonproliferative retinopathy.* Ophthalmologica, 2009. **223**(5): p. 292-7.
- 19. Shimizu, K., Y. Kobayashi, and K. Muraoka, *Midperipheral fundus involvement in diabetic retinopathy*. Ophthalmology, 1981. **88**(7): p. 601-12.

- 20. Gastinger, M.J., et al., Dendrite remodeling and other abnormalities in the retinal ganglion cells of Ins2 Akita diabetic mice. Invest Ophthalmol Vis Sci, 2008. **49**(6): p. 2635-42.
- 21. Kern, T.S. and A.J. Barber, *Retinal ganglion cells in diabetes*. J Physiol, 2008. **586**(Pt 18): p. 4401-8.
- 22. Ogden, C.L., et al., *Prevalence of childhood and adult obesity in the United States*, 2011-2012. JAMA, 2014. **311**(8): p. 806-14.
- 23. Association, A.H. *Obesity Statistics*. 2012 May 5, 2011.; Available from: http://www.heart.org/HEARTORG/GettingHealthy/WeightManagement/Obesity/Obesity-Information_UCM_307908_Article.jsp#.Tx2sA4G8ioA.
- 24. Center for Disease Control and Prevention; Division of Nutrition, P.A., and Obesity (DNPAO), *Overweight and Obesity statistics*. 2014.
- 25. Association, A.M., American Medical Association's Council on Science and Public Health Report 4, Resolution: 420 (A-13). 2013.
- 26. Klein, R., et al., 15-year cumulative incidence and associated risk factors for retinopathy in nondiabetic persons. Arch Ophthalmol, 2010. **128**(12): p. 1568-75.
- 27. van Leiden, H.A., et al., *Risk factors for incident retinopathy in a diabetic and nondiabetic population: the Hoorn study.* Arch Ophthalmol, 2003. **121**(2): p. 245-51.
- 28. Cheung, N. and T.Y. Wong, *Obesity and eye diseases*. Surv Ophthalmol, 2007. **52**(2): p. 180-95.
- 29. Habot-Wilner, Z. and M. Belkin, [Obesity is a risk factor for eye diseases]. Harefuah, 2005. **144**(11): p. 805-9, 821.
- 30. Nguyen, T.T. and T.Y. Wong, *Retinal vascular manifestations of metabolic disorders*. Trends Endocrinol Metab, 2006. **17**(7): p. 262-8.
- 31. Wong, T.Y., et al., Associations between the metabolic syndrome and retinal microvascular signs: the Atherosclerosis Risk In Communities study. Invest Ophthalmol Vis Sci, 2004. **45**(9): p. 2949-54.
- 32. Kawasaki, R., et al., *The metabolic syndrome and retinal microvascular signs in a Japanese population: the Funagata study.* Br J Ophthalmol, 2008. **92**(2): p. 161-6.
- 33. Gonzalez-Chavez, A., et al., *Pathophysiological implications between chronic inflammation and the development of diabetes and obesity.* Cir Cir. **79**(2): p. 209-16.
- 34. Gustafson, B., *Adipose tissue*, *inflammation and atherosclerosis*. J Atheroscler Thromb. **17**(4): p. 332-41.
- 35. Caballero, A.E., *Metabolic and vascular abnormalities in subjects at risk for type 2 diabetes: the early start of a dangerous situation.* Arch Med Res, 2005. **36**(3): p. 241-9.
- 36. Couillard, C., et al., Circulating levels of oxidative stress markers and endothelial adhesion molecules in men with abdominal obesity. J Clin Endocrinol Metab, 2005. **90**(12): p. 6454-9.
- 37. Hackman, A., et al., Levels of soluble cell adhesion molecules in patients with dyslipidemia. Circulation, 1996. **93**(7): p. 1334-8.
- 38. Medzhitov, R., *Origin and physiological roles of inflammation*. Nature, 2008. **454**(7203): p. 428-35.
- 39. Rubartelli, A., et al., *Mechanisms of sterile inflammation*. Front Immunol, 2013. **4**: p. 398
- 40. Chen, G.Y. and G. Nunez, *Sterile inflammation: sensing and reacting to damage*. Nat Rev Immunol, 2010. **10**(12): p. 826-37.

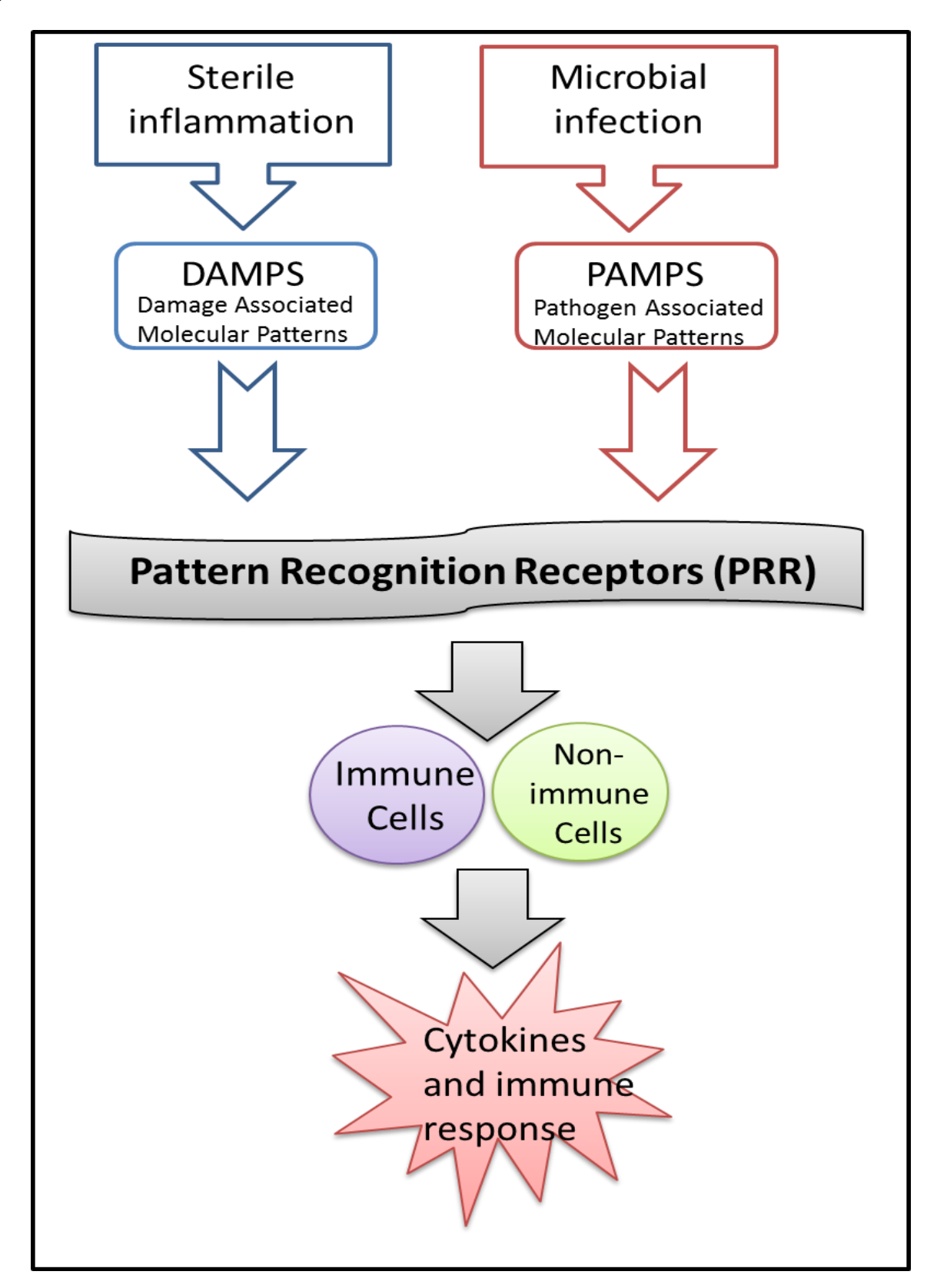
- 41. Kono, H., A. Onda, and T. Yanagida, *Molecular determinants of sterile inflammation*. Curr Opin Immunol, 2014. **26**: p. 147-56.
- 42. Janeway, C.A., Jr., *Pillars article: approaching the asymptote? Evolution and revolution in immunology. Cold spring harb symp quant biol. 1989.* 54: 1-13. J Immunol, 2013. **191**(9): p. 4475-87.
- 43. Tang, D., et al., *PAMPs and DAMPs: signal 0s that spur autophagy and immunity*. Immunol Rev, 2012. **249**(1): p. 158-75.
- 44. Matzinger, P., *Tolerance, danger, and the extended family*. Annu Rev Immunol, 1994. **12**: p. 991-1045.
- 45. Takeuchi, O. and S. Akira, *Pattern recognition receptors and inflammation*. Cell, 2010. **140**(6): p. 805-20.
- 46. Suresh, R. and D.M. Mosser, *Pattern recognition receptors in innate immunity, host defense, and immunopathology.* Adv Physiol Educ, 2013. **37**(4): p. 284-91.
- 47. Davis, B.K., H. Wen, and J.P. Ting, *The inflammasome NLRs in immunity, inflammation, and associated diseases.* Annu Rev Immunol, 2011. **29**: p. 707-35.
- 48. Schroder, K., R. Zhou, and J. Tschopp, *The NLRP3 inflammasome: a sensor for metabolic danger?* Science, 2010. **327**(5963): p. 296-300.
- 49. Tschopp, J. and K. Schroder, *NLRP3 inflammasome activation: The convergence of multiple signalling pathways on ROS production?* Nat Rev Immunol, 2010. **10**(3): p. 210-5.
- 50. Gross, O., et al., *The inflammasome: an integrated view.* Immunol Rev, 2011. **243**(1): p. 136-51.
- 51. Tsuchiya, K. and H. Hara, *The inflammasome and its regulation*. Crit Rev Immunol, 2014. **34**(1): p. 41-80.
- 52. Vandanmagsar, B., et al., *The NLRP3 inflammasome instigates obesity-induced inflammation and insulin resistance*. Nat Med, 2011. **17**(2): p. 179-88.
- 53. Stienstra, R., et al., *The inflammasome-mediated caspase-1 activation controls adipocyte differentiation and insulin sensitivity.* Cell Metab, 2010. **12**(6): p. 593-605.
- 54. Jha, S., et al., *The inflammasome sensor, NLRP3, regulates CNS inflammation and demyelination via caspase-1 and interleukin-18.* J Neurosci, 2010. **30**(47): p. 15811-20.
- 55. Lamkanfi, M. and V.M. Dixit, *Inflammasomes and their roles in health and disease*. Annu Rev Cell Dev Biol, 2012. **28**: p. 137-61.
- 56. Strowig, T., et al., *Inflammasomes in health and disease*. Nature, 2012. **481**(7381): p. 278-86.
- 57. Liu, L. and C. Chan, *The role of inflammasome in Alzheimer's disease*. Ageing Res Rev, 2014. **15C**: p. 6-15.
- 58. Adamis, A.P. and A.J. Berman, *Immunological mechanisms in the pathogenesis of diabetic retinopathy*. Semin Immunopathol, 2008. **30**(2): p. 65-84.
- 59. Krizaj, D., et al., From mechanosensitivity to inflammatory responses: new players in the pathology of glaucoma. Curr Eye Res, 2014. **39**(2): p. 105-19.
- 60. Demircan, N., et al., Determination of vitreous interleukin-1 (IL-1) and tumour necrosis factor (TNF) levels in proliferative diabetic retinopathy. Eye (Lond), 2006. **20**(12): p. 1366-9.
- 61. Dong, N., et al., Study of 27 aqueous humor cytokines in patients with type 2 diabetes with or without retinopathy. Mol Vis, 2013. **19**: p. 1734-46.

- 62. Koleva-Georgieva, D.N., N.P. Sivkova, and D. Terzieva, *Serum inflammatory cytokines IL-1beta, IL-6, TNF-alpha and VEGF have influence on the development of diabetic retinopathy.* Folia Med (Plovdiv), 2011. **53**(2): p. 44-50.
- 63. Mohr, S., et al., Caspase activation in retinas of diabetic and galactosemic mice and diabetic patients. Diabetes, 2002. **51**(4): p. 1172-9.
- 64. Kowluru, R.A. and S. Odenbach, *Role of interleukin-1beta in the development of retinopathy in rats: effect of antioxidants.* Invest Ophthalmol Vis Sci, 2004. **45**(11): p. 4161-6.
- 65. Vincent, J.A. and S. Mohr, *Inhibition of caspase-1/interleukin-1beta signaling prevents degeneration of retinal capillaries in diabetes and galactosemia.* Diabetes, 2007. **56**(1): p. 224-30.
- 66. Kowluru, R.A. and S. Odenbach, *Role of interleukin-1beta in the pathogenesis of diabetic retinopathy*. Br J Ophthalmol, 2004. **88**(10): p. 1343-7.
- 67. Yego, E.C., et al., Differential regulation of high glucose-induced glyceraldehyde-3-phosphate dehydrogenase nuclear accumulation in Muller cells by IL-1beta and IL-6. Invest Ophthalmol Vis Sci, 2009. **50**(4): p. 1920-8.
- 68. Liu, Y., M. Biarnes Costa, and C. Gerhardinger, *IL-1beta is upregulated in the diabetic retina and retinal vessels: cell-specific effect of high glucose and IL-1beta autostimulation*. PLoS One, 2012. **7**(5): p. e36949.
- 69. Krady, J.K., et al., *Minocycline reduces proinflammatory cytokine expression, microglial activation, and caspase-3 activation in a rodent model of diabetic retinopathy.* Diabetes, 2005. **54**(5): p. 1559-65.
- 70. Rivera, J.C., et al., *Microglia and interleukin-1beta in ischemic retinopathy elicit microvascular degeneration through neuronal semaphorin-3A*. Arterioscler Thromb Vasc Biol, 2013. **33**(8): p. 1881-91.
- 71. Meyer, Y., et al., *Thioredoxins and glutaredoxins: unifying elements in redox biology*. Annu Rev Genet, 2009. **43**: p. 335-67.
- 72. Mahmood, D.F., et al., *The thioredoxin system as a therapeutic target in human health and disease.* Antioxid Redox Signal, 2013. **19**(11): p. 1266-303.
- 73. Nishiyama, A., et al., *Identification of thioredoxin-binding protein-2/vitamin D(3) up-* regulated protein 1 as a negative regulator of thioredoxin function and expression. J Biol Chem, 1999. **274**(31): p. 21645-50.
- 74. Patwari, P., et al., *The interaction of thioredoxin with Txnip. Evidence for formation of a mixed disulfide by disulfide exchange.* J Biol Chem, 2006. **281**(31): p. 21884-91.
- 75. Masutani, H., et al., *Thioredoxin binding protein (TBP)-2/Txnip and alpha-arrestin proteins in cancer and diabetes mellitus.* J Clin Biochem Nutr, 2012. **50**(1): p. 23-34.
- 76. Chung, J.W., et al., Vitamin D3 upregulated protein 1 (VDUP1) is a regulator for redox signaling and stress-mediated diseases. J Dermatol, 2006. **33**(10): p. 662-9.
- 77. Junn, E., et al., Vitamin D3 up-regulated protein 1 mediates oxidative stress via suppressing the thioredoxin function. J Immunol, 2000. **164**(12): p. 6287-95.
- 78. El-Azab, M.F., et al., Deletion of thioredoxin-interacting protein preserves retinal neuronal function by preventing inflammation and vascular injury. Br J Pharmacol, 2014. **171**(5): p. 1299-313.
- 79. Perrone, L., et al., *Thioredoxin interacting protein (TXNIP) induces inflammation through chromatin modification in retinal capillary endothelial cells under diabetic conditions.* J Cell Physiol, 2009. **221**(1): p. 262-72.

- 80. Dunn, L.L., et al., A critical role for thioredoxin-interacting protein in diabetes-related impairment of angiogenesis. Diabetes, 2014. **63**(2): p. 675-87.
- 81. Singh, L.P., *Thioredoxin Interacting Protein (TXNIP) and Pathogenesis of Diabetic Retinopathy*. J Clin Exp Ophthalmol, 2013. **4**.
- 82. Huang, C., et al., *Thioredoxin-interacting protein mediates dysfunction of tubular autophagy in diabetic kidneys through inhibiting autophagic flux.* Lab Invest, 2014. **94**(3): p. 309-20.
- 83. Chen, J., et al., *Diabetes induces and calcium channel blockers prevent cardiac expression of proapoptotic thioredoxin-interacting protein.* Am J Physiol Endocrinol Metab, 2009. **296**(5): p. E1133-9.
- 84. Al-Gayyar, M.M., et al., Neurovascular protective effect of FeTPPs in N-methyl-D-aspartate model: similarities to diabetes. Am J Pathol, 2010. **177**(3): p. 1187-97.
- 85. Al-Gayyar, M.M., et al., *Thioredoxin interacting protein is a novel mediator of retinal inflammation and neurotoxicity.* Br J Pharmacol, 2011. **164**(1): p. 170-80.
- 86. Polekhina, G., et al., *Crystallization and preliminary X-ray analysis of the N-terminal domain of human thioredoxin-interacting protein.* Acta Crystallogr Sect F Struct Biol Cryst Commun, 2011. **67**(Pt 5): p. 613-7.
- 87. Spindel, O.N., C. World, and B.C. Berk, *Thioredoxin interacting protein: redox dependent and independent regulatory mechanisms*. Antioxid Redox Signal, 2012. **16**(6): p. 587-96.
- 88. Lane, T., et al., TXNIP shuttling: missing link between oxidative stress and inflammasome activation. Front Physiol, 2013. 4: p. 50.
- 89. AB, A.M.a.E.-R., *Role of Thioredoxin Interacting Protein (TXNIP) in VEGF angiogenic signal.* (In revision) Journal of Cell Science, 2012.
- 90. Abdelsaid, M.A., S. Matragoon, and A.B. El-Remessy, *Thioredoxin-interacting protein expression is required for VEGF-mediated angiogenic signal in endothelial cells*. Antioxid Redox Signal, 2013. **19**(18): p. 2199-212.
- 91. World, C., O.N. Spindel, and B.C. Berk, *Thioredoxin-interacting protein mediates TRX1 translocation to the plasma membrane in response to tumor necrosis factor-alpha: a key mechanism for vascular endothelial growth factor receptor-2 transactivation by reactive oxygen species.* Arterioscler Thromb Vasc Biol, 2011. **31**(8): p. 1890-7.
- 92. Saxena, G., J. Chen, and A. Shalev, *Intracellular shuttling and mitochondrial function of thioredoxin-interacting protein.* J Biol Chem, 2010. **285**(6): p. 3997-4005.
- 93. Wu, N., et al., AMPK-dependent degradation of TXNIP upon energy stress leads to enhanced glucose uptake via GLUT1. Mol Cell, 2013. **49**(6): p. 1167-75.
- 94. Perrone, L., et al., *Inhibition of TXNIP expression in vivo blocks early pathologies of diabetic retinopathy*. Cell Death Dis, 2010. **1**: p. e65.
- 95. Mohamed, I.N., et al., *Thioredoxin-interacting protein is required for endothelial NLRP3 inflammasome activation and cell death in a rat model of high-fat diet.* Diabetologia, 2014. **57**(2): p. 413-23.
- 96. Yamawaki, H., et al., Fluid shear stress inhibits vascular inflammation by decreasing thioredoxin-interacting protein in endothelial cells. J Clin Invest, 2005. 115(3): p. 733-8.
- 97. Masters, S.L., et al., Activation of the NLRP3 inflammasome by islet amyloid polypeptide provides a mechanism for enhanced IL-1beta in type 2 diabetes. Nat Immunol, 2010. **11**(10): p. 897-904.
- 98. Koenen, T.B., et al., *Hyperglycemia activates caspase-1 and TXNIP-mediated IL-1beta transcription in human adipose tissue.* Diabetes, 2011. **60**(2): p. 517-24.

- 99. Zhou, R., et al., A role for mitochondria in NLRP3 inflammasome activation. Nature, 2011. **469**(7329): p. 221-5.
- 100. Lunov, O., et al., Amino-functionalized polystyrene nanoparticles activate the NLRP3 inflammasome in human macrophages. ACS Nano, 2011. **5**(12): p. 9648-57.
- 101. Park, Y.J., et al., TXNIP deficiency exacerbates endotoxic shock via the induction of excessive nitric oxide synthesis. PLoS Pathog, 2013. 9(10): p. e1003646.
- 102. Xiang, M., et al., *Hemorrhagic shock activation of NLRP3 inflammasome in lung endothelial cells.* J Immunol, 2011. **187**(9): p. 4809-17.
- 103. Anthony, T.G. and R.C. Wek, *TXNIP switches tracks toward a terminal UPR*. Cell Metab, 2012. **16**(2): p. 135-7.
- 104. Zhang, Q.Y., et al., Quercetin inhibits AMPK/TXNIP activation and reduces inflammatory lesions to improve insulin signaling defect in the hypothalamus of high fructose-fed rats. J Nutr Biochem, 2014. 25(4): p. 420-8.
- 105. Wang, W., et al., Quercetin and allopurinol reduce liver thioredoxin-interacting protein to alleviate inflammation and lipid accumulation in diabetic rats. Br J Pharmacol, 2013. **169**(6): p. 1352-71.
- 106. Kim, S.J. and S.M. Lee, *NLRP3 inflammasome activation in D-galactosamine and lipopolysaccharide-induced acute liver failure: role of heme oxygenase-1.* Free Radic Biol Med, 2013. **65**: p. 997-1004.
- 107. Luo, B., et al., Rosuvastatin alleviates diabetic cardiomyopathy by inhibiting NLRP3 inflammasome and MAPK pathways in a type 2 diabetes rat model. Cardiovasc Drugs Ther, 2014. **28**(1): p. 33-43.
- 108. Devi, T.S., et al., TXNIP links innate host defense mechanisms to oxidative stress and inflammation in retinal Muller glia under chronic hyperglycemia: implications for diabetic retinopathy. Exp Diabetes Res, 2012. 2012: p. 438238.
- 109. Trueblood, K.E., S. Mohr, and G.R. Dubyak, *Purinergic regulation of high-glucose-induced caspase-1 activation in the rat retinal Muller cell line rMC-1*. Am J Physiol Cell Physiol, 2011. **301**(5): p. C1213-23.
- 110. Tezel, G., et al., *An astrocyte-specific proteomic approach to inflammatory responses in experimental rat glaucoma*. Invest Ophthalmol Vis Sci, 2012. **53**(7): p. 4220-33.
- 111. Dvoriantchikova, G., et al., Genetic ablation of Pannexin1 protects retinal neurons from ischemic injury. PLoS One, 2012. **7**(2): p. e31991.
- 112. Tseng, W.A., et al., *NLRP3 inflammasome activation in retinal pigment epithelial cells by lysosomal destabilization: implications for age-related macular degeneration.* Invest Ophthalmol Vis Sci, 2013. **54**(1): p. 110-20.
- 113. Liu, R.T., et al., *Inflammatory mediators induced by amyloid-beta in the retina and RPE in vivo: implications for inflammasome activation in age-related macular degeneration.* Invest Ophthalmol Vis Sci, 2013. **54**(3): p. 2225-37.
- 114. Anderson, O.A., A. Finkelstein, and D.T. Shima, A2E induces IL-1ss production in retinal pigment epithelial cells via the NLRP3 inflammasome. PLoS One, 2013. 8(6): p. e67263.
- 115. Tarallo, V., et al., *DICER1 loss and Alu RNA induce age-related macular degeneration via the NLRP3 inflammasome and MyD88.* Cell, 2012. **149**(4): p. 847-59.
- 116. Kerur, N., et al., *TLR-independent and P2X7-dependent signaling mediate Alu RNA-induced NLRP3 inflammasome activation in geographic atrophy*. Invest Ophthalmol Vis Sci, 2013. **54**(12): p. 7395-401.

Fig.1.1



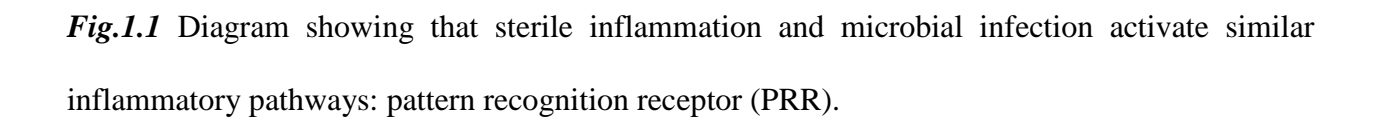
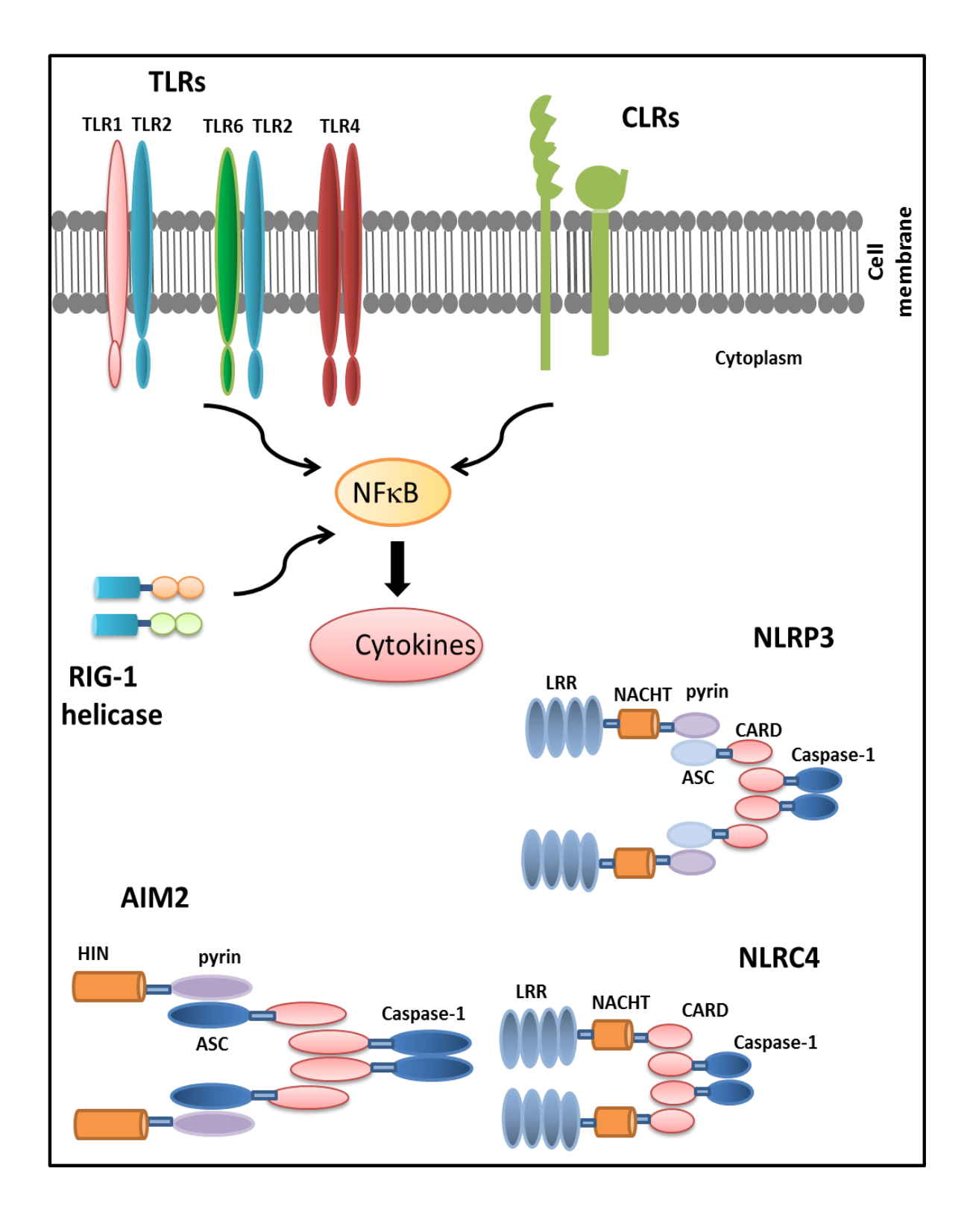


Fig.1.2



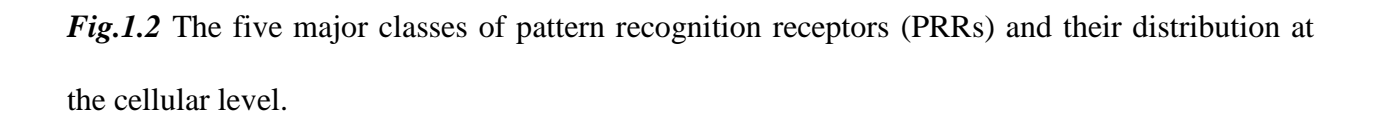


Fig.1.3

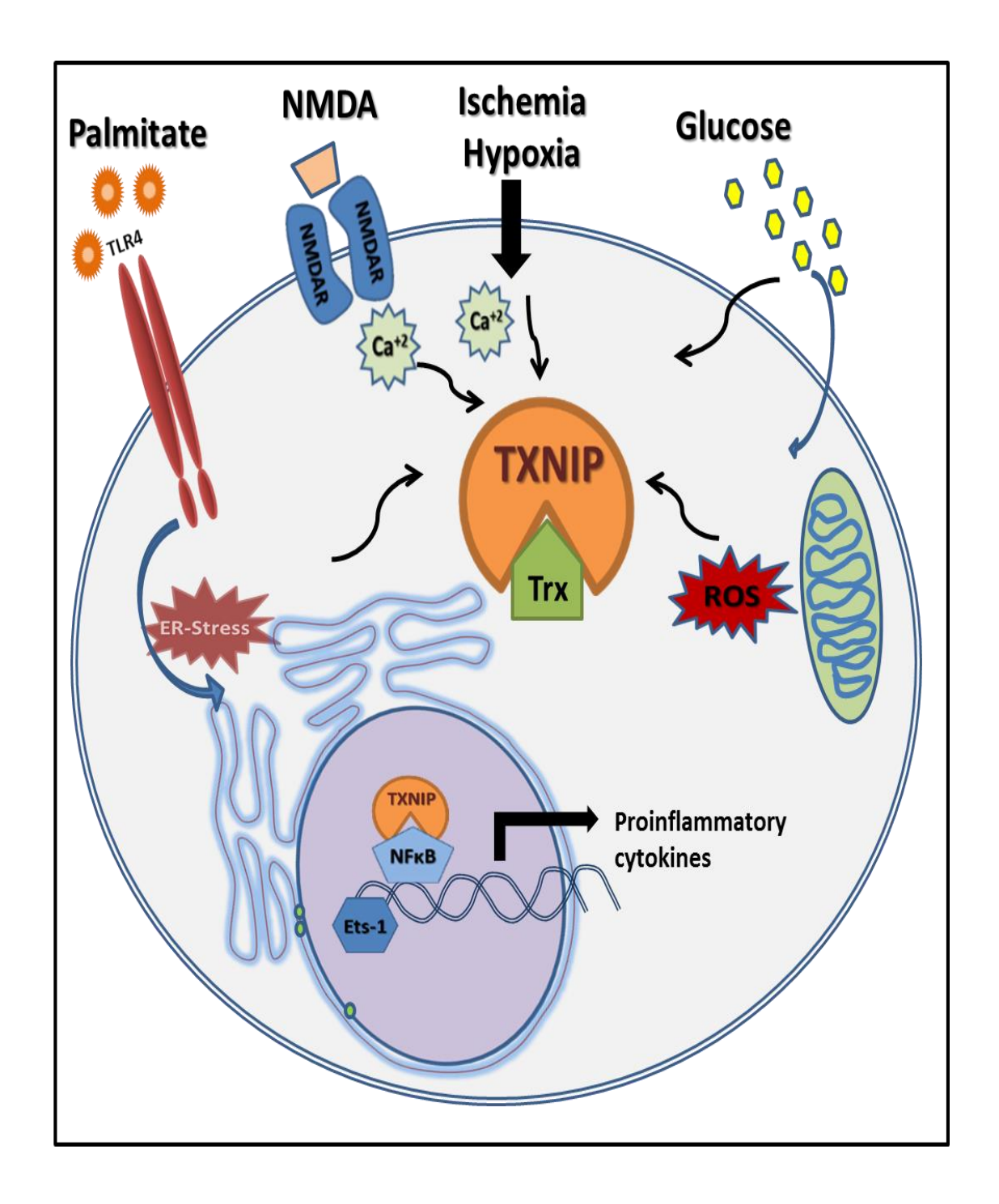


Fig.1.3 The major upstream activators of TXNIP expression; glucose, palmitate, NMDA and ischemia. Enhanced TXNIP expression contributes to proinflammatory cytokines production via activation of NFκB at the transcription level.

Fig.1.4

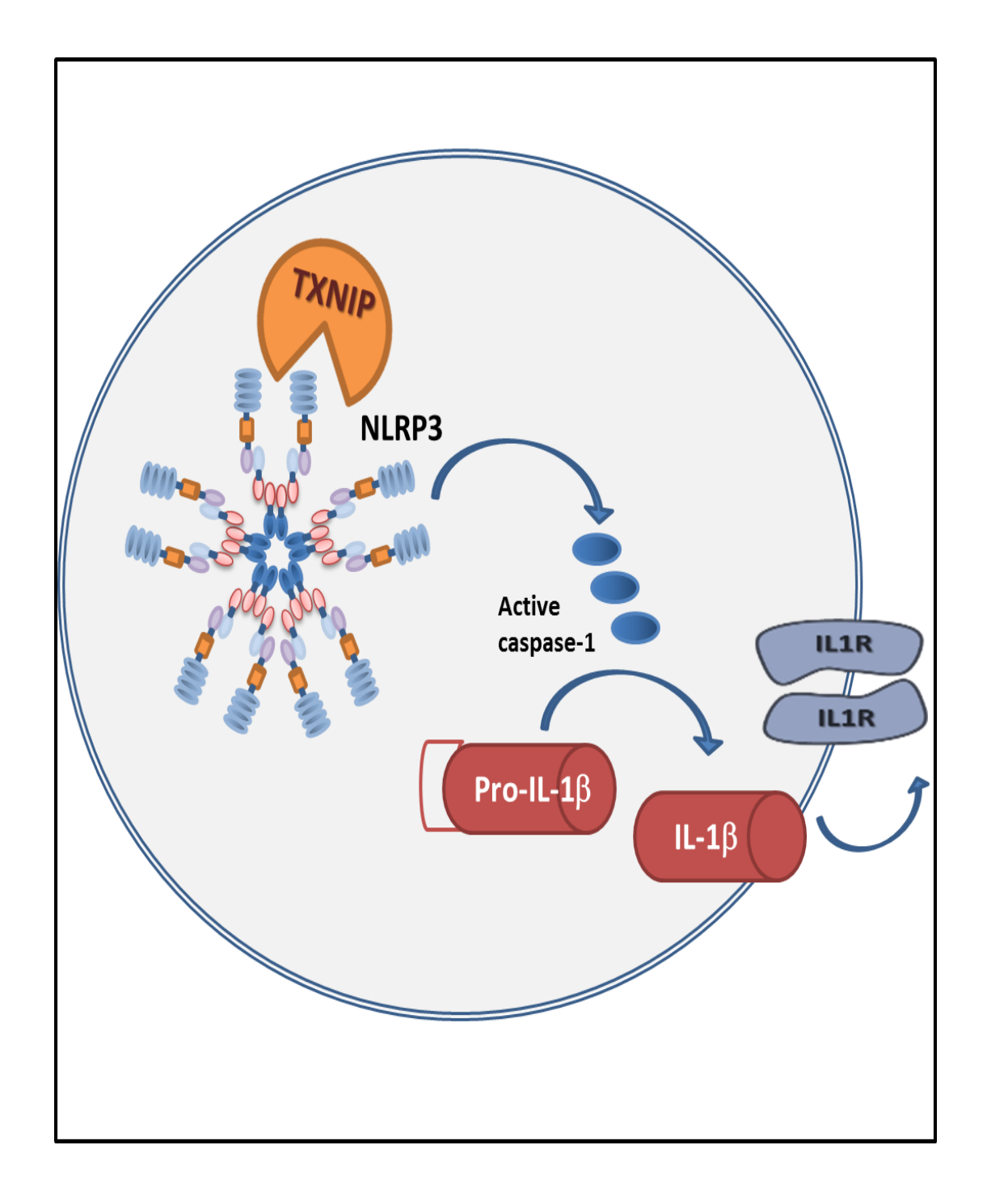


Fig.1.4 Depicted role of TXNIP as a direct activator of NLRP3-inflammasome resulting in activation of caspase-1 that in turn causes maturation and cleavage of pro-IL1 β to IL-1 β . IL-1 β can activate its receptor and sustain its own expression and auto-inflammation loop.

Fig.1.5

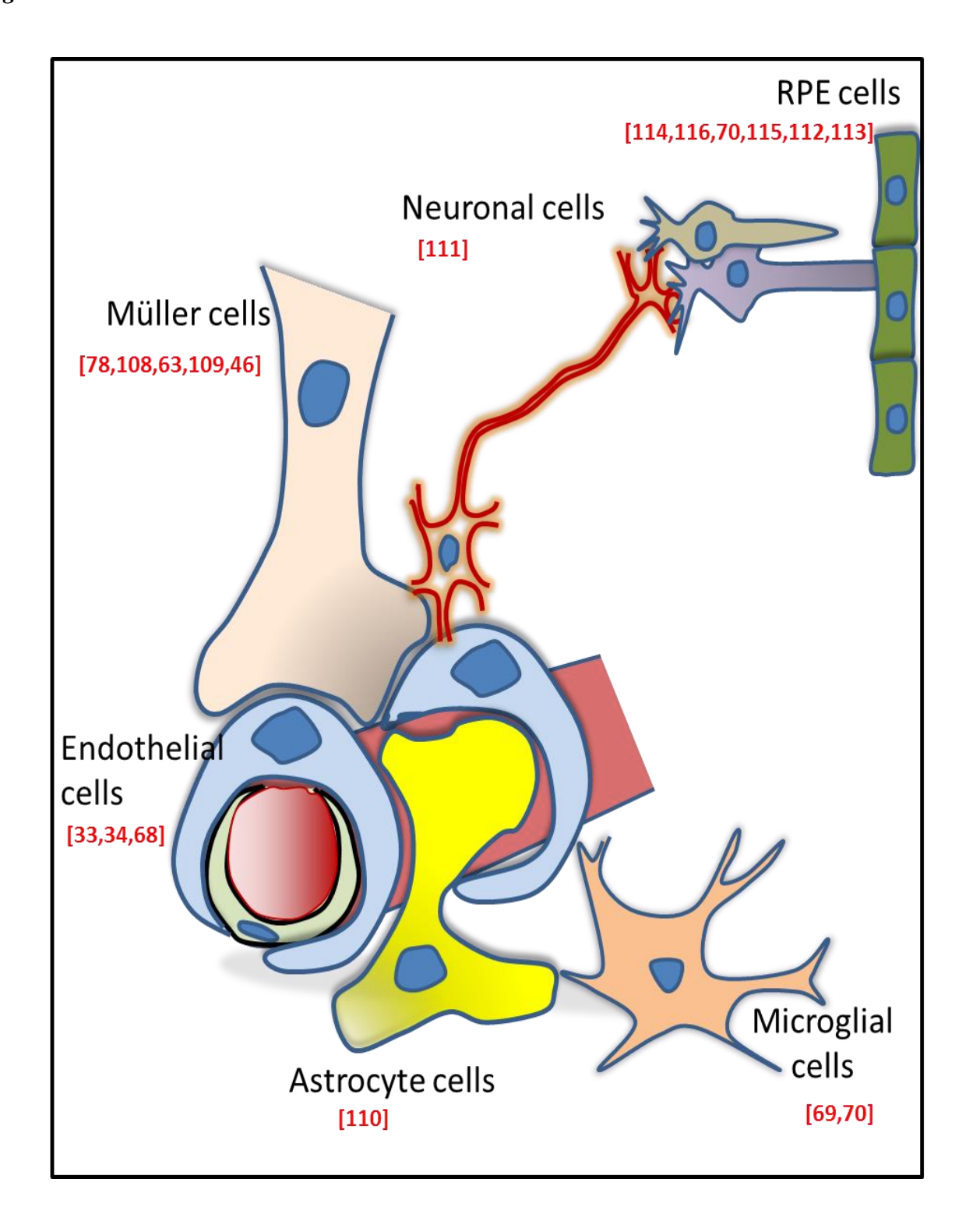


Fig.1.5 Schematic representation that illustrates NLRP3-inflammasome activation in various cell types of the NVU of the retina

CHAPTER 2

PROBLEM STATEMENT, GAP IN KNOWLEDGE AND CENTRAL HYPOTHESIS

2.1 Problem statement and gap in knowledge.

Several population studies have established each of glycemia, hypertension or obesity, the known components of metabolic syndrome, as an independent risk factor for developing retinopathy and retinal microvascular abnormalities in the general non-diabetic population [1-4] or in addition to type 1 or type 2 diabetes [5]. Retinal leukostasis, defined by increased attraction and abnormal adhesion between activated leukocytes and retinal microvasculature, is a well-characterized pathophysiologic landmark in metabolic pro-inflammatory retinal conditions such as diabetic retinopathy [6, 7]. Increased retinal leukostasis occurs as a result of retinal endothelial dysfunction and upregulation of pro-inflammatory cytokines and vascular adhesion molecules and can directly induce blood retinal barrier (BRB) breakdown followed by exacerbated loss of retinal endothelial cells and increased formation of non-perfused acellular capillaries. Such events comprise the hallmark foundation for establishing focal retinal ischemia and triggering pathologic retinal neovascularization in advanced stages of diabetic retinopathy [8-10]. However, it is unclear whether retinal leukostasis can also contribute to the early pathological findings in metabolic syndrome or obese pre-diabetic retinopathy stages.

On the other hand, free fatty acid (FFA) plasma levels are relatively higher in obesity and are one of the major factors for inducing obesity and metabolic syndrome-associated

inflammation and insulin resistance [11-14]. Previous reports have established palmitate, which is one of the most abundant circulating saturated fatty acid in plasma [15], as an inducer of proinflammatory response in human coronary endothelial cells versus other unsaturated fatty acids [16, 17] and an activator of the NLRP3-inflammasome [18-20]. In addition, TXNIP has been also identified as a direct activator of the NLRP3 inflammasome, the upstream multi-protein complex responsible for activating the Caspase-1/IL-1β axis and one of the most established pathways for instigating obesity-induced inflammation [21, 22]. Nevertheless, there is a gap in knowledge whether high fat diet (HFD)-induced obesity can up-regulate TXNIP expression and retinal and endothelial inflammasome activation and whether this TXNIP-NLRP3 inflammasome axis can trigger retinal microvascular inflammation, leukostasis and microvascular degeneration.

2.2 Central hypothesis

As outlined in Fig2.1, our central hypothesis predicts that HFD-induced obesity can result in retinal leukostasis, microvascular inflammation, and degeneration through TXNIP-NLRP3 inflammasome activation. Of note, the relationship between HFD-induced retinal and endothelial TXNIP expression and NLRP3 inflammasome activation in obesity and their role in mediating microvascular inflammation and degeneration has not been examined before.

2.3 The central hypothesis will be examined by two specific aims:

- **2.3.1 Specific Aim 1:** To test the hypothesis that HFD-induced obesity or metabolic syndrome results in TXNIP-mediated retinal NLRP3 inflammasome activation and microvascular inflammation.
- 2.3.1.1 Rationale: TXNIP has been recognized as a direct activator of the NLRP3 inflammasome in macrophages, endothelial cells and pancreatic beta cells [23-28]. However,

there is a gap in knowledge whether TXNIP results in retinal NLRP3 inflammasome activation in response to HFD or metabolic syndrome and whether TXNIP is required for NLRP3 inflammasome activation in retinal endothelial cells.

2.3.1.2 *The working hypothesis* is that HFD alone or as a component of metabolic syndrome will result in retinal TXNIP-NLRP3 inflammasome activation in vivo, and that TXNIP is required for NLRP3 inflammasome activation in retinal endothelial cells in-vitro.

In vivo, in order to model the effect of HFD alone or as a component of the metabolic syndrome, control Wistar kyoto rats (W) and spontaneously hypertensive rats (SHR) fed *ad libitum* with normal rat chow, will be compared to their respective groups (W+F) and (SHR+F) groups; fed with HFD. TXNIP expression and its association with NLRP3, along with markers for NLRP3 inflammasome activation (expression of cleaved Caspase-1 and cleaved IL-1β) will be assessed after 8-10-weeks of HFD. In addition, other markers for retinal inflammation, oxidative/nitrative stress, and acellular capillary formation combined with immunohistochemical co-localization studies will be used to characterize the effect of HFD on retinal microvascular degeneration and to identify the tissue distribution of TXNIP expression in HFD retinas.

NLRP3 inflammasome activation will be also assessed in human retinal endothelial (HRE) cells incubated with saturated fatty acid "Palmitate" coupled to bovine serum albumin (Pal-BSA) as a model of HFD in-vitro. Palmitate is one of the most abundant saturated fatty acids in plasma after HFD. This model resembles increased dietary intake of saturated/trans-fat responsible for significantly higher plasma levels of fatty acids in obese subjects [11, 29]. Knockdown studies for silencing TXNIP expression using a specific siRNA will be used to determine the impact of TXNIP on endothelial inflammasome activation.

Results pertained to Specific Aim 1 are compiled and presented in chapter (3). The manuscript: "Thioredoxin interacting protein is required for endothelial NLRP3-inflammasome

activation and cell death in a rat model of high fat diet" was published in Diabetologia; 2014 Feb;57(2):413-23.

2.3.2 Specific Aim 2: To test the hypothesis that HFD induces retinal microvascular inflammation and degeneration through the interplay between TXNIP-NLRP3 inflammasome axis and leukostasis.

2.3.2.1 Rationale: Increased retinal leukostasis is positively correlated with enhanced expression of adhesion molecules in dysfunctional endothelium and can result in accelerated blood retinal barrier (BRB) breakdown on the short term, and exacerbated loss of retinal endothelial cells and increased formation of non-perfused acellular capillaries on the longer term [8, 9]. Yet, the contribution of retinal leukostasis to the early microvascular injury at the obese pre-diabetic level remained unexplored. On the other hand, TXNIP and IL-1β are both known for NFκB pathway activation and induction of its downstream pro-inflammatory mediators including IL-1β (its own self) and TNF-α and endothelial adhesion molecules as: ICAM-1, PECAM-1, Eselectin, VCAM-1 in vivo and in isolated microvascular cells [30-36]. Therefore, there is a need to determine the specific contribution of the inflammasome induced IL-1β production in mediating and maintaining microvascular inflammation adhesion molecule expression in an autocrine fashion, versus the pro-inflammatory upstream role mediated by TXNIP.

2.3.2.2 The working hypothesis predicts that targeting TXNIP will protect against HFD-induced TXNIP-NLRP3 inflammasome activation and its associated leukostasis, BRB breakdown and acellular capillaries formation in vivo. Moreover, upregulation of the TXNIP-NLRP3 axis is also expected to act as an essential contributor to retinal microvascular inflammation and induction of adhesion molecules expression in HRE cells in-vitro.

In order to study both the short and long term effect of high fat diet (HFD) on retinal microvascular inflammation, 6-weeks old age and gender matched C57Bl/6J wild type mice

(WT) and TXNIP knock out (TKO) mice fed with HFD will be compared to their littermates fed with standard mice chow for both 8 and 18 weeks. TXNIP-NLRP3 inflammasome activation and its associated leukostasis and BRB breakdown will be evaluated after 8-weeks (short term) and acellular capillaries formation and retinal microvascular morphological changes will be evaluated at 18-weeks (long term) of HFD.

Genetic knockdown and overexpression studies using a specific siRNA and commercially available human TXNIP plasmid for manipulating TXNIP expression will be used to disect the role of TXNIP-NLRP3 inflammasome axis on endothelial adhesion molecule expression in cultured HRE cells. Moreover, isolated peripheral blood mononuclear cells (PBMCs) from obese and lean subjects and from all WT and TKO animal groups involved in the study will be used to asses the role of circulating leukocytes exposed to HFD in mediating leukostasis and endothelial cell death in culture.

Results pertained to Specific Aim 2 are compiled and presented in chapter (4). The manuscript: "High fat diet-induced obesity drives leukostasis, barrier dysfunction and microvascular degeneration through TXNIP-NLRP3 inflammasome activation." will be submitted to Circulation Research.

2.4 Significance.

Our findings in conjunction with the fact that obesity has been upgraded from a mere risk factor to a disease-state highlight the detrimental effect of HFD-induced obesity on the vasculature in general and development of retinal microvascular lesions even before reaching a state of hyperglycemia and frank diabetes. Current treatment approaches focus only on late stages of retinopathy or type 2 diabetes microvascular complications, while missing opportunities for earlier intervention during obesity or pre-diabetic stages. In absence of successful specific pharmacological therapies, delineating this proposed mechanism suggests TXNIP-NLRP3 inflammasome activation

axis as a novel therapeutic target for earlier intervention or prevention of obesity and pre-diabetes-induced retinal and general microvascular complications affecting millions of patients world-wide.

2.5 References

- 1. Klein, R., et al., 15-year cumulative incidence and associated risk factors for retinopathy in nondiabetic persons. Arch Ophthalmol, 2010. **128**(12): p. 1568-75.
- 2. van Leiden, H.A., et al., *Risk factors for incident retinopathy in a diabetic and nondiabetic population: the Hoorn study.* Arch Ophthalmol, 2003. **121**(2): p. 245-51.
- 3. Cheung, N. and T.Y. Wong, *Obesity and eye diseases*. Surv Ophthalmol, 2007. **52**(2): p. 180-95.
- 4. Habot-Wilner, Z. and M. Belkin, [Obesity is a risk factor for eye diseases]. Harefuah, 2005. **144**(11): p. 805-9, 821.
- 5. Nguyen, T.T. and T.Y. Wong, *Retinal vascular manifestations of metabolic disorders*. Trends Endocrinol Metab, 2006. **17**(7): p. 262-8.
- 6. Kohner, E.M. and P. Henkind, *Correlation of fluorescein angiogram and retinal digest in diabetic retinopathy*. Am J Ophthalmol, 1970. **69**(3): p. 403-14.
- 7. Tang, J. and T.S. Kern, *Inflammation in diabetic retinopathy*. Prog Retin Eye Res, 2011. **30**(5): p. 343-58.
- 8. Kern, T.S., Contributions of inflammatory processes to the development of the early stages of diabetic retinopathy. Exp Diabetes Res, 2007. **2007**: p. 95103.
- 9. Adamis, A.P. and A.J. Berman, *Immunological mechanisms in the pathogenesis of diabetic retinopathy*. Semin Immunopathol, 2008. **30**(2): p. 65-84.
- 10. Joussen, A.M., et al., A central role for inflammation in the pathogenesis of diabetic retinopathy. FASEB J, 2004. **18**(12): p. 1450-2.
- 11. Boden, G., *Interaction between free fatty acids and glucose metabolism*. Curr Opin Clin Nutr Metab Care, 2002. **5**(5): p. 545-9.
- 12. Boden, G., *Obesity, insulin resistance and free fatty acids*. Curr Opin Endocrinol Diabetes Obes, 2011. **18**(2): p. 139-43.
- 13. Eckel, R.H., S.M. Grundy, and P.Z. Zimmet, *The metabolic syndrome*. Lancet, 2005. **365**(9468): p. 1415-28.
- 14. Karpe, F., J.R. Dickmann, and K.N. Frayn, *Fatty acids, obesity, and insulin resistance: time for a reevaluation.* Diabetes, 2011. **60**(10): p. 2441-9.
- 15. Knopp, R.H., et al., *One-year effects of increasingly fat-restricted, carbohydrate-enriched diets on lipoprotein levels in free-living subjects.* Proc Soc Exp Biol Med, 2000. **225**(3): p. 191-9.
- 16. Krogmann, A., et al., *Inflammatory response of human coronary artery endothelial cells to saturated long-chain fatty acids.* Microvasc Res, 2011. **81**(1): p. 52-9.
- 17. Staiger, H., et al., *Palmitate-induced interleukin-6 expression in human coronary artery endothelial cells.* Diabetes, 2004. **53**(12): p. 3209-16.
- 18. Wen, H., et al., *Fatty acid-induced NLRP3-ASC inflammasome activation interferes with insulin signaling.* Nat Immunol, 2011. **12**(5): p. 408-15.
- 19. Matsuzaka, T., et al., *Elovl6 promotes nonalcoholic steatohepatitis*. Hepatology, 2012. **56**(6): p. 2199-208.
- 20. Pejnovic, N.N., et al., Galectin-3 deficiency accelerates high-fat diet-induced obesity and amplifies inflammation in adipose tissue and pancreatic islets. Diabetes, 2013. **62**(6): p. 1932-44.
- 21. Vandanmagsar, B., et al., *The NLRP3 inflammasome instigates obesity-induced inflammation and insulin resistance*. Nat Med. **17**(2): p. 179-88.

- 22. Stienstra, R., et al., *The inflammasome-mediated caspase-1 activation controls adipocyte differentiation and insulin sensitivity*. Cell Metab. **12**(6): p. 593-605.
- 23. Zhou, R., et al., *Thioredoxin-interacting protein links oxidative stress to inflammasome activation*. Nat Immunol, 2010. **11**(2): p. 136-40.
- 24. Zhou, R., et al., *A role for mitochondria in NLRP3 inflammasome activation*. Nature, 2011. **469**(7329): p. 221-5.
- 25. Lunov, O., et al., *Amino-functionalized polystyrene nanoparticles activate the NLRP3 inflammasome in human macrophages.* ACS Nano, 2011. **5**(12): p. 9648-57.
- 26. Park, Y.J., et al., TXNIP deficiency exacerbates endotoxic shock via the induction of excessive nitric oxide synthesis. PLoS Pathog, 2013. **9**(10): p. e1003646.
- 27. Xiang, M., et al., *Hemorrhagic shock activation of NLRP3 inflammasome in lung endothelial cells.* J Immunol, 2011. **187**(9): p. 4809-17.
- 28. Anthony, T.G. and R.C. Wek, *TXNIP switches tracks toward a terminal UPR*. Cell Metab, 2012. **16**(2): p. 135-7.
- 29. Wen, H., et al., Fatty acid-induced NLRP3-ASC inflammasome activation interferes with insulin signaling. Nat Immunol. **12**(5): p. 408-15.
- 30. Al-Gayyar, M.M., et al., *Thioredoxin interacting protein is a novel mediator of retinal inflammation and neurotoxicity*. Br J Pharmacol. **164**(1): p. 170-80.
- 31. Perrone, L., et al., *Thioredoxin interacting protein (TXNIP) induces inflammation through chromatin modification in retinal capillary endothelial cells under diabetic conditions*. J Cell Physiol, 2009. **221**(1): p. 262-72.
- 32. Perrone, L., et al., *Inhibition of TXNIP expression in vivo blocks early pathologies of diabetic retinopathy*. Cell Death Dis. 1: p. e65.
- 33. Kowluru, R.A. and S. Odenbach, *Role of interleukin-1beta in the pathogenesis of diabetic retinopathy*. Br J Ophthalmol, 2004. **88**(10): p. 1343-7.
- 34. Kowluru, R.A. and S. Odenbach, *Role of interleukin-1beta in the development of retinopathy in rats: effect of antioxidants.* Invest Ophthalmol Vis Sci, 2004. **45**(11): p. 4161-6.
- 35. Wang, J.G., et al., *Monocytic microparticles activate endothelial cells in an IL-1beta-dependent manner*. Blood, 2011. **118**(8): p. 2366-74.
- 36. Brown, G.T. and T.M. McIntyre, *Lipopolysaccharide signaling without a nucleus: kinase cascades stimulate platelet shedding of proinflammatory IL-1beta-rich microparticles.* J Immunol, 2011. **186**(9): p. 5489-96.

Fig.2.1

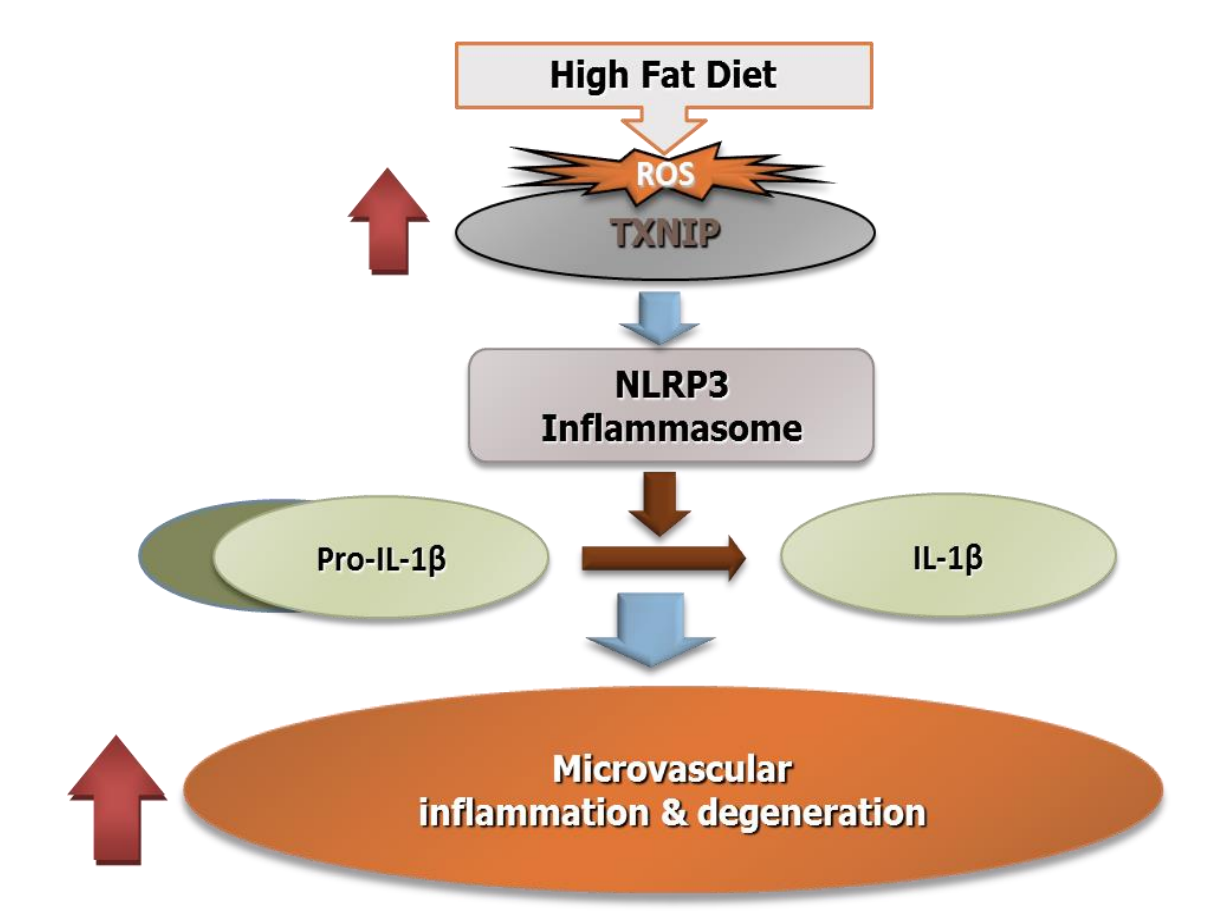


Fig.2.1 Diagram outlining the central hypothesis which predicts that TXNIP is the upstream molecular switch that connects between HFD-induced oxidative stress and downstream microvascular dysfunction via NLRP3 inflammasome activation.

CHAPTER 3

THIOREDOXIN INTERACTING PROTEIN IS REQUIRED FOR ENDOTHELIAL NLRP3-INFLAMMASOME ACTIVATION AND CELL DEATH IN A RAT MODEL OF HIGH FAT DIET. 1

¹ Mohamed IN, Hafez SS, Fairaq A, Ergul A, Imig JD, El-Remessy AB. Diabetologia. 2014 Feb;57(2):413-23.Reprinted with permission from Springer on behalf of the European Association for the Study of Diabetes (EASD). All rights reserved.

3.1 Abstract

Aims/hypothesis Obesity and hypertension, known pro-inflammatory states are identified determinants for increased retinal microvascular abnormalities. However, the molecular link between inflammation and microvascular degeneration remain elusive. Thioredoxin interacting protein (TXNIP) is recognized as an activator of NOD-like receptor protein (NLRP3)inflammasome. This study aims to examine TXNIP expression and elucidate its role in endothelial inflammasome activation and retinal lesions. Methods/results Spontaneously hypertensive (SHR) and control Wistar (W) rats were compared to groups fed with high-fat diet (W+F and SHR+F) for 8-10 weeks. Compared to W-controls, HFD alone or in combination with hypertension significantly induced acellular capillaries formation, a hallmark of retinal ischemic lesions. These effects were accompanied by significant increases in lipid peroxidation, nitrotyrosine, and expression of TXNIP, NFκB, TNFα and IL-β. HFD significantly increased interaction of TXNIP-NLRP3 and expression of cleaved casp-1 and cleaved IL-1β expression. Immunolocalization studies identified retinal vasculature as prominent tissue for enhanced TXNIP expression. To model HFD in vitro, human retinal endothelial (HRE) cells were stimulated with 400µmol/l-palmitate coupled to bovine serum-albumin (Pal-BSA). Pal-BSA triggered expression of TXNIP and its interaction with NLRP3 resulting in activation of caspase-1 and IL-1\beta in HRE cells. Silencing TXNIP expression in HRE cells abolished Pal-BSAmediated cleaved IL-1β release to medium and cell death evident by decreases in cleavedcaspase-3 expression and percentage of live to dead cells. Conclusions/interpretation These findings provide first evidence for enhanced TXNIP expression in hypertension and HFDinduced retinal oxidative/inflammatory response and that TXNIP is required for HFD-mediated activation of NLRP3-inflammasome and release of IL-1β in endothelial cells.

3.2 Introduction

Obesity and hypertension, the hallmarks of metabolic syndrome characterized by prediabetic insulin resistance, are identified as independent risk factors for the development of retinopathy [1-2]. Population studies have established obesity and hypertension as determinants for increased incidence of retinopathy and retinal microvascular abnormalities in the general non-diabetic population [3-4]. Increased caloric intake and consumption of saturated/trans-fat and cholesterol are the most plausible reasons behind obesity and metabolic syndrome alarming epidemic rates [5]. High levels of plasma free fatty acids and the saturated fatty acid palmitate in particular, are the result of high fat intake [6-7] that contribute to metabolic syndrome-associated inflammation and insulin resistance [8-9]. Palmitate has been shown to induce the activation of the NLRP3 (NOD-like receptor protein) inflammasome [6, 10-11], a well-established multiprotein complex responsible for instigating obesity-induced inflammation [12-13]. Activated NLRP3 oligomerizes with the ASC (apoptosis-associated specklike) adaptor protein which recruits procaspase-1, allowing its autocleavage and activation. Activated caspase-1 enzyme in turn cleaves upregulated premature pro-inflammatory cytokines: IL-1\beta and IL-18 and causes their release [14].

Thioredoxin interacting protein (TXNIP) is the endogenous inhibitor and regulator of the thioredoxin (Trx), a major cellular antioxidant and anti-apoptotic system [15]. TXNIP expression, a well-established mediator of insulin resistance has been shown to be consistently elevated in the muscles of pre-diabetics and diabetics [16-17]. In THP-1 human macrophages, inflammasome activators induced the dissociation of TXNIP from thioredoxin in a reactive oxygen species (ROS)-sensitive manner, allowing it to bind and activate NLRP3 [18]. We and others have demonstrated a pivotal role of enhanced retinal TXNIP expression in induction of

pro-inflammatory cytokines expression including IL-1 β , ICAM-1 and TNF- α in-vivo and in isolated retinal cultures [19-22]. Increased levels of IL-1 β were shown to increase number of retinal acellular capillaries in-vivo [23]. Nevertheless, there is a gap in knowledge whether TXNIP can mediate HFD-induced retinal inflammasome activation and whether this can occur directly within retinal endothelial cells to trigger inflammation and microvascular degeneration. Here, we test the hypothesis that high fat diet (HFD), as an essential component of the metabolic syndrome, results in up-regulation of retinal TXNIP expression, NLRP3-inflammasome activation and microvascular degeneration *in vivo* and *in vitro*.

3.3 Materials and Methods

3.3.1 Animal preparation.

All animal studies were in accordance with the Association for Research in Vision and Ophthalmology (ARVO) and the Georgia Reagents University Animal Care and Use Committee. Retinas were obtained from two separate animal studies that examined the effect of HFD, either alone or in combination with hypertension. In the first study, 8-week old male wistar kyoto control rats (W) and spontaneously hypertensive rats (SHR) were randomly assigned to four groups: (W) and (SHR) control groups; fed ad libitum with normal rat chow (7%fat), or (W+F) and (SHR+F) groups; fed with high-fat diet (HFD) (36gm%-60kcal%fat, #F2685 Bioserv.), respectively for 10-weeks. Rats were weighted weekly and metabolic parameters, plasma insulin, and blood glucose measurements were examined and published previously [24]. In the second study, retinas were obtained from sham control 4-5 week old male wistar control rats (W) fed ad libitum with an isocaloric control diet (10% fat), compared to W fed with HFD (24gm%-45kcal%fat,#D12451 Research Diets) (W+F) for 8-weeks. Rats were weighed weekly and metabolic parameters were examined and published recently [25]. Of note, in both studies, HFD resulted in significant increases in total body weights as an indicator for obesity. HFD induced

increases in plasma cholesterol levels in the first study [24], but not in the second study [25] and there was no effect on blood-pressure, blood-glucose levels or insulin resistance in either study.

3.3.2 Determination of retinal acellular (degenerated) capillaries.

Retinal vasculatures were isolated as described previously [26]. Transparent vasculature was laid out on slides and stained with periodic acid-Schiff and hematoxylin. Acellular capillaries counts were quantified under AxioObserver.Z1 Microscope (Zeiss, Germany). Acellular capillaries were identified as capillary-sized blood vessel tubes having no nuclei anywhere along their length. The number of acellular capillaries were averaged from 8 different fields of the midretinal area and calculated as the average number/mm² of retinal area.

3.3.3 Immunoprecipitation and western blot analysis.

Retinas were lysed in modified RIPA buffer (Millipore, Billerica, MA). 30μg of total protein were separated on a 4–20% SDS-polyacrylamide gel by electrophoresis, transferred to nitrocellulose membranes and then reacted with specific primary antibodies and their corresponding horseradish peroxidase-conjugated secondary antibodies then detected using and enhanced chemiluminescence (Pierce/Thermo Scientific, Rockford IL). Antibodies used were: anti-TXNIP (Santa Cruz Biotechnology, Dallas, TX), anti-NFκB p65 (Santa Cruz Biotechnology), Anti-TNF-α (Novus Biologicals), Anti-caspase-1, Anti-NLRP-3 (Enzo lifesciences) and anti-IL-1β (Abcam). 100μg of total protein was immunoprecipitated with anti-TXNIP antibody (5μg/ml) and incubated with A/G agarose beads overnight. Precipitated proteins were analyzed by SDS-PAGE and blotted with primary antibodies anti-TXNIP and anti-NLRP-3. X-ray films were scanned, and band intensities were quantified using (Alpa Innotech) imaging and densitometry software and expressed as relative optical density (ROD).

3.3.4 Detection of lipid peroxides.

Levels of lipid peroxides (Malondialdehyde, MDA) were assayed using thiobarbituric acid reactive substances as described before [26]. The Bradford assay (Bio-Rad, Hercules, CA) was performed to determine the protein concentration of retinal lysate. Lipid peroxides were expressed in micromoles MDA/mg total protein.

3.3.5 Detection of retinal nitrative stress.

Slot-blot analysis was used to measure nitrative stress marker, nitrotyrosine (NY) as described previously [26]. 5µg of retinal homogenate were immobilized onto a nitrocellulose membrane that was reacted with polyclonal anti-nitrotyrosine (Calbiochem/EMD Bioscience, La Jolla, CA) and the relative optical densities (ROD) were calculated compared to controls.

3.3.6 Quantitative real time PCR.

The One-Step qRT-PCR kit (Invitrogen) was used to amplify 10ng retinal mRNA as described previously [27]. PCR primers were purchased from Integrated DNA Technologies Inc. (Coralville, IA). Quantitative PCR was performed using a Realplex Master cycler (Eppendorf, Germany). Expression of TXNIP, NLRP3, NLRC4, or caspase-1 was normalized to the 18S level and expressed relative to W-control.

3.3.7 Immunolocalization studies.

10μmol/l OCT-frozen sections of the eyes were fixed using 2% paraformaldehyde and reacted with the primary antibody (1:200 dilution) including polyclonal anti-TXNIP (Santa Cruz Biotechnology), polyclonal anti-GFAP (Pierce Biotect, Rockford, IL), monoclonal anti-GFAP, monoclonal anti-glutamine synthetase (Chemicon-Millipore, Billerica, MA) or negative control at 4°C overnight, followed by Oregon-green-conjugated goat anti-rabbit antibody or Texas-red goat anti-mouse antibody (Invitrogen, Carlsbad, CA). Retinal vasculature was localized using

isolectin-B4 (Invitrogen). Images were collected using AxioObserver.Z1 Microscope (Zeiss, Germany).

3.3.8 Human retinal endothelial (HRE) cell culture studies.

All HRE cell studies were in accordance with the Association for Research in Vision and Ophthalmology (ARVO) and the Charlie Norwood Veterans Affairs Medical Center, research and ethics committee. HRE cells and supplies were purchased from Cell Systems Corporations (Kirkland, WA) and VEC Technology as described previously [27]. Sodium palmitate (Sigma, Cat# P9767) was dissolved in 50% ethyl alcohol solution, then added drop-wise to pre-heated 10% endotoxin- and fatty acid-free bovine serum albumin (BSA, Sigma, Cat#A8806) in M199 at 50°C to create an intermediate stock solution of palmitate coupled to BSA (Pal-BSA). Confluent cells were switched to serum-free medium for 6-hours then treated with Pal-BSA solutions in a ratio of 1:10 to produce final concentrations of 200, 400 and 800µmol/l of Pal-BSA for 12 hours. Equal volumes of 50% ethyl alcohol solution without any palmitate dissolved in BSA served as a control (BSA-alone). Peroxynitrite (PN) was purchased from Calbiochem and diluted in 0.1N NaOH and added at a final concentration of 100µmol/l.

3.3.9 Silencing TXNIP expressiom.

Transfection of HRE cells with 0.6 µmol/l TXNIP siRNA was performed using Amaxa nucleofector primary endothelial cells kit (Lonza, Germany) as described previously [27]. Additionally, a chemical-transfection kit was used according to the manufacturer's protocol. 80%-confluent HRE cells were incubated in the conditioned transfection medium with 300ng of FITC-labeled scrambled (SC) or TXNIP siRNA (Txsi) for 6-hours, then left to recover in complete medium for 24hours before performing experiments. Transfection efficiency was 70-80%, for both methods as indicated by the number of cells expressing GFP or FITC-labeled

scrambled (SC) siRNA (data not shown). Silencing TXNIP expression was verified by Western blot analysis (Fig.3.6).

3.3.10 Determination of IL-1\beta release.

Secreted cleaved-IL-1 β into the HRE cell conditioned media was determined using IL-1 β ELISA sensitive kit (R&D systems). Briefly, equal volumes of conditioned media for each group were concentrated using Ambion10K concentration columns (Millipore, Temecula CA), then loaded into IL-1 β capture antibody pre-coated wells and processed per manufacturer protocol. IL-1 β concentrations were expressed pg/ml of the cell conditioned media used.

3.3.11 Life and death cell viability assay.

HRE cell viability was tested by a Live/Dead assay (Invitrogen, USA) following manufacture's protocol. A working assay solution of 4μM ethidium homodimer-1 and 2μM calcein-AM was prepared that was added on top of each culture well for 15 min at 37 C in a humidified- atmosphere (20%O₂) with 5%CO₂. The staining solution was removed and samples were then viewed under a Ziess fluorescence microscope with filters 494 nm (green, viable) and 528 nm (red, non-viable) and the percentage was calculated.

3.3.12 Data analysis.

Results were expressed as mean \pm SEM. Two-way analysis of variance (ANOVA), followed by Bonferroni Multiple comparison test were used for testing differences among all the multiple experimental groups and for testing the interaction between the types of diet (HFD versus normal diet) across the animal groups (W control versus SHR group; for the animal experiments) and between the presence or absence of peroxynitrite (PN) across palmitate treated or control cell groups (for the in-vitro studies). Two-sided student's t-test was used for testing differences between two experimental groups (w and W+F). Significance was defined as P < 0.05.

3.4 Results

3.4.1 HFD causes retinal microvascular degeneration, oxidative and inflammatory stress.

To assess the impact of HFD by itself or in combination with co-morbid condition of hypertension on the development of retinopathy lesion, we examined 10-weeks of HFD in W or SHR on retinal microvascular degeneration. As shown in Fig.3.1a and supplementary Fig.3.1, HFD alone (W+F) significantly induced the number of acellular capillaries by 2-folds, compared to control (W) group. SHR alone significantly induced the number of acellular capillaries by 2.6fold, which was further exacerbated to 4-fold upon combination with HFD compared to W control. These effects were associated with increases in retinal oxidative and inflammatory stress (Fig.3.1b-e). Retinal lipid peroxides were higher in W+F group by 1.7-fold when compared to control W group. SHR and combined SHR+F groups had higher levels by 2- and 2.7-fold, respectively, compared to control W group (Fig. 3.1b). Retinal NY levels were higher by 1.3and 1.5-fold in W+F and SHR groups, which was exacerbated to 2-fold in the SHR+F relative to control W group (Fig.3.1c). Oxidative stress was paralleled with increases in NFkB p65 expression in the W+F alone group by 2-folds, SHR group by 1.8-folds, and in the combined SHR+F group by 2.8-folds respectively, when compared to control W group (Fig.3.1d). Furthermore, TNF- α , a downstream target for NF \square B pathway was also higher in the W+F group by 3.3 folds, in the SHR group by 2.7-fold which was further exacerbated in the combined SHR+F group to 5.2 folds respectively, when compared to control W group (Fig. 3.1e).

3.4.2 HFD induces retinal TXNIP expression and NLRP3 inflammasome activation.

TXNIP has been shown to be an effective link coupling between increased oxidative stress and inflammation and activation of the innate immune response mediated by the NLRP3 inflammasome [17-18, 21]. Therefore, we sought to examine the potential involvement of HFD-

induced TXNIP expression in mediating NLRP3 inflammasome activation. As shown in Fig.3.2, HFD alone (W+F) or in combination with hypertension (SHR+F) significantly induced retinal TXNIP expression by 1.9- and 2-folds, and NLRP3 by 1.6- and 1.7-fold, respectively, compared to W-controls (Fig.3.2a-c). Cleaved caspase-1 and cleaved IL-1β expression, the final products of inflammasome activation, were also higher in the W+F by 1.4- and 1.5-fold and in the SHR+F groups by 1.9- and 1.7-fold, respectively compared to W-controls (Fig. 3.2 d-e). In comparison to W-controls, SHR did not show significant changes in inflammasome protein expression except 1.4-fold increase in TXNIP (Fig.3.2b). These results highlight the selective effect of HFD alone, independently from other components of the metabolic syndrome like hypertension. Therefore, the rest of the study will focus on studying effects of HFD alone from a parallel study utilizing wistar rats fed with HFD for 8-weeks.

3.4.3 HFD induces TXNIP-NLRP3 interaction associated with retinal inflammasome activation.

Other inflammasome members, like NLRP1 and NLRC4 have been also suggested to play a role in HFD-induced inflammatory pathologies [28-29]. On the mRNA level, HFD induced a significant 2-fold increase in TXNIP mRNA expression (Fig.3.3a) and a strong trend in the mRNA expression of NLRP3 (Fig. 3.3b). However, there were no changes observed in NLRP1 (Fig.3.3c) or NLRC4 mRNA expression levels (Fig.3.3d). On the protein expression and interaction level, as shown in Fig.3.4a, HFD-induced 2-fold increase in TXNIP expression (W+F) compared to W-controls. This effect was associated with 1.3-fold increase in NLRP3 expression, the intracellular receptor for the inflammasome (Fig.3.4b) and 2.5-fold in TXNIP-NLRP3 interaction assessed by immuno-precipitation (Fig.3.4c). Moreover, HFD stimulated cleaved Casp-1 and cleaved IL-1β expression by 1.4- and 1.7-fold, respectively, compared to

control W group (Fig.3.4d-e). These results confirm activation of TXNIP-NLRP3-inflammasome in the retina in response to HFD.

3.4.4 HFD-induced TXNIP expression co-localizes within retinal microvasculature.

TXNIP expression was found to be highly glucose-responsive in retinal endothelial cells and diabetic vasculature [19, 22]. On the other hand, TXNIP-mediated NLRP3 inflammasome activation was reported in rat Muller glia cells cultured in hyperglycemic conditions [21]. As shown in Fig.3.5a, W+F retinas showed higher TXNIP expression in both the ganglion cell layer (GCL) and inner nuclear layer (INL) compared to W-controls. HFD also was associated with increased staining of Glial fibrillary acidic protein (GFAP), a marker for glial Muller cell activation, in W+F group compared to control W group (Fig.3.5b). We next attempted to investigate HFD-induced TXNIP expression colocalization within different retinal layers. Colcalization with glutamine synthase (GS), the specific Muller cell marker showed minimal association of TXNIP within Muller cells (Fig.3.5c). Colocalization with of TXNIP and GFAP showed strong association within the GCL suggesting astrocytes and Muller endfeet surrounding retinal blood vessels (Fig.3.4d). Colocalization of TXNIP expression with the vascular endothelial marker Isolectin-B4 showed strong TXNIP expression within retinal cappilaries in GCL as well as deep retinal blood vessels in INL (Fig. 3.4 e-f). These findings highlight retinal microvascular tissue as a prominent site for HFD-induced TXNIP expression.

3.4.5 Palmitate induces TXNIP and activates caspase-1/IL-1 β in human retinal endothelial cells.

Palmitate is a commonly elevated saturated FFA in plasma, with a well established proinflammatory effect, versus other unsaturated fatty acids [7, 30-31]. In addition, palmitate is a major component (60%) of the saturated fatty acids both in the #F2685 Bioserv and # D12451 Research Diets. In order to test the hypothesis that HFD can directly activate NLRP3inflammsome in endothelial cells, we have examined different levels of palmitate coupled to bovine serum albumin (Pal-BSA) 200μM, 400μM and 800μM in human retinal endothelial (HRE) cells. Pal-BSA induced a bell shaped dose-response curve, (supplementary Fig.3.2a-d) reaching the maximum response at 400μM that induced TXNIP, cleaved caspase-1 and cleaved IL-1β expression by 1.6-, 1.8- and 1.75-fold respectively, compared to BSA-controls. Of note, 800μM induced HRE cell toxicity; hence 400μM of Pal-BSA was used for the rest of *in vitro* studies to probe the role of HFD in NLRP3-inflammasome activation in endothelial cells.

3.4.6 TXNIP is required for palmitate-induced NLRP3-inflammasome activation in HRE cells.

TXNIP, as an oxidative stress sensor, was shown to induce NLRP3-inflammasome activation in ROS-sensitive manner [18, 32]. Therefore, we tested the hypothesis that TXNIP is required for NLRP3-inflammasome activation in HRE cells and that combining 100μmol/l PN with 400μmol/l Pal-BSA (Pal-BSA+PN) would exacerbate palmitate-induced inflammasome activation. 400μmol/l Pal-BSA (Pal-BSA) alone or in combination with 100μmol/l PN (Pal-BSA+PN) resulted in significant increases in interaction of TXNIP-NLRP3 by 2 and 2.5-fold respectively, compared to control BSA treatment. PN alone did not result in a significant increase in TXNIP-NLRP3 interaction, nor a significant exacerbation of the Pal-BSA effect (Fig.3.6a). Next, we tested the hypothesis that TXNIP is required for palmitate-induced NLRP3 inflammasome activation in HRE cells. As shown in Fig.3.6b-e, Pal-BSA alone or in combination with PN, but not PN alone increased TXNIP, NLRP3 and cleaved caspase-1 by 2.7-, 2- and 1.7-fold for PAL-BSA and 2.45- 2.7- and 2.4-fold for PAL+PN, respectively, relative to BSA-controls in the scrambled-siRNA group. Silencing TXNIP expression using siRNA abolished such responses (Fig.3.6b-e).

3.4.7 TXNIP is required for palmitate-induced IL-1 β maturation in HRE cells.

As shown in Fig.3.7a, Pal-BSA and Pal-BSA+PN but not PN alone increased cleaved IL-1β expression by 1.75- and 1.9-fold respectively, compared to control BSA in scrambled-treated groups. Silencing TXNIP expression significantly abolished cellular IL-1β expression in the Txsi-group. IL-1β levels released into the conditioning medium were assessed by an ELISA assay. In the scrambled-control group, PN-alone stimulated the maximum release of IL-1β by 4-fold compared to BSA-controls. Pal-BSA alone or Pal-BSA+PN significantly induced IL-1β release by 1.8- and 1.6-fold, respectively, relative to BSA-controls. Silencing TXNIP expression blunted Pal-BSA-mediated but did not affect PN alone or Pal-BSA+PN stimulated release of IL-1β compared to BSA-control (Fig.3.7b). These results indicate that TXNIP is required for palmitate-induced intracellular inflammasome activation and IL-1β maturation, but not for PN-mediated mature IL-1β release.

3.4.8 TXNIP is required for palmitate-induced apoptosis and cell death in HRE cells.

We next assessed the impact of Pal-BSA-induced IL-1β release on HRE cell death. As shown in Fig.3.8a, Pal-BSA induced expression of apoptotic marker cleaved caspase-3 by 2.5-fold compared to BSA-controls in the SC-group, which was abolished by silencing TXNIP. Furthermore, reduced cell viability was also observed in HRE cells after treatment with PN, Pal-BSA and Pal-BSA+PN in the SC group by 1.3, 1.8 and 2 folds respectively, compared to SC control BSA group. Silencing TXNIP expression resulted in a significant decrease in cell death in all Txsi treatment groups compared to their relative SC treatment group (Fig.3.8b & supplementary Fig.3.3).

3.5 Discussion

Although clinical evidence signifies metabolic syndrome for increasing the risk for retinopathy [3-4], data from experimental models are lacking. Therefore, we attempted to model

and characterize the detrimental elements of the metabolic syndrome on the early development of retinal microvascular lesions. The major findings of the current study are: 1- HFD-induced obesity, hypertension or their combination showed early retinal microvascular lesions, significant increases in retinal TXNIP expression, oxidative stress and inflammation. 2-HFD selectively induces retinal TXNIP-NLRP3 interaction and activates inflammasome resulting in increased expression of cleaved Caspase-1 and IL-1 β . 3- Retinal vasculature is a prominent site for HFD-induced TXNIP up-regulation and for palmitate-induced activation of the NLRP3-inflammasome in retinal endothelial cells.

Population studies have shown that subjects with various components of the metabolic syndrome including obesity, dyslipidemia and hypertension were more likely to have retinal microvascular abnormalities such as focal and generalized retinal arteriolar narrowing and venular dilatation [33-34]. In our study, HFD-induced obesity or hypertension alone demonstrated significant increases in retinal acellular capillaries formation that was further exacerbated upon their combination as early as 10-weeks. Accelerated retinal capillary dropout, vascular tortuosity, and vascular leakage were previously reported in obese SHR rats starting at 12-weeks. [35].

The thioredoxin system is one of the major anti-oxidant and anti-apoptotic defense systems, which is directly inhibited by TXNIP. Increased levels of TXNIP bind more thioredoxin, limiting its availability for scavenging cellular ROS [15]. Indeed, exposure to HFD, hypertension or their combination significantly triggered retinal TXNIP expression, retinal lipid peroxides and nitrotyrosine levels, the foot-print of peroxynitrite formation implicating endothelial dysfunction compared to control group (Fig.3.1 and 3.2). Increased lipid peroxidation and peroxynitrite generation and endothelial dysfunction were also reported in patients with hypertension-related microvascular changes [36-37] and in retinas from BBZ rat, an obese and

noninsulin-dependent model of diabetes [38] as well as coronary endothelial cells in response to HFD [39-40]. Nevertheless, this is the first report to demonstrate increases in retinal TXNIP expression in HFD, SHR or their combination. TXNIP can directly activate the redox-sensitive NF-κB and its downstream inflammatory cytokines and adhesion molecules. HFD alone, hypertension alone or their combination significantly enhanced levels of NFκB and downstream TNF-α. In line with our findings, animals fed with a HFD or a high sucrose and cholesterol diet have higher expression of inflammation in isolated retinal vasculature and higher levels of retinal microaneurysms respectively [41-42].

Lipotoxcicty or impaired tissue-homeostasis, occurs as a result of lipid-induced changes in intracellular signaling or increased lipid utilization [9, 43]. Previous reports have established that saturated fatty acids, mainly palmitate, but not unsaturated fatty acids were able to induce pro-inflammatory response in human corornary endothelial cells [7, 31] and NLRP3 inflammasome activation in cultured macrophages [6]. Accumulated literature provides evidence supporting TXNIP as an important mediator of NLRP3 inflammasome activation. However, the relationship between HFD-induced retinal and endothelial TXNIP expression and inflammasome activation in HFD-induced obesity has not been examined. Here we show that HFD alone selectively induced expression and interaction of TXNIP and NLRP3 resulting in cleaved caspase-1 and IL-1\beta expression independently from hypertension, and that retinal microvasculature is a prominent site for increased TXNIP expression (Fig.3.3-3.5). These results lend further support to previously documented TXNIP-induced NLRP3 inflammasome activation in lung endothelial cells, macrophages, adipose tissue and pancreatic beta cells in response to ROS, obesity/hyperglycemia and endoplasmic reticulum stress, respectively [18, 32, 44-45]. To model HFD in vitro, we examined the effects of saturated fatty acid palmitate alone or in combination with exogenous peroxynitrite in HRE cells. Indeed, Silencing TXNIP abrogated palmitate-induced NLRP3 inflammasome activation and its associated increases in pro-apoptotic caspase-3 expression and reduced cell viability of HRE cells (Fig.3.6-3.8). These findings establish TXNIP as an essential activator of NRLP3 inflammasome in HRE cells, which can result in increased retinal endothelial death/apoptosis. In line with our findings, pharmacological inhibition of caspase-1 or deletion of IL-1receptor suppressed IL-1β-dependent retinal acellular capillaries formation in diabetic animals [23, 46]. Together, these findings support the proposed link between inflammasome activation and accelerated retinal microvascular degeneration. Further studies are warranted to study the effect of HFD-induced retinal microvascular inflammation and degeneration in TXNIP knockout mice. To the best of our knowledge, this is the first report of increased retinal TXNIP expression and activation of endothelial TXNIP-NLRP3 inflammasome in experimental models of HFD.

Our data suggest an inverse relationship between accumulation of intracellular cleavage/ maturation of IL-1β and its release. Pal-BSA alone was able to induce both intracellular maturation and release of IL-1β in HRE cells which was mitigated by silencing TXNIP expression (Fig. 3.7). On the other hand, exogenous PN alone resulted in a higher surge of IL-1β release that was independent of TXNIP inhibition, although it was not able to induce significant changes in its intracellular cleavage/maturation, suggesting accelerated activation and trafficking of IL-1β. Furthermore, this effect was quenched when exogenous PN was combined with Pal-BSA in presence of TXNIP, whereas TXNIP inhibition reversed this process and facilitated PN-induced IL-1β release despite its combination with Pal-BSA. This data indicate that, while TXNIP is required for palmitate-induced NLRP3 inflammasome activation and IL-1β maturation in HRE cells, it does not facilitate the maximum IL-1β release. Recent evidence suggests that caspase-1 activation/processing of pro-IL-1β by caspase-1 and the release of mature IL-1β from human monocytes are distinct and separable events [47]. TXNIP has been shown to shuffle

between different cellular compartments, including the nucleus, mitochondria [48] and plasma membrane [49]. A possible explanation for this intriguing observation might be due the nature of TXNIP as a member of the alpha arrestin scaffolding proteins, which are believed to play an important role in intracelleular cargo trafficking and/or internalization of different proteins [49-50]. Hence, subcellular localization of TXNIP in response to different insults might reflect on enhancement or inhibition of mature IL-1β release.

In summary, our findings in conjunction with the fact that obesity has been upgraded from a mere risk factor to a disease-state highlight the detrimental effect of HFD-induced obesity on the vasculature in general and development of retinal microvascular lesions even before reaching a state of hyperglycemia and frank diabetes. Characterizing the early impact of HFD-induced obesity on development of retinopathy and developing TXNIP as a therapeutic target will help identifying innovative strategies for intervention in obesity and pre-diabetes related vascular complications affecting millions of patients world-wide.

3.6 References

- [1]Nguyen TT, Wong TY (2006) Retinal vascular manifestations of metabolic disorders. Trends Endocrinol Metab 17: 262-268
- [2]Liew G, Wang JJ (2007) Retinal vascular signs in diabetes and hypertension--review. Arq Bras Endocrinol Metabol 51: 352-362
- [3] Klein R, Myers CE, Lee KE, Klein BE (2010) 15-year cumulative incidence and associated risk factors for retinopathy in nondiabetic persons. Arch Ophthalmol 128: 1568-1575
- [4]van Leiden HA, Dekker JM, Moll AC, et al. (2003) Risk factors for incident retinopathy in a diabetic and nondiabetic population: the Hoorn study. Arch Ophthalmol 121: 245-251
- [5] Kratz M, Baars T, Guyenet S (2013) The relationship between high-fat dairy consumption and obesity, cardiovascular, and metabolic disease. Eur J Nutr 52: 1-24
- [6] Wen H, Gris D, Lei Y, et al. (2011) Fatty acid-induced NLRP3-ASC inflammasome activation interferes with insulin signaling. Nat Immunol 12: 408-415
- [7]Staiger H, Staiger K, Stefan N, et al. (2004) Palmitate-induced interleukin-6 expression in human coronary artery endothelial cells. Diabetes 53: 3209-3216
- [8]Boden G (2011) Obesity, insulin resistance and free fatty acids. Curr Opin Endocrinol Diabetes Obes 18: 139-143
- [9] Karpe F, Dickmann JR, Frayn KN (2011) Fatty acids, obesity, and insulin resistance: time for a reevaluation. Diabetes 60: 2441-2449
- [10]Pejnovic NN, Pantic JM, Jovanovic IP, et al. (2013) Galectin-3 deficiency accelerates high-fat diet-induced obesity and amplifies inflammation in adipose tissue and pancreatic islets. Diabetes 62: 1932-1944
- [11]Matsuzaka T, Atsumi A, Matsumori R, et al. (2012) Elovl6 promotes nonalcoholic steatohepatitis. Hepatology 56: 2199-2208
- [12]Stienstra R, van Diepen JA, Tack CJ, et al. (2011) Inflammasome is a central player in the induction of obesity and insulin resistance. Proc Natl Acad Sci U S A 108: 15324-15329
- [13] Vandanmagsar B, Youm YH, Ravussin A, et al. (2011) The NLRP3 inflammasome instigates obesity-induced inflammation and insulin resistance. Nat Med 17: 179-188
- [14]Schroder K, Zhou R, Tschopp J (2010) The NLRP3 inflammasome: a sensor for metabolic danger? Science 327: 296-300
- [15]Nishiyama A, Matsui M, Iwata S, et al. (1999) Identification of thioredoxin-binding protein-2/vitamin D(3) up-regulated protein 1 as a negative regulator of thioredoxin function and expression. J Biol Chem 274: 21645-21650
- [16]Parikh H, Carlsson E, Chutkow WA, et al. (2007) TXNIP regulates peripheral glucose metabolism in humans. PLoS Med 4: e158
- [17] Muoio DM (2007) TXNIP links redox circuitry to glucose control. Cell Metab 5: 412-414
- [18]Zhou R, Tardivel A, Thorens B, Choi I, Tschopp J (2010) Thioredoxin-interacting protein links oxidative stress to inflammasome activation. Nat Immunol 11: 136-140
- [19]Perrone L, Devi TS, Hosoya K, Terasaki T, Singh LP (2009) Thioredoxin interacting protein (TXNIP) induces inflammation through chromatin modification in retinal capillary endothelial cells under diabetic conditions. J Cell Physiol 221: 262-272
- [20]Al-Gayyar MM, Abdelsaid MA, Matragoon S, Pillai BA, El-Remessy AB (2011) Thioredoxin interacting protein is a novel mediator of retinal inflammation and neurotoxicity. Br J Pharmacol 164: 170-180

- [21]Devi TS, Lee I, Huttemann M, Kumar A, Nantwi KD, Singh LP (2012) TXNIP links innate host defense mechanisms to oxidative stress and inflammation in retinal Muller glia under chronic hyperglycemia: implications for diabetic retinopathy. Exp Diabetes Res 2012: 438238
- [22]Schulze PC, Yoshioka J, Takahashi T, He Z, King GL, Lee RT (2004) Hyperglycemia promotes oxidative stress through inhibition of thioredoxin function by thioredoxin-interacting protein. J Biol Chem 279: 30369-30374
- [23]Kowluru RA, Odenbach S (2004) Role of interleukin-1beta in the development of retinopathy in rats: effect of antioxidants. Invest Ophthalmol Vis Sci 45: 4161-4166
- [24]Knight SF, Quigley JE, Yuan J, Roy SS, Elmarakby A, Imig JD (2008) Endothelial dysfunction and the development of renal injury in spontaneously hypertensive rats fed a high-fat diet. Hypertension 51: 352-359
- [25]Li W, Prakash R, Chawla D, et al. (2013) Early effects of high-fat diet on neurovascular function and focal ischemic brain injury. Am J Physiol Regul Integr Comp Physiol 304: R1001-1008
- [26]Al-Gayyar MM, Abdelsaid MA, Matragoon S, Pillai BA, El-Remessy AB (2010) Neurovascular protective effect of FeTPPs in N-methyl-D-aspartate model: similarities to diabetes. Am J Pathol 177: 1187-1197
- [27] Abdelsaid MA, Matragoon S, El-Remessy AB (2013) Thioredoxin Interacting Protein (TXNIP) expression is required for VEGF-mediated angiogenic signal in endothelial cells. Antioxidant and Redox Signal
- [28] Faustin B, Reed JC (2013) Reconstituting the NLRP1 Inflammasome In Vitro. Methods Mol Biol 1040: 137-152
- [29]Luo X, Yang Y, Shen T, et al. (2012) Docosahexaenoic acid ameliorates palmitate-induced lipid accumulation and inflammation through repressing NLRC4 inflammasome activation in HepG2 cells. Nutr Metab (Lond) 9: 34
- [30]Knopp RH, Retzlaff B, Walden C, Fish B, Buck B, McCann B (2000) One-year effects of increasingly fat-restricted, carbohydrate-enriched diets on lipoprotein levels in free-living subjects. Proc Soc Exp Biol Med 225: 191-199
- [31]Krogmann A, Staiger K, Haas C, et al. (2011) Inflammatory response of human coronary artery endothelial cells to saturated long-chain fatty acids. Microvasc Res 81: 52-59
- [32]Xiang M, Shi X, Li Y, et al. (2011) Hemorrhagic shock activation of NLRP3 inflammasome in lung endothelial cells. J Immunol 187: 4809-4817
- [33]Wong TY, Duncan BB, Golden SH, et al. (2004) Associations between the metabolic syndrome and retinal microvascular signs: the Atherosclerosis Risk In Communities study. Invest Ophthalmol Vis Sci 45: 2949-2954
- [34] Kawasaki R, Tielsch JM, Wang JJ, et al. (2008) The metabolic syndrome and retinal microvascular signs in a Japanese population: the Funagata study. Br J Ophthalmol 92: 161-166
- [35]Huang SS, Khosrof SA, Koletsky RJ, Benetz BA, Ernsberger P (1995) Characterization of retinal vascular abnormalities in lean and obese spontaneously hypertensive rats. Clin Exp Pharmacol Physiol Suppl 22: S129-131
- [36] Ferroni P, Basili S, Paoletti V, Davi G (2006) Endothelial dysfunction and oxidative stress in arterial hypertension. Nutr Metab Cardiovasc Dis 16: 222-233
- [37]Coban E, Nizam I, Topal C, Akar Y (2010) The association of low-grade systemic inflammation with hypertensive retinopathy. Clin Exp Hypertens 32: 528-531
- [38]Ellis EA, Grant MB, Murray FT, et al. (1998) Increased NADH oxidase activity in the retina of the BBZ/Wor diabetic rat. Free Radic Biol Med 24: 111-120

- [39]Galili O, Versari D, Sattler KJ, et al. (2007) Early experimental obesity is associated with coronary endothelial dysfunction and oxidative stress. Am J Physiol Heart Circ Physiol 292: H904-911
- [40] Jebelovszki E, Kiraly C, Erdei N, et al. (2008) High-fat diet-induced obesity leads to increased NO sensitivity of rat coronary arterioles: role of soluble guanylate cyclase activation. Am J Physiol Heart Circ Physiol 294: H2558-2564
- [41]Gustavsson C, Agardh CD, Zetterqvist AV, Nilsson J, Agardh E, Gomez MF (2010) Vascular cellular adhesion molecule-1 (VCAM-1) expression in mice retinal vessels is affected by both hyperglycemia and hyperlipidemia. PLoS One 5: e12699
- [42]Helfenstein T, Fonseca FA, Ihara SS, et al. (2011) Impaired glucose tolerance plus hyperlipidaemia induced by diet promotes retina microaneurysms in New Zealand rabbits. Int J Exp Pathol 92: 40-49
- [43]Symons JD, Abel ED (2013) Lipotoxicity contributes to endothelial dysfunction: a focus on the contribution from ceramide. Rev Endocr Metab Disord 14: 59-68
- [44]Koenen TB, Stienstra R, van Tits LJ, et al. (2011) Hyperglycemia activates caspase-1 and TXNIP-mediated IL-1beta transcription in human adipose tissue. Diabetes 60: 517-524
- [45]Lerner AG, Upton JP, Praveen PV, et al. (2012) IRE1alpha induces thioredoxin-interacting protein to activate the NLRP3 inflammasome and promote programmed cell death under irremediable ER stress. Cell Metab 16: 250-264
- [46] Vincent JA, Mohr S (2007) Inhibition of caspase-1/interleukin-1beta signaling prevents degeneration of retinal capillaries in diabetes and galactosemia. Diabetes 56: 224-230
- [47]Galliher-Beckley AJ, Lan LQ, Aono S, Wang L, Shi J (2013) Caspase-1 activation and mature interleukin-1beta release are uncoupled events in monocytes. World J Biol Chem 4: 30-34
- [48]Lane T, Flam B, Lockey R, Kolliputi N (2013) TXNIP shuttling: missing link between oxidative stress and inflammasome activation. Front Physiol 4: 50
- [49]Park SY, Shi X, Pang J, Yan C, Berk BC (2013) Thioredoxin-interacting protein mediates sustained VEGFR2 signaling in endothelial cells required for angiogenesis. Arterioscler Thromb Vasc Biol 33: 737-743
- [50]Wu N, Zheng B, Shaywitz A, et al. (2013) AMPK-Dependent Degradation of TXNIP upon Energy Stress Leads to Enhanced Glucose Uptake via GLUT1. Mol Cell 49: 1167-1175

Fig.3.1

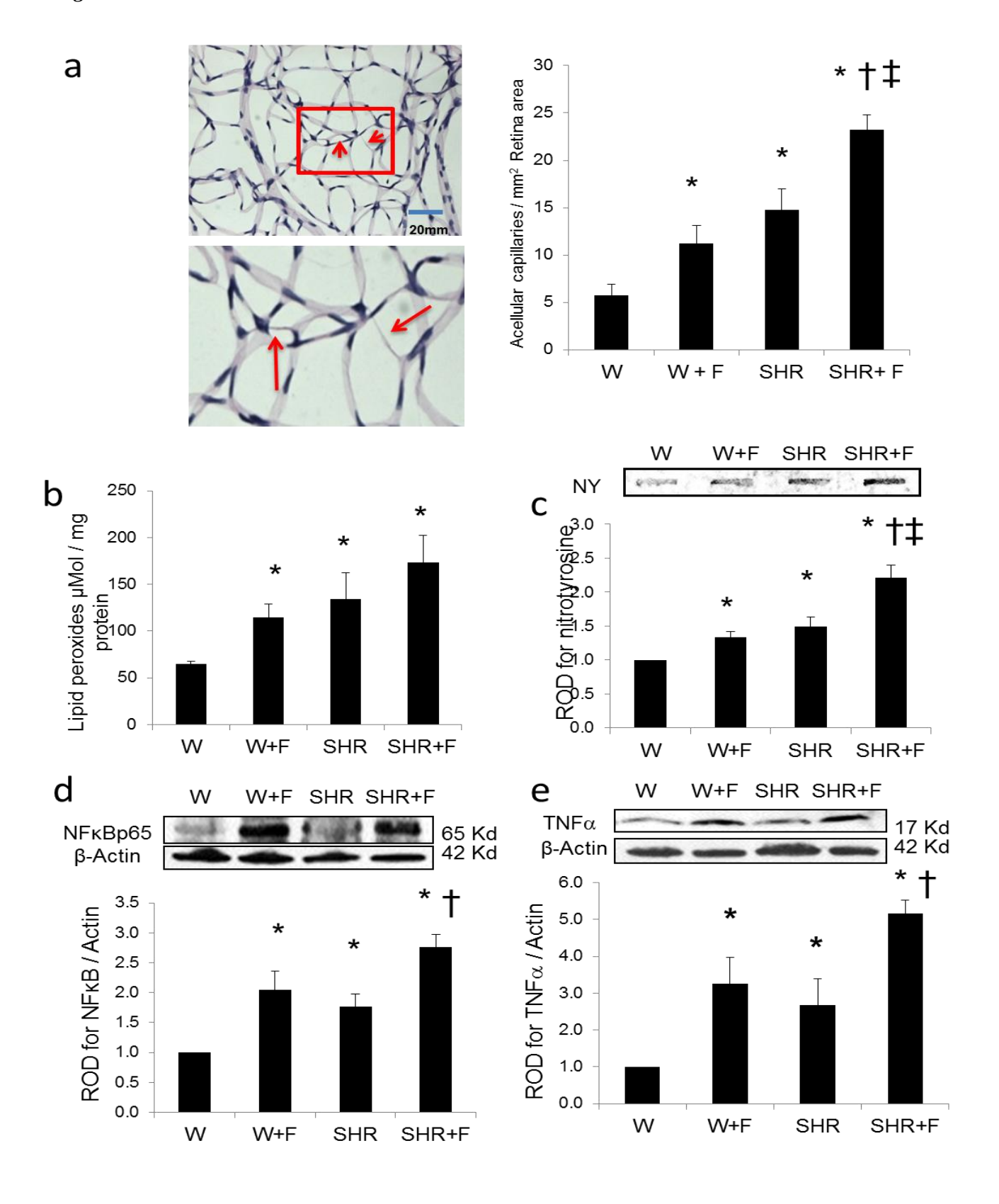


Fig.3.1 HFD causes retinal microvascular degeneration, oxidative and inflammatory stress. (a) Representative images and quantification of retinal trypsin digests with enlarged subset identifying retinal acellular capillaries in control wistar rats (W) and spontaneously hypertensive rats (SHR) fed with normal diet or with HFD (W+F) and (SHR+F), respectively, for 10-weeks. Two-way ANOVA showed significant interaction between HFD and hypertension. Oxidative stress markers were assessed using retinal lipid-peroxidation levels (b) and NY levels (c) in all groups. Two-way ANOVA showed significant interaction between HFD and hypertension in retinal NY levels. Representative blots and western blot (WB) analyses of NFκB p65 expression (d) and TNF-α expression (e) in all groups. Protein levels were normalized to β-actin and respective control W group. (n=4-5; * P value <0.05 vs W, † vs SHR and ‡ vs W+F).

Fig.3.2

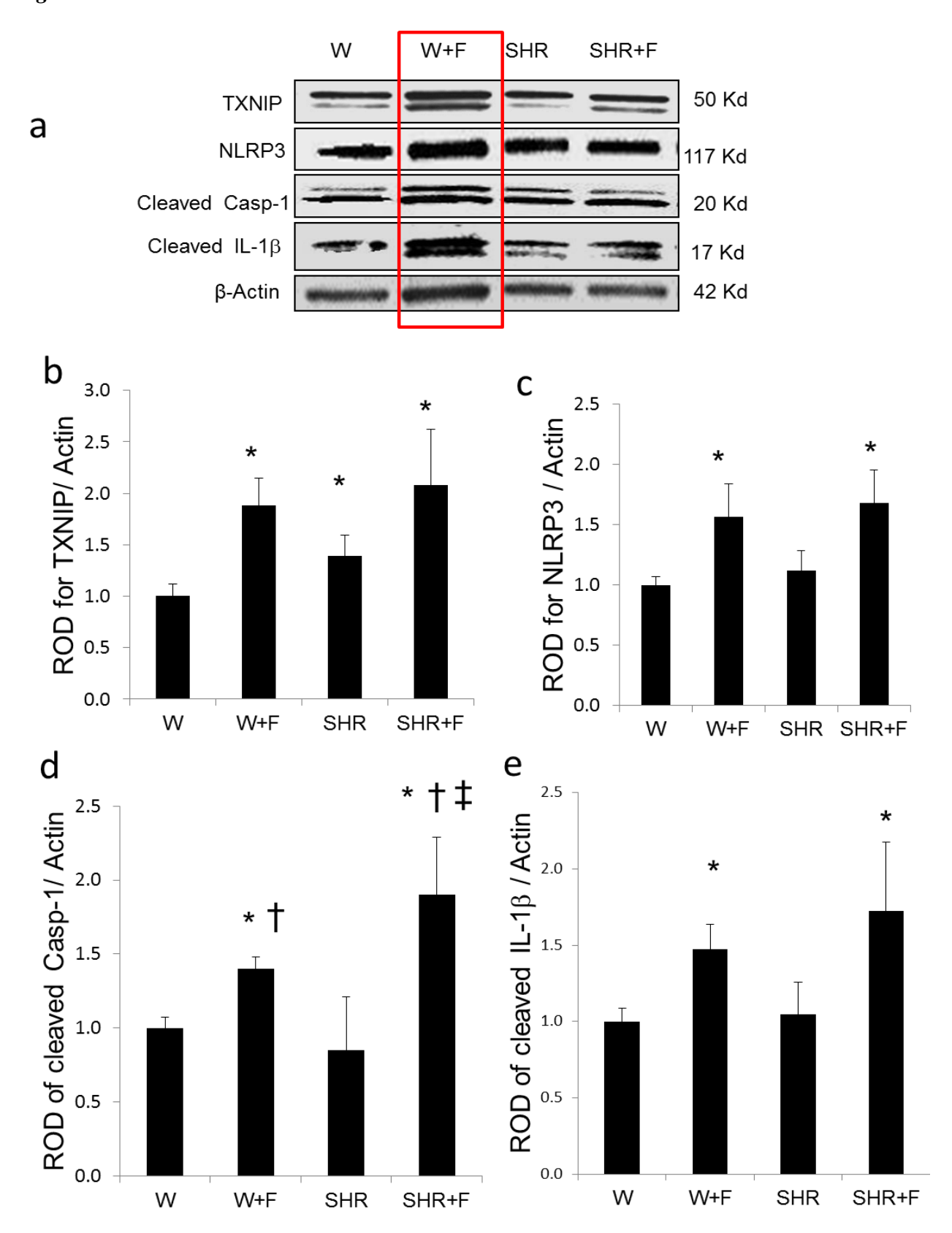


Fig.3.2 HFD induces retinal TXNIP expression and NLRP3 inflammasome activation. Representative blots (a) and WB analysis of TXNIP (b), NLRP3 (c), cleaved caspase-1 (d) and cleaved IL-1β (d) protein levels in retinas of Wistar (W) or spontaneously hypertensive rats (SHR) controls or fed with normal diet or HFD (W+F and SHR+F) for 10-weeks of. HFD had selectively increased the levels of TXNIP-inflammasome target proteins. Protein levels were normalized to actin and respective W-controls (n=3-8, * P value <0.05 vs W, † vs SHR and ‡ vs W+F).

Fig.3.3

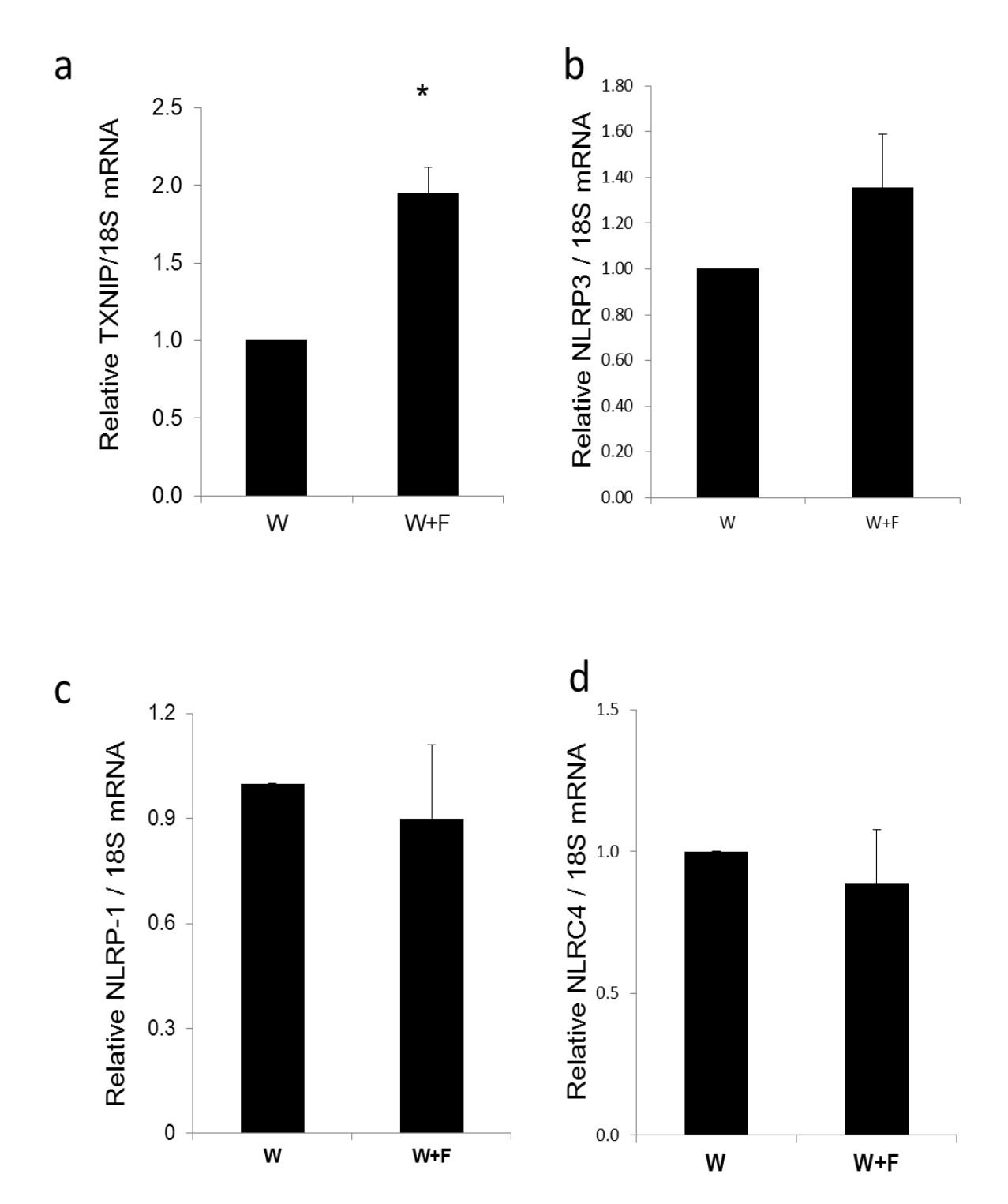


Fig.3.3 Gene expression levels of TXNIP (a), and other inflammasome members; NLRP3 (b), NLRP1 (c) and NLRC4 (d) in wistar rats fed with HFD for 8-weeks compared to control W rats. HFD induced significant increases in TXNIP gene expression and a strong trend in that of NLRP3 versus other inflammasome members. (n=3-6; * P value <0.05 vs W).

Fig.3.4

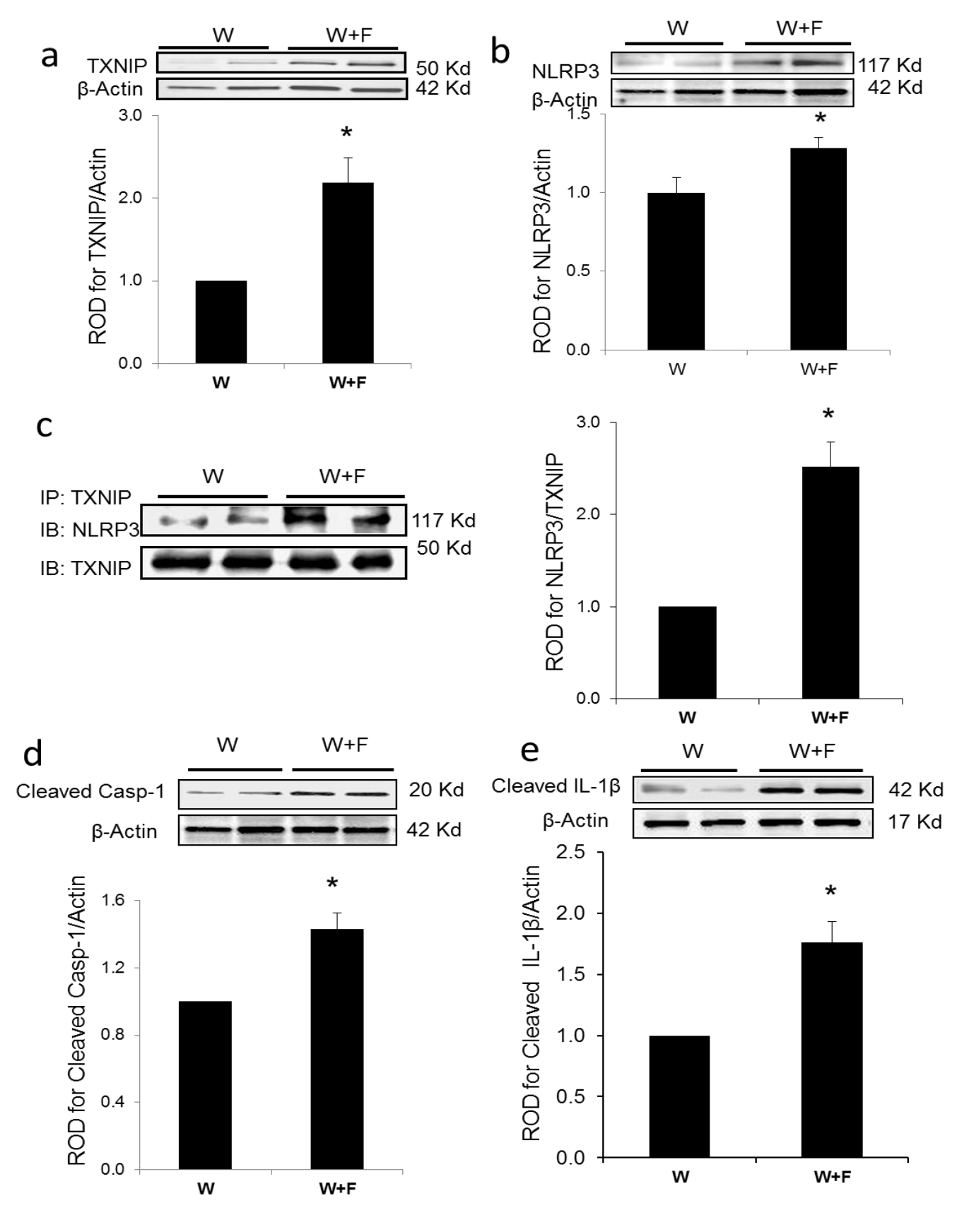


Fig.3.4 HFD induces TXNIP-NLRP3 interaction associated with retinal inflammasome activation. Representative blots and WB analyses of TXNIP (a) and NLRP3 (b) protein expression in wistar rats after 8-weeks of HFD versus W-controls (n=4-5; * P value <0.05). (c) Representative blot and quantification of immunoprecipitation with TXNIP and blotting with NLRP3 showed higher association of TXNIP with NLRP3 (n= 3-4; * P value <0.05), which was associated with increased cleaved casp-1 (e) and cleaved IL-1β expression in W+F compared to control W group. Protein levels were normalized to actin and respective wild-type controls (n= 4; * P value <0.05).

Fig.3.5

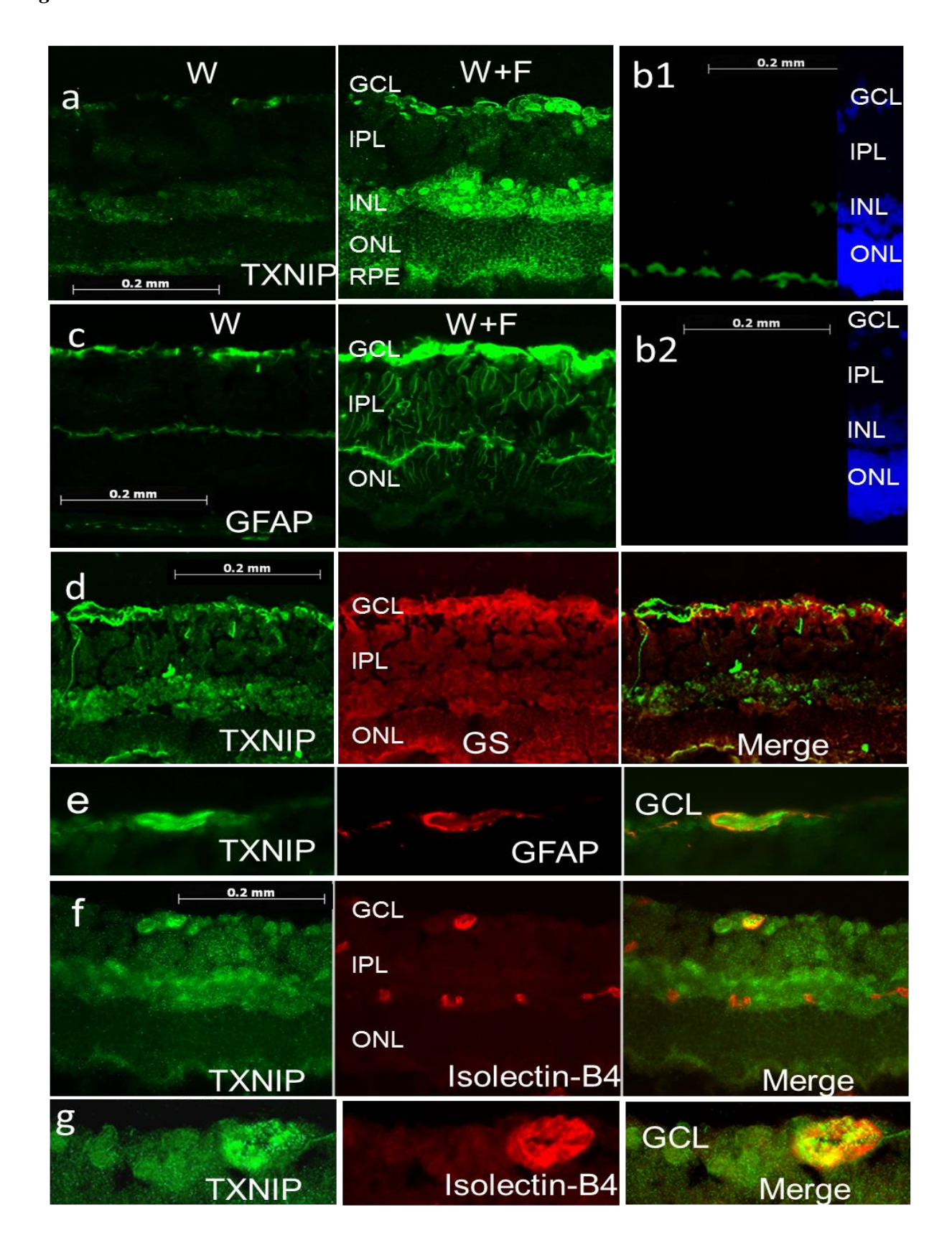
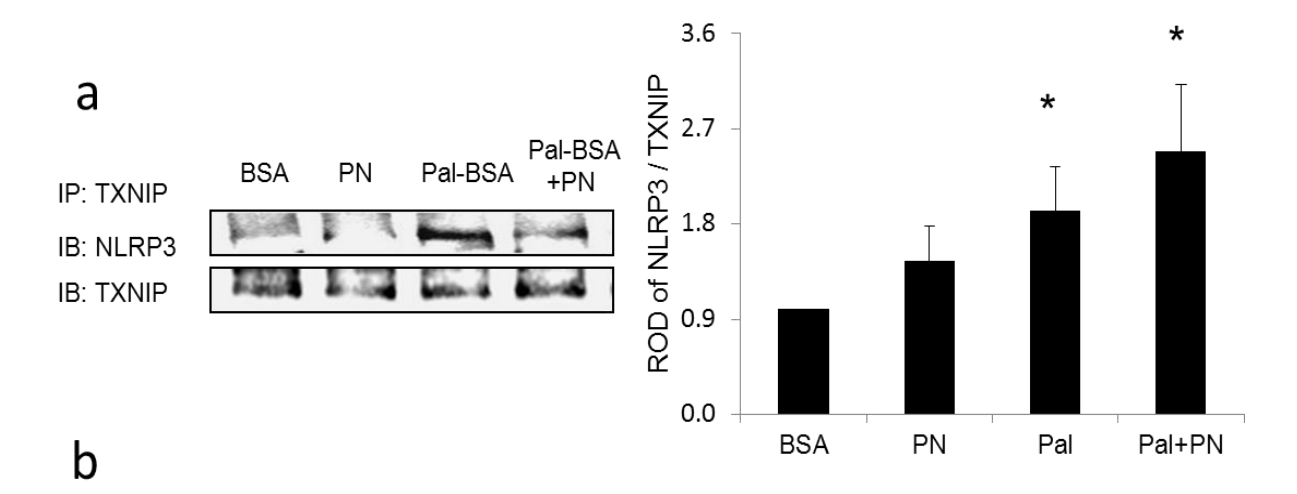
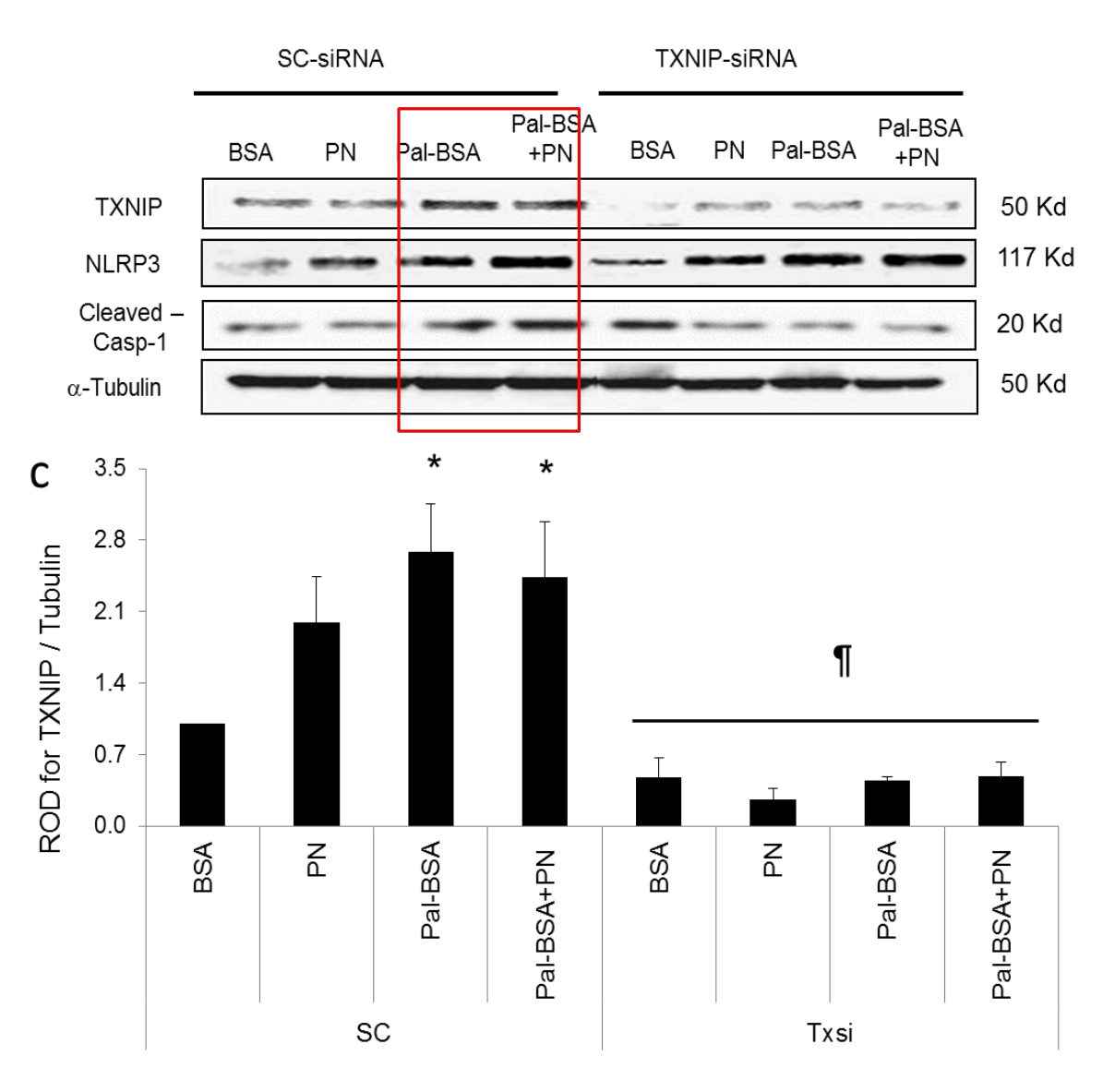
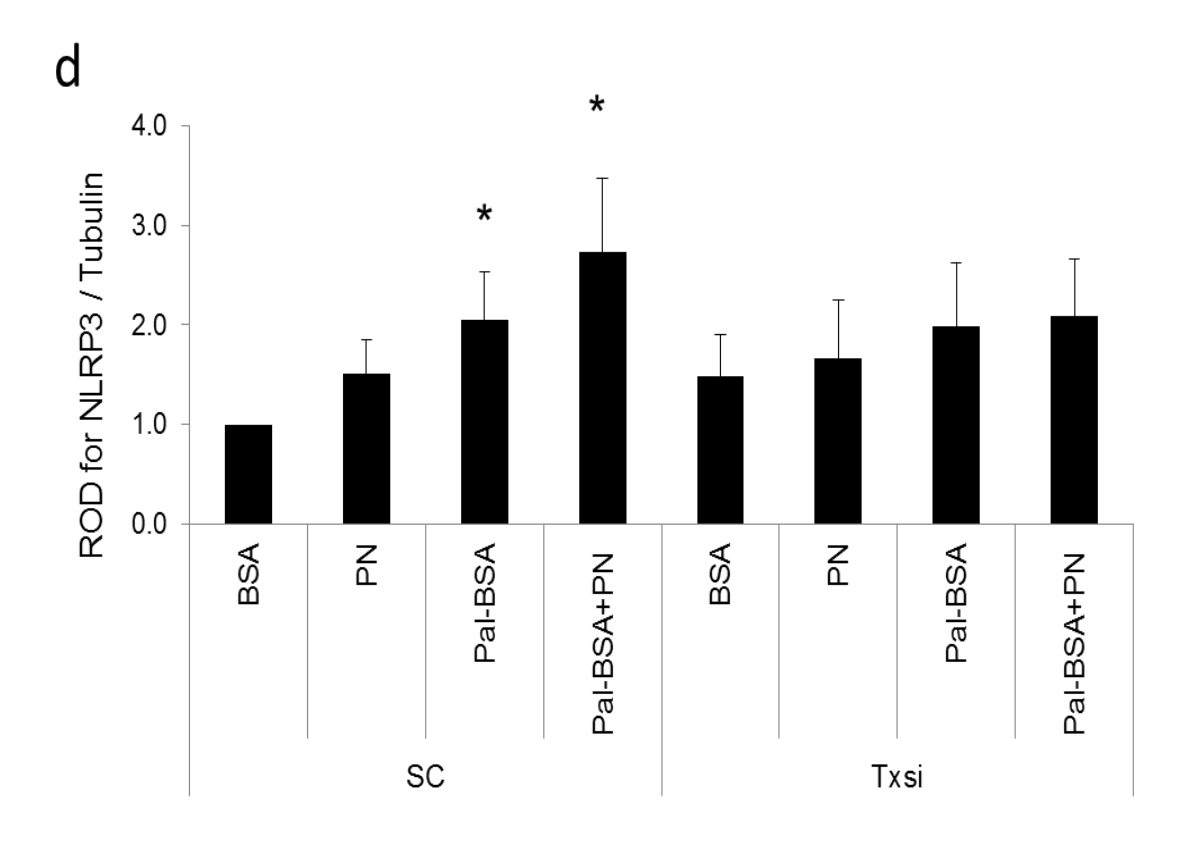


Fig.3.5 HFD-induced TXNIP expression co-localizes within retinal microvasculature. (a) Increased TXNIP expression was observed in ganglion cell layer (GCL), inner nuclear layer (INL), to less extent in retinal pigment epethelium (RPE) in W+F group relative to control W group. (b) Negative controls (b1; normal rabbit serum and b2; no primary antibody) showed specific binding for TXNIP antibody in GCL and INL layers but not in RPE. (c) HFD caused Muller cell activation as evident by increased expresssion of GFAP in W+F group. (d) Colocalization of TXNIP showed minimal association with with glutamine synthase (GS), the specific Muller cell marker. (e) Colocalization of TXNIP with GFAP showed strong association in the GCL layer, suggesting astrocytes and Muller cell endfeet surrounding retinal blood vessels. On the other hand, co-localization of TXNIP expression with isolectin-B4 staining showed higher TXNIP expression within retinal microvasculature in GCL as well as deep retinal capillaries in inner nuclear layer (INL) (f) and enlarged GCL layer (g).

Fig.3.6







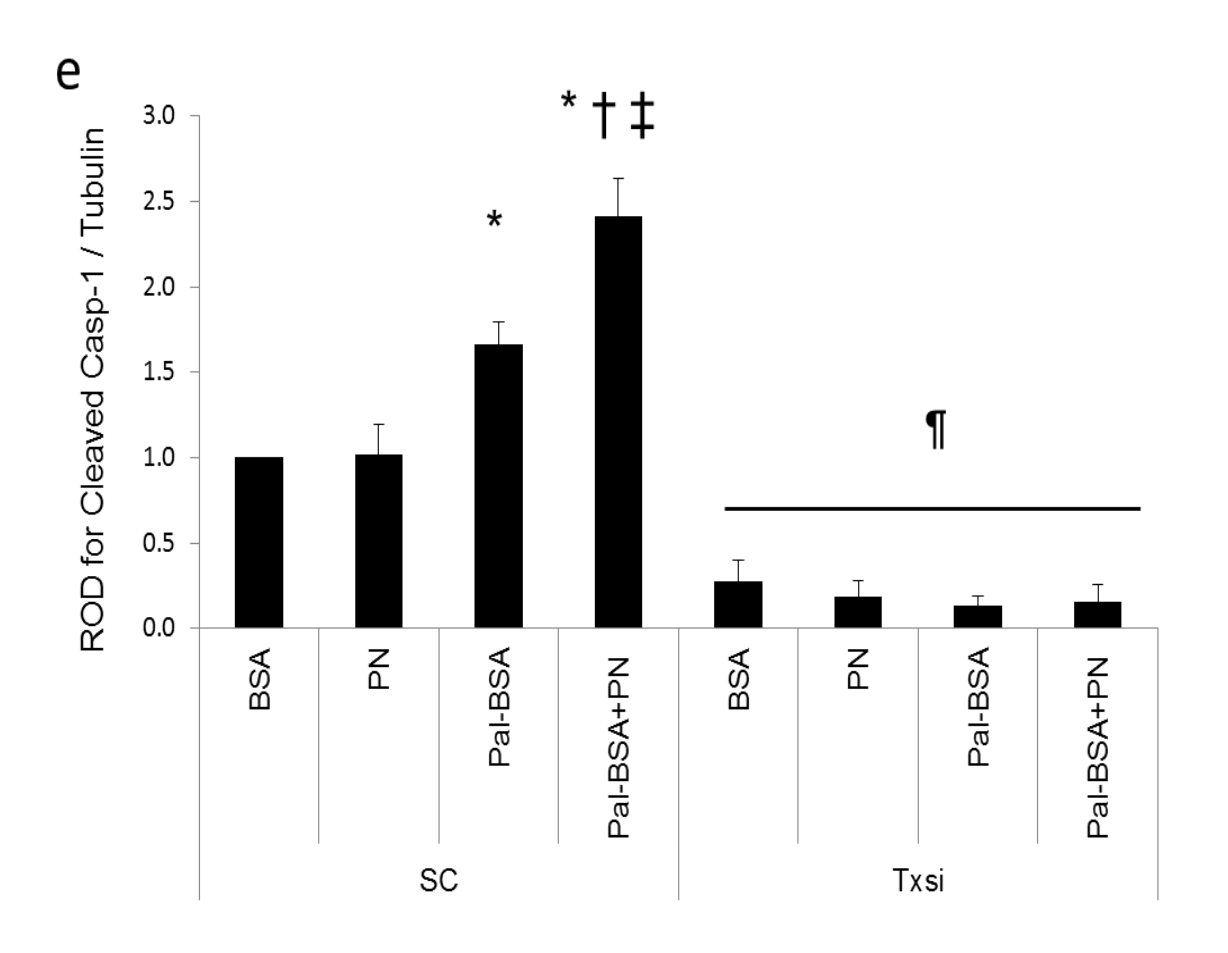


Fig.3.6 TXNIP is required for palmitate-induced NLRP3-inflammasome activation in HRE cells.

(a) Representative blot and quantification of immunoprecipitation with TXNIP and blotting with NLRP3 after incubation with 100μmol/l peroxynitrite (PN) alone, 400 μmol/l palmitate alone (Pal-BSA) or both (Pal-BSA+PN), showed higher association of TXNIP with NLRP3 in Pal-BSA and Pal-BSA+PN treatments only (n= 4; * P value <0.05). Representative blots (b) and WB analysis of TXNIP (c), NLRP3 (d), and cleaved-caspase-1 (e), in HRE cells transfected with either 0.6μmol/l scrambled siRNA (SC group) or TXNIP (Txsi group) after incubation with PN alone, Pal-BSA alone or both (Pal-BSA+PN) in comparison to control BSA in the SC group. TXNIP-knockdown resulted in abrogating Pal-BSA-mediated activation of cleaved casp-1. Two-way ANOVA showed significant interaction between PN and Pal-BSA in the combined Pal-BSA+PN group regarding cleaved caspase-1 expression in the SC group. Protein levels were normalized to tubulin and SC BSA control (n=3-4; * P value <0.05 vs SC BSA, † P value <0.05 vs SC PN-BSA, ‡ P value <0.05 vs SC Pal-BSA and ¶ P value <0.05 vs all SC groups).

Fig.3.7

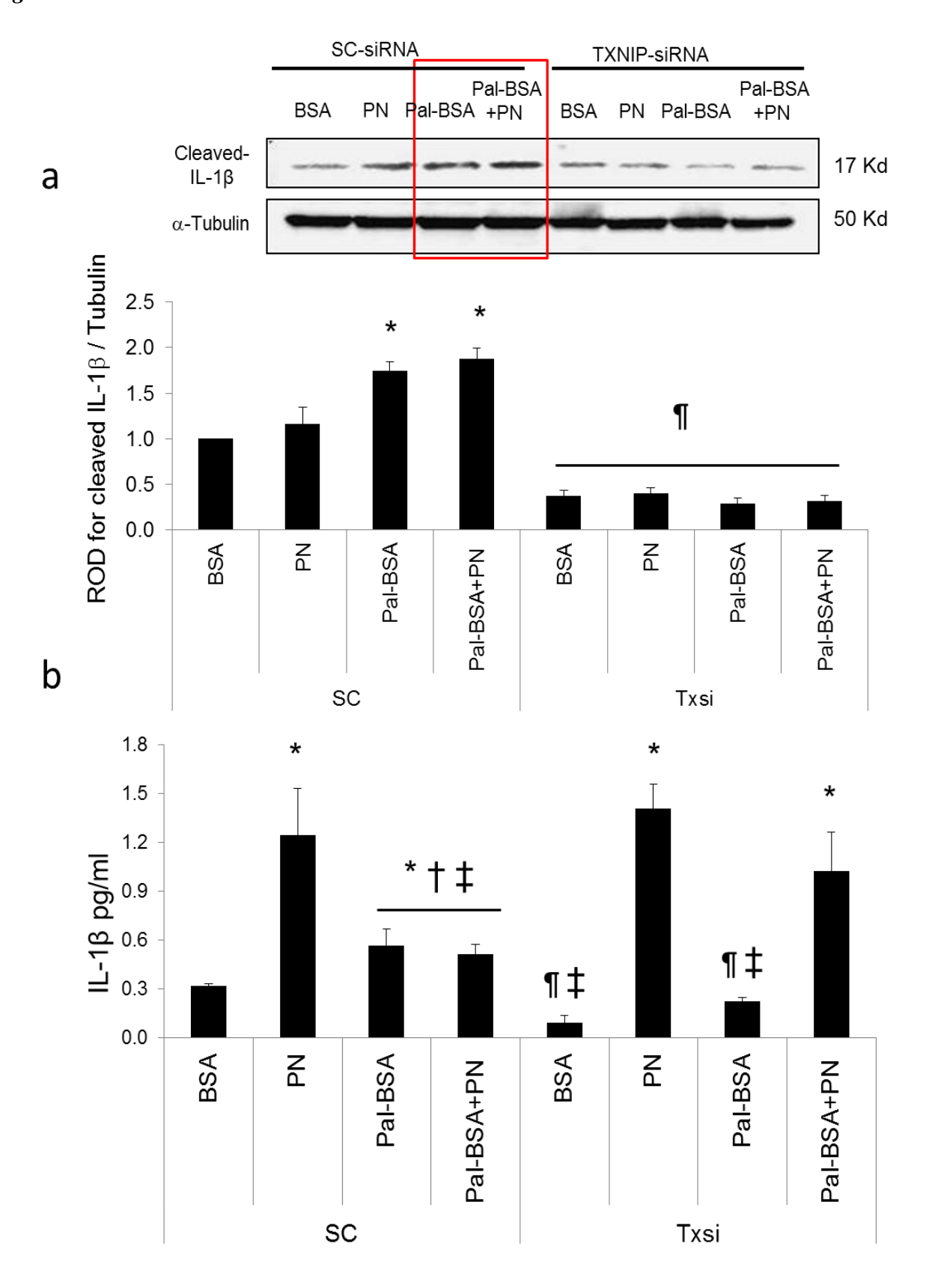


Fig. 3.7 TXNIP is required for palmitate-induced IL-1β maturation in HRE cells. Representative blot and WB analysis of cleaved IL-1β (a) in HRE cells transfected with either 0.6μmol/l scrambled siRNA (SC group) or TXNIP (Txsi group) after incubation with PN alone, Pal-BSA alone or both (Pal-BSA+PN) in comparison to control BSA in the SC group. TXNIP-knockdown resulted in abrogating Pal-BSA-mediated maturation of cleaved IL-1β. Protein levels were normalized to tubulin and SC BSA control (n=3-4; * P value <0.05 vs SC BSA, † P value <0.05 vs SC PN-BSA, ‡ P value <0.05 vs SC Pal-BSA and ¶ P value <0.05 vs all SC groups). (b) IL-1β release into the HRE cell conditioned media was quantified using IL-1β sensitive ELISA kit. (n=3-4; * P value <0.05 vs SC BSA, † P value <0.05 vs SC PN-BSA, ‡ P value <0.05 vs SC Pal-BSA and ¶ P value <0.05 vs SC Pal-BSA and ¶ P value <0.05 vs all SC groups)

Fig.3.8

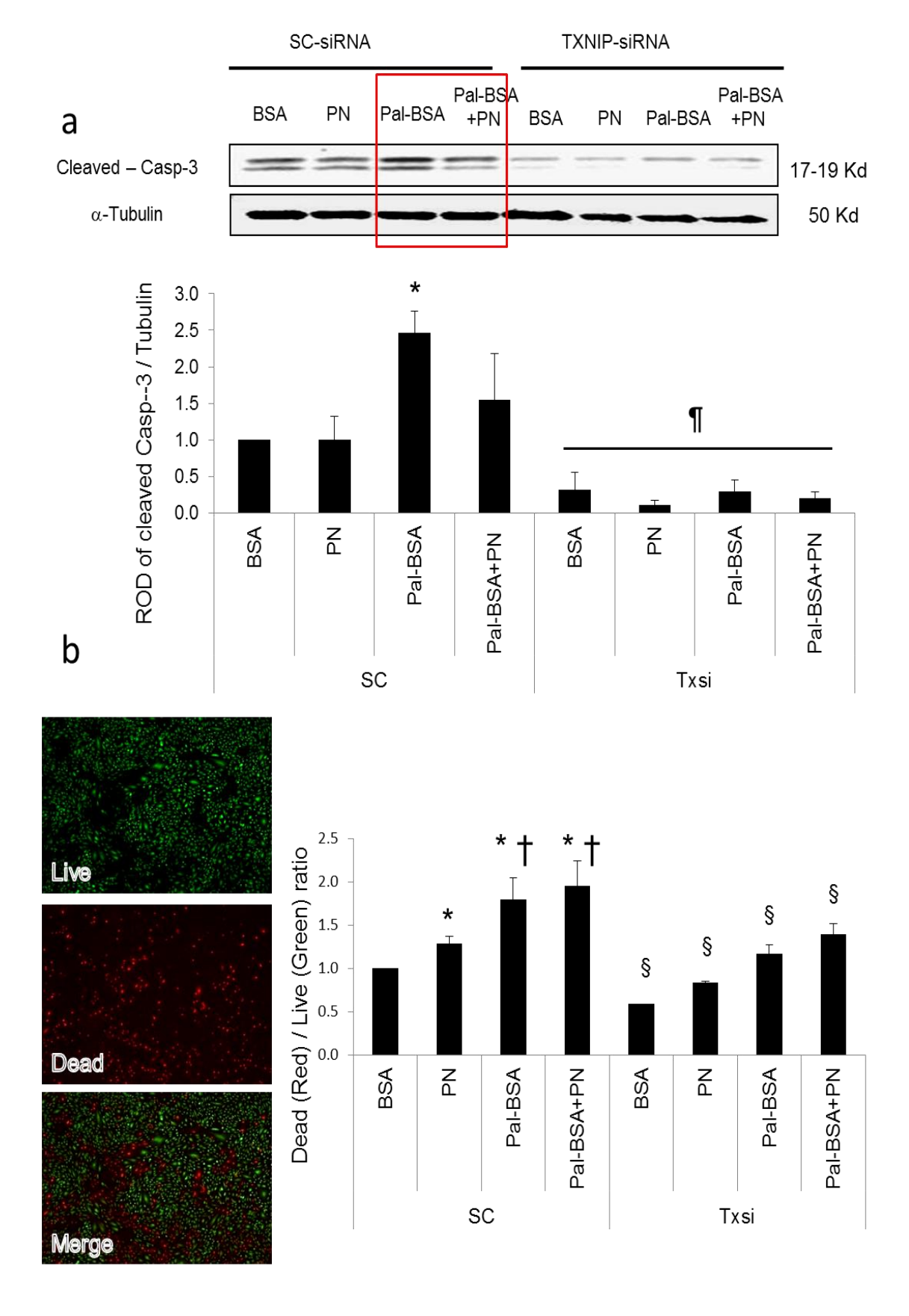
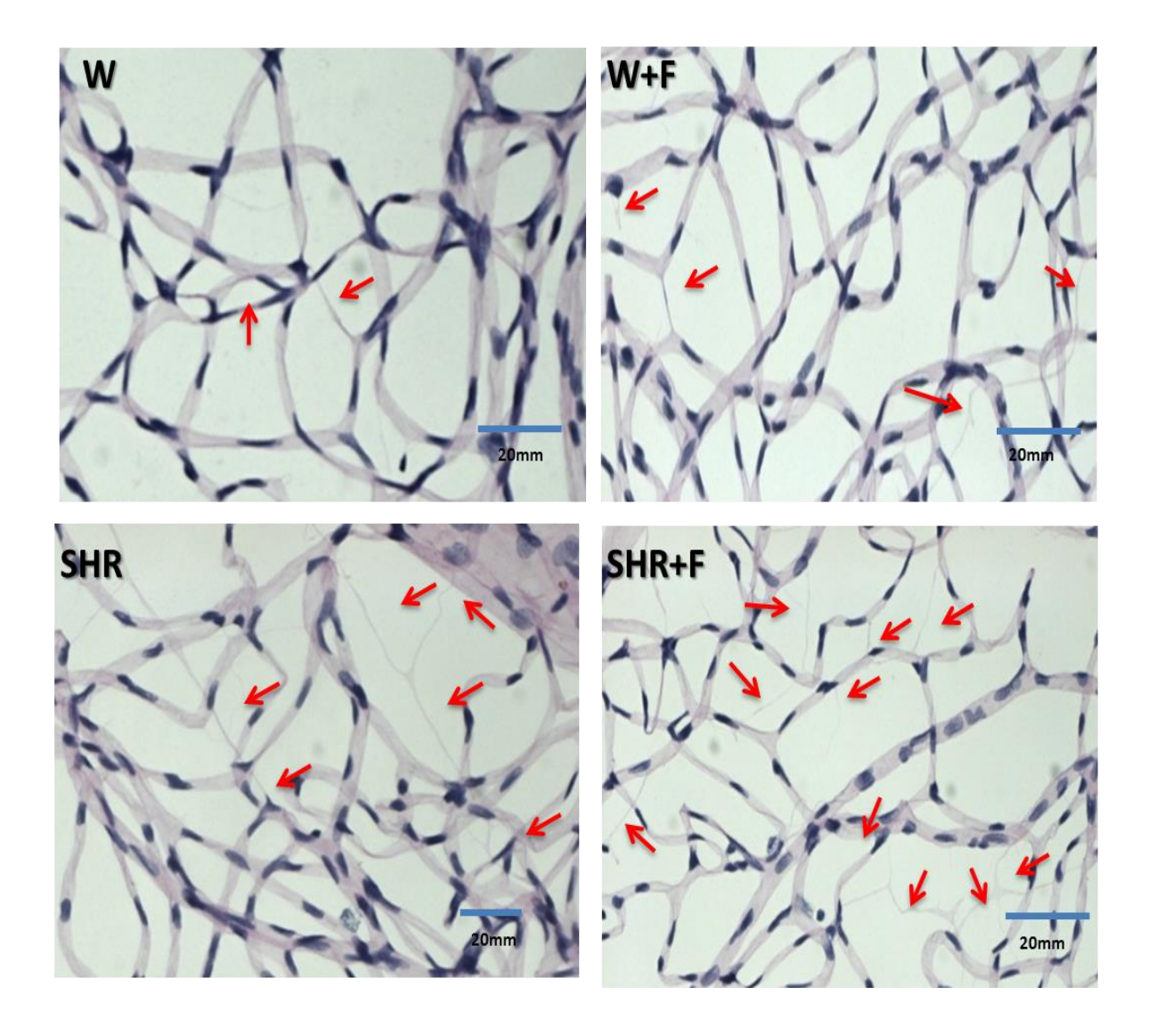


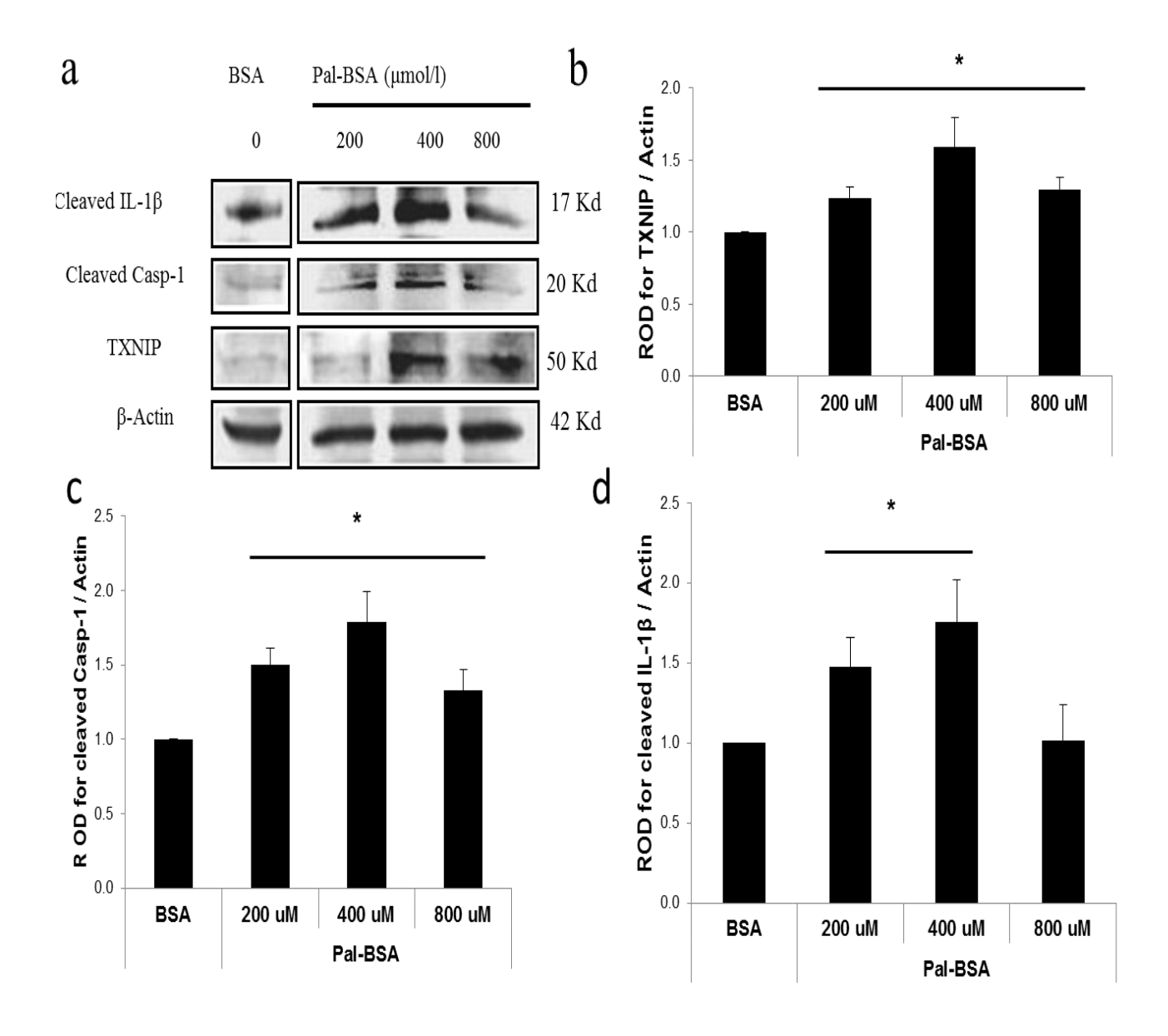
Fig.3.8 TXNIP is required for palmitate-induced apoptosis and cell death in HRE cells. Representative blot and WB analysis of cleaved casp-3 (a) in HRE cells transfected with either 0.6μmol/l scrambled siRNA (SC group) or TXNIP (Txsi group) after incubation with PN alone, Pal-BSA alone or both (Pal-BSA+PN) in comparison to control BSA in the SC group. TXNIP-knockdown resulted in abrogating Pal-BSA-mediated increase in cleaved casp-3 expression. Protein levels were normalized to tubulin and SC BSA control (n=3-4; * P value <0.05 vs SC BSA, † P value <0.05 vs SC PN-BSA, ‡ P value <0.05 vs SC Pal-BSA and ¶ P value <0.05 vs all SC groups). (b) Representative image of HRE cell viability quantified using the ratio of dead cells (stained red) to the live cells (stained green) in both SC and Txsi groups. TXNIP-knockdown resulted in significant decrease in cell death in all Txsi treatment groups compared to their relative SC treatment group. (n=3; * P value <0.05 vs SC BSA, † P value <0.05 vs SC PN and § P value <0.05 vs corresponding SC group).

Supplementary Fig.3.1

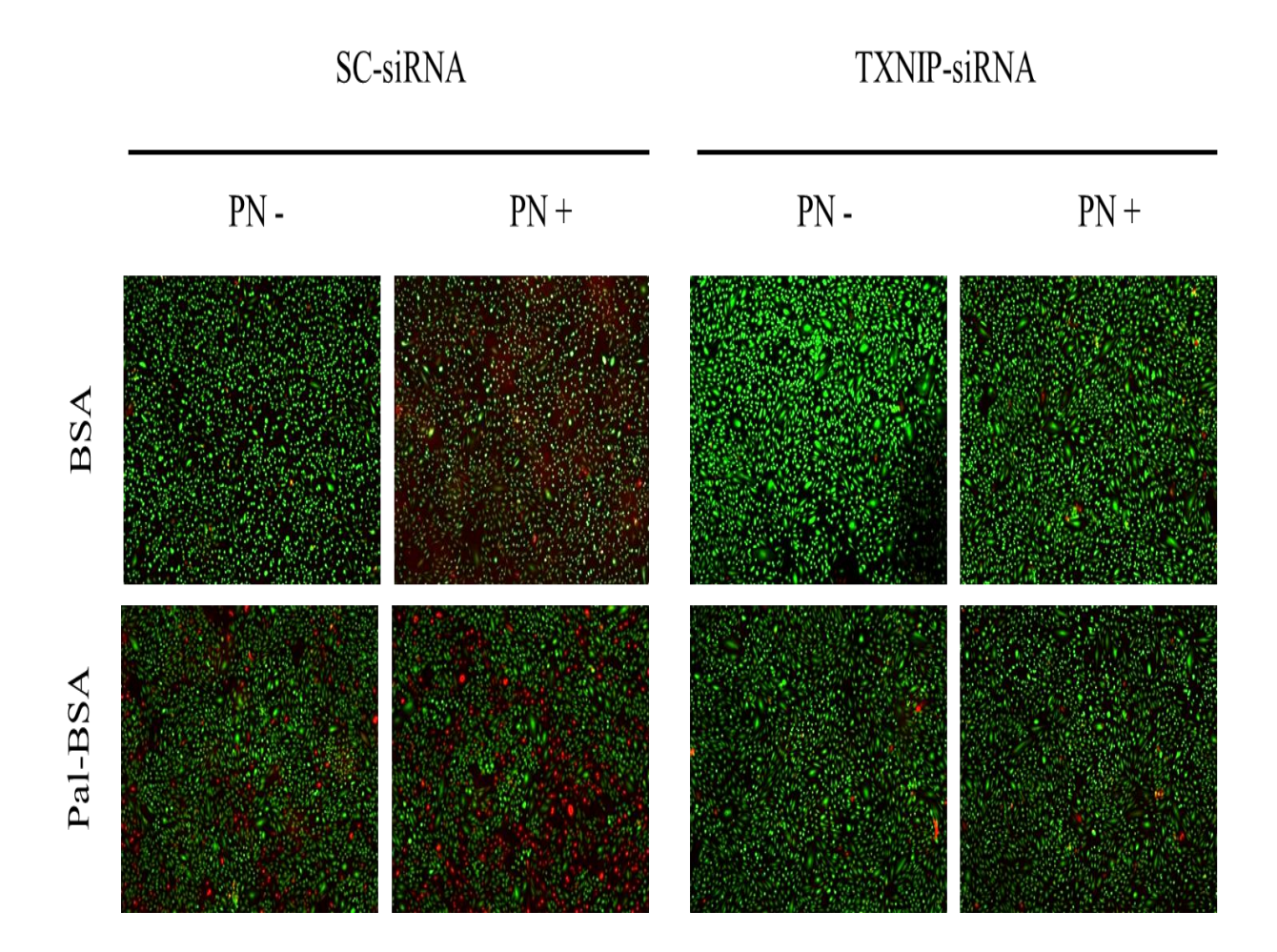


Supplementary Fig.3.1 representative images for number of acellular capillaries (arrows) identified in tryptic-digest of retinas stained with PASH staining as described in Methods. Groups included control wistar rats (W) and spontaneously hypertensive rats (SHR) fed with normal diet or with HFD (W+F) and (SHR+F), respectively, for 10-weeks.

Supplementary Fig.3.2



Supplementary Fig.3.2 Dose-response proinflammatory effects of palmitate in human retinal endothelial (HRE) cells. Representative blots (a) and WB analyses of TXNIP (a), cleaved Caspase-1 (b) and cleaved IL-1 β (c) in HRE cells after incubation with Pal-BSA at 200, 400 and 800 μmol/l concentrations in comparison to control BSA group. (n=6 for cleaved caspase-1 and IL-1 β and n=3 for TXNIP; * P value <0.05 vs BSA-controls).



Supplementary Fig.3.3 Representative images of HRE cell viability transfected with either 0.6μmol/l scrambled siRNA (SC group) or TXNIP (Txsi group) after incubation with PN alone, Pal-BSA alone or both (Pal-BSA+PN).

CHAPTER 4

HIGH FAT DIET-INDUCED OBESITY DRIVES LEUKOSTASIS, BARRIER DYSFUNCTION AND MICROVASCULAR DEGENERATION THROUGH TXNIP-NLRP3 INFLAMMASOME ACTIVATION.¹

¹ Islam N. Mohamed, Megan Bartasis, Modesto Rojas, Ruth Caldwell, Xiaoling Wang, Nader Sheibani, and Azza B. El-Remessy. To be submitted to Circulation Research, 7/15/2014.

4.1 Abstract

Obesity is recently upgraded to a disease state on top of being the fastest growing risk factor for vascular diseases. Our group has recently shown that high fat diet (HFD) induces endothelial NOD-like receptor protein (NLRP3)-inflammasome activation that was associated with enhanced thioredoxin interacting protein (TXNIP). Here, we examine the specific contribution of TXNIP-NLRP3 inflammasome activation and its impact on microvasculature. Age-matched wild-type (WT) and TXNIP knockout (TKO) mice fed with normal diet (ND) were compared to their littermates fed with 60%-HFD for 8-18 weeks. TXNIP was stably overexpressed or silenced in human endothelial cells (EC). After 8-weeks, HFD significantly increased total body weight, insulin resistance and retinal NLRP3 inflammasome activation evidenced by increased NLRP3, cleaved caspase-1 and cleaved IL-1β by 1.6, 2.3 and 2.7 -fold, respectively in WT-HFD compared to WT-ND mice. These coincided with increased retinal adhesion molecule ICAM-1, leukostasis and microvascular permeability by 1.4 and 1.8-fold, respectively at 8-weeks and retinal microvascular degeneration by ~2-fold after 18-weeks in WT-HFD mice compared to WT-ND. Despite equal increases in total body weight, TKO mice were protected against HFD-induced NLRP3-inflammasome activation and the subsequent microvascular injury. In-vitro, silencing TXNIP inhibited palmitate- induced ICAM-1 and PECAM-1 in EC. Overexpression of TXNIP induced NLRP3-inflammasome activation and adhesion molecules, an effect that was mitigated by blocking IL-1\beta effect. Ex-vivo studies showed that peripheral leukocytes isolated from WT-HFD mice or obese subjects are able to induce leukostasis and EC death but not from TKO-HFD. Targeting TXNIP seems a potential therapeutic strategy for obesity-mediated microvascular complications.

4.2 Introduction

Obesity is recently upgraded to a disease state from a mere risk factor for developing dyslipidemia, and insulin resistance, which then culminates into the complex metabolic syndrome disorder and type 2 diabetes. Several population studies have characterized each of these metabolic conditions as an independent risk factor for developing retinopathy and retinal microvascular abnormalities such as focal and generalized retinal arteriolar narrowing, venular dilatation and alteration of the arteriolar wall reflex in the general non diabetic population [1-4] or in addition to type 1 or type 2 diabetes [4]. Systemic low grade inflammation, oxidative stress and its associated endothelial dysfunction/activation has been suggested as the most plausible reasons for such clinical observations [5-7], however, little is known about the exact molecular mechanisms involved in instigating these retinal microvascular insults.

Retinal leukostasis, defined by increased attraction and abnormal adhesion between activated leukocytes and retinal microvasculature as a result of retinal endothelial dysfunction and upregulation of pro-inflammatory cytokines and vascular adhesion molecules, is a well-characterized pathophysiologic landmark in metabolic pro-inflammatory retinal conditions such as diabetic retinopathy [8, 9]. Increased retinal leukostasis can directly result in blood retinal barrier (BRB) breakdown followed by exacerbated loss of retinal endothelial cells and increased formation of non-perfused acellular capillaries on the long term. Such events comprise the foundation for establishing focal retinal ischemia and triggering pathologic retinal neovascularization in advanced stages of the disease [10-12]. On the other hand, sterile inflammation manifested by increased retinal caspase-1 activation and interleukin-1β (IL-1β) levels has been increasingly recognized to have a causative role in initiating and sustaining retinal microvascular dysfunction and degeneration. Clinically, patients with diabetic retinopathy were found to have increased levels of IL-1β in both the aqueous and vitreous humors and

plasma samples versus control subjects, which was directly correlated with the severity and progression from mild non-proliferative into proliferative diabetic retinopathy (PDR) [13-15]. Experimentally, exogenous administration of IL-1 β into the vitreous of healthy non-diabetic wistar rats resulted in massive increases in the number of degenerated retinal acellular capillaries and apoptotic capillary endothelial cells in isolated retinal microvascularture [16, 17]. Nevertheless, there is a gap in knowledge whether retinal leukostasis can also contribute to the early pathological findings in pre-diabetic retinopathy, and whether caspase-1 activation/IL-1 β axis can directly contribute to such early stage detrimental event.

Our group was the first to report the activation of the upstream signaling complex, the NLRP3 (NOD-like receptor protein) inflammasome responsible for the activation of the Caspase-1/IL-1β axis, in retinas of high fat diet (HFD)-fed rats as a model of obesity and prediabetes [18]. NLRP3 inflammasome is one of the most established multi-protein complexes known for instigating obesity-induced inflammation [19, 20]. As a sensor for metabolic danger, activated NLRP3 oligomerizes with the ASC (apoptosis-associated specklike) adaptor protein which recruits procaspase-1, allowing its autocleavage and activation. Activated caspase-1 enzyme in turn cleaves upregulated IL-1β into its active mature form before its release [21]. HFD-induced obesity, hypertension or their combination resulted in accelerated induction of retinal microvascular degeneration, significant increases in retinal oxidative stress, inflammation and increased thioredoxin interacting protein (TXNIP) expression, which co-localized within retinal vasculature and its surrounding macroglial cells (astrocytes and Müller cell endfeet) [18]. TXNIP, is the endogenous inhibitor of the ubiquitous antioxidant defense protein system: thioredoxin, known for its pro-inflammatory, pro-oxidative stress and pro-apoptotic activity [22-24]. Recently, TXNIP has been also found to act as a direct activator for the NLRP3 inflammasome [25-31]. In our study, HFD selectively induced retinal TXNIP-NLRP3 interaction

and inflammasome activation resulting in increased expression of cleaved Caspase-1 and IL-1β. TXNIP-mediated NLRP3-inflammasome activation in human retinal endothelial (HRE) cells was further confirmed in-vitro in response to incubation with saturated fatty acid "palmitate" coupled to bovine serum albumin (Pal-BSA), as one of the most abundant circulating saturated fatty acid in plasma [32], and a direct activator of the NLRP3-inflammasome [33-35]. Therefore, we hypothesized that HFD can induce retinal microvascular degeneration through increased retinal leukostasis and microvascular inflammation and that TXNIP-NLRP3 inflammasome axis plays a direct role in mediating this pathological manifestation.

4.3 Materials and Methods

4.3.1 Animal preparation.

All animal studies were in accordance with the Association for Research in Vision and Ophthalmology (ARVO) and the Georgia Reagents University Animal Care and Use Committee. In order to study both the short and long term effect of high fat diet (HFD) on retinal microvascular inflammation, 5-6 weeks old age and gender matched C57Bl/6J wild type mice (WT) and TXNIP knock out (TKO) mice fed with standard mice chow (normal diet; ND)(WT-ND and TKO-ND) were compared to their littermates fed with high fat diet (HFD, 60% fat: Research diets, Product #D12492) (WT-HFD and TKO-HFD) for both 8-weeks (short term) and 18-weeks (long term). TKO mice were a kind gift from Dr. Lusis AJ, San Diego State University [36] and have been previously studied by our group [37]. In our studies, TKO phenotyping showed that they are similar in weight and activity to WT with no differences in food consumption or litter sizes with normal retinal microvascular development [37]. All mice were weighted weekly and fasting peripheral blood glucose (FPBG) measurement using a small tail tip needle prick and a standard commercially available glucometer (Reli on®, Abott Diabetes care Inc.) throughout the study at 8, 12 and 18-weeks (summarized in Table.4.1). Full metabolic

parameters including assessment of HFD-induced glucose intolerance and plasma levels of total cholesterol and triglycerides were performed after 8-weeks of HFD as detailed in each section below.

4.3.2 Intra-peritoneal glucose tolerance test (IPGTT).

As previously reported [38, 39], all animal groups were fasted overnight except from water. In the next morning, FPBG levels were recorded as the baseline and then all groups were challenged with a bolus intra-peritoneal injection of an equal dose of 2 grams of glucose/kg mouse body weight. After which, PBG levels was followed using a small tail tip needle prick and a standard commercially available glucometer (Reli on®, Abott Diabetes care Inc.) at 20, 40, 60, 90 and 120 minutes after the glucose dose injection. Analysis of the area under the curve (AUC) was performed using NCSS software (NCSS, LLC, Utah, USA) and used to assess the differences in PBG response across all groups (Fig.4.1 b&d).

4.3.3 Determination of plasma total cholesterol levels.

Plasma total cholesterol levels of all animal groups were determined using a commercially available Cholesterol/Cholesteryl Ester Quantitation Colorimetric Kit (Biovision, Catalog # K613-100) according to the manufacture protocol. In brief, 20µl plasma samples were diluted into 50µl total using assay buffer. An equal volume of the reaction mix containing Cholesterol Enzyme Mix, Cholesterol Esterase enzyme and Cholesterol Probe dissolved in assay buffer were added per well and incubated for 60 minutes at 37°C and then color absorbance was measured at 570 nm. Plasma total cholesterol concentrations were expressed in mg/dl.

4.3.4 Determination of plasma triglycerides levels.

Plasma triglycerides (TGs) levels of all animal groups were determined using a commercially available Triglyceride Quantification Colorimetric Kit (Biovision, Catalog

#K622-100) according to the manufacture protocol. In brief, 20μl plasma samples were diluted into 50μl total using assay buffer. 2μl of lipase enzyme was added to each standard and sample well and incubated for 20 min at room temperature to convert plasma triglycerides to glycerol and fatty acid. An equal volume of the reaction mix containing Triglyceride Probe and Triglyceride enzyme mix dissolved in assay buffer were added per well and incubated for 60 minutes at room temperature and then color absorbance was measured at 570 nm. Plasma total cholesterol concentrations were expressed in mMole/liter.

4.3.5 Western blot analysis.

Retinas were lysed in modified RIPA buffer (Millipore, Billerica, MA) and 30μg of total protein were separated by SDS-PAGE. Antibodies used were: anti-TXNIP (Invitrogen, Carlsbad, CA), anti-NLRP-3 (LifeSpan Biosciences, Inc, Seatle, WA), anti-Caspase-1, anti-ICAM-1, anti-PECAM-1 and anti PARP (cell signaling, Danvers, MA) and anti-IL-1β and Anti-TNF-α (Abcam, Cambridge, MA). Band intensities were quantified using (Alpa Innotech) imaging and densitometry software and expressed as relative optical density (ROD).

4.3.6 Determination of blood—retina barrier function.

Integrity of the BRB was measured as described by our group [40]. Mice received jugular vein injections of 10 mg/kg BSA-conjugated fluorescein (Invitrogen, Grand Island, NY, USA). After 20 min, animals were killed and blood and retinas collected. Retinas were homogenized in RIPA-buffer to detect the fluorescence of retinal lysates using a fluorescent plate reader (BioTek Synergy2, Winooski, VT, USA) (excitation 370 nm, emission 460 nm). Retina fluorescence was then normalized to that of serum.

4.3.7 Leukostasis.

Leukostasis was assessed by Concanavalin A labeling and quantitation of adherent leukocytes using the method first described by Joussen et al. [41] and our group [42]. Briefly, mice were

transcardially perfused with 10 mL of phosphate-buffered saline (PBS) to wash out non-adherent blood cells, followed by perfusion with 10 mL fluorescent isothiocyanate (FITC)—labeled concanavalin A (Con A) lectin (40 µg/mL in PBS, pH 7.4; Vector Laboratories, Burlingame, CA) to label the adherent leukocytes and vascular endothelial cells. Residual unbound Con A was removed by perfusion with PBS. The eyes were removed, fixed with 4% paraformaldehyde overnight and retinal flat mounts were prepared. The flat mounts were imaged using a fluorescence microscope and adherent leukocytes were counted. The Con A positive blood cells were identified as leukocytes based on their size (7 – 20 µm diameter), morphology (round or oval shape) and intraluminal position (as verified by focusing through the vessel).

4.3.8 Mice leukocyte isolation and labeling.

Circulating total peripheral blood mononucalear cells (PBMCs) were isolated by density gradient centrifugation method using Ficoll-Paque technique (according to manufacturer protocol) from all animal groups after 18-weeks of ND or HFD. Briefly, 40µl of 2% sodium citrate at pH 7.2 was first injected into the left ventricle of deeply anesthetized mice and left to circulate for 1 minute, then 0.5-1mL of whole blood was drawn via cardiac puncture using a 21 gauge syringe containing 40µl of 4% sodium citrate at pH 7.2. Within 2 hours, all blood samples were the diluted into a total volume of 1.5 ml using sterile PBS and laid carefully on top of 1.125ml (a ratio of 3:4) of Ficoll-Paque PREMIUM 1.084 (Product code:17-5446-02, GE Healthcare life sciences, Pittsburgh PA) in a 4ml sterile culture tube and centrifuged at 300g for 30 minutes at room temperature with no brakes used. PBMCs layer was carefully aspirated and Isolated PBMCs were washed twice in 2ml volume of Gibco® RPMI 1640 medium (life technologies, Gand Island NY) and then frozen in freezing medium (90% endotoxin free fetal bovine serum albumin in DMSO) at a density of 0.5-1 million cells/ml.

4.3.9 Human leukocyte isolation.

Human PBMNCs from both obese and lean subjects were obtained from Dr. Xiaolin Wang, at the Georgia Prevention Institute (GPI). Patients were consented and samples were collected according to an IRB protocol approved at the Georgia Regents University. Subjects 15-20 year old who were obese and glucose intolerant but had no signs of diabetes, significant hyperglycemia or hypertension and clinically diagnosed as "Prediabetic". Physical and metabolic parameters of both lean and obese subjects enrolled are summarized in Table 4.2.

4.3.10 Ex-vivo co-culture studies of EC and determination of leukostasis.

Immortalized mouse retinal endothelial cells (mREC) [43] were grown in control medium (DMEM with 5 mM glucose) containing 10% serum. Media was changed every other day for 4 days. When mREC reached 80% confluence (500,000 cells) in 24-well plates they were first switched to serum-free medium for 6-hours. Isolated PBMCs were then labeled first with fluorescent cell tracker (CellTracker CM-DiI, Life technologies; 5µg/ml in RPMI culture medium) and immediately co-cultured with mREC and incubated for either 2 hours for assessment of leukostasis or 24 additional hours for assessment of mREC cell death. Cell death of the retinal endothelial cells was measured by Terminal deoxynucleotidyl transferase dUTP nick end labeling (TUNEL) assay kit (ApopTag® Fluorescein Direct In Situ Apoptosis Detection Kit, Catalogue # S7160, Millipore, Bellirica, MA) according to the manufacturer protocol. Same experimental protocol was used for experiments that utilized Human retinal endothelial cells (EC) and isolated Human PBMCs.

4.3.11 Determination of retinal acellular (degenerated) capillaries.

Retinal vasculatures were isolated as described previously [44]. Transparent vasculature were laid out on slides and stained with periodic acid-Schiff and hematoxylin. Acellular capillaries were identified as capillary-sized blood vessel tubes having no nuclei anywhere along

their length. The number of acellular capillaries were averaged from 8 different fields of the midretinal area and calculated as the average number/mm² of retinal area using AxioObserver.Z1 Microscope (Zeiss, Germany).

4.3.12 Vascular morphology analyses.

All animal groups after 18-weeks of ND or HFD were systemically perfused with (FITC)–labeled concanavalin A (Con A) lectin (40 µg/mL in PBS, pH 7.4; Vector Laboratories, Burlingame, CA) using the same protocol used for the leukostasis experiments to label all retinal microvasculature. The eyes were removed, fixed with 4% paraformaldehyde overnight and retinal flat mounts were prepared. A series of Z-stack (ZS) images (5-6 slices, 18-20µm thickness) were taken in 3-4 different fields in the mid-retinal area spanning all three layers of retinal vasculature (innermost, intermediate and deep capillary plexus) using AxioObserver.Z1 Microscope (Zeiss, Germany). ZS images were then compressed into one plane using FIJI software with maximum intensity projection, transformed into a binary (black and white mode) and skeletonized (SKTN) for comparison between groups.

4.3.13 Human endothelial cell (EC) culture studies.

EC and supplies were purchased from Cell Systems Corporations (Kirkland, WA) and VEC Technology as described previously [37]. Sodium palmitate (Sigma, Cat# P9767) was dissolved in 50% ethyl alcohol solution, then added drop-wise to pre-heated 10% endotoxin- and fatty acid-free bovine serum albumin (BSA, Sigma, Cat#A8806) in M199 at 50°C to create an intermediate stock solution of palmitate coupled to BSA (Pal-BSA). Confluent cells were switched to serum-free medium for 6-hours then treated with Pal-BSA solutions in a ratio of 1:10 to produce final concentrations of 400 μmol/l of Pal-BSA for 12 hours. Equal volumes of 50% ethyl alcohol solution without any palmitate dissolved in BSA served as a control (BSA-alone).

4.3.14 Silencing TXNIP expression.

Transfection of ECs with 0.6 µmol/1 *TXNIP* siRNA was performed using Amaxa nucleofector primary endothelial cells kit (Lonza, Germany) as described previously [37]. 80%-confluent ECs were incubated in the conditioned transfection medium with 300ng of FITC-labeled scrambled (SC) or *TXNIP* siRNA (Txsi) for 6-hours, then left to recover in complete medium for 24hours before performing experiments. Transfection efficiency was 70-80%, for both methods as indicated by the number of cells expressing *GFP* or FITC-labeled scrambled (SC) siRNA (data not shown). Silencing *TXNIP* expression was verified by Western blot analysis as previously shown by our group [18].

4.3.15 TXNIP overexpression.

Overexpression of TXNIP in human EC cultures isolated was performed as described previously [37] using Amaxa nucleofector and a kit for primary endothelial cells according to the manufacture protocol (Lonza, Germany). Optimization experiments that were performed showed that T005 program and 300ng of commercially available GFP-tagged open reading frame cDNA clone of Homo sapiens-TXNIP (Origene, Rockville, MD) gave the maximum transfection efficacy. Transfection efficiency was between 85 to 90% as indicated by number of GFP expressing cells and Western blots for TXNIP expression showed a 2.5-fold increase in expression (Supplementary Fig.4.1). Cells suspended in a nucleofection mixture with the TXNIP plasmid (TXNIP⁺⁺) and pmaxGFP (empty vector-GFP; EV-GFP) were zapped and left in complete medium for 24 hours to recover before treatment with Interleukin-1 receptor antagonist (IL-1RA; 100 ng/ml, R&D Systems) in indicated groups for additional 24 hours.

4.3.16 Statistical analysis.

Results were expressed as mean \pm SEM. Statistical analyses was performed using NCSS software (NCSS, LLC, Utah, USA) and three-way analysis of variance (a 2X2X2 ANOVA)

followed by Bonferroni Multiple comparison test for testing for differences among all experimental groups and for any interaction between the type of diet (HFD versus normal diet), genotype (WT versus TKO mice) and gender (Males versus Females) for all in-vivo experiments. Of note, three-way analyses indicated no differences in response or interaction between males and females for all experiments performed, and hence data from both males and females within each experimental group were pooled together. Same statistical analyses were also applied for all other animal experiments including the in-vitro leukostasis experiments utilizing isolated PBMCs from all animal groups. Two-way ANOVA followed by Bonferroni Multiple comparison test was used to test the interaction between the presence and absence of Pal-BSA across silencing TXNIP expression and between IL-1RA treatment and TXNIP overexpression. Two-sided student's t-test was used for testing differences between obese and lean human subject groups and for the in-vitro leukostasis experiments utilizing isolated PBMCs from both groups. Significance was defined as P < 0.05.

4.4 Results

4.4.1 HFD results in weight gain, impaired glucose tolerance and dyslipidemia in both WT and TKO mice.

As depicted in (Fig.4.1a.), 8-weeks of HFD resulted in significant comparable increases in total body weight, as a marker for obesity, in both WT-HFD and TKO-HFD animal groups, compared to their normal diet control groups (WT-ND and WT-HFD). However, the TKO-HFD group was relatively more protected against HFD-induced impaired glucose tolerance in the WT-HFD group, indicated by their lower peripheral blood glucose levels in the IPGTT, a standard test for assessing glucose intolerance (Fig.4.1.a). AUC analysis for IPGTT indicated that HFD resulted in a 1.5-fold change in peripheral blood glucose response in WT-HFD group, versus 0.7-fold and no change in both TKO-ND and TKO-HFD groups, compared to WT-ND group

(Fig.4.1c). HFD also resulted in inducing dyslipidemia in both WT-HFD and TKO-HFD groups indicated by increased plasma total cholesterol (Fig. 4.1d) and triglyceride levels (Fig.4.1e) by 1.5 and 1.7-fold for total cholesterol and 2.3- and 2.6-fold for triglycerides, respectively, compared to WT-ND. TKO-ND group showed no change in plasma total cholesterol levels, but higher basal levels of triglycerides by 2-fold compared to WT-ND. Of note, fasting peripheral blood glucose (FPBG) levels were either insignificantly different or slightly higher in the WT-HFD compared to WT-ND group throughout the whole study (summarized in Table.4.1), whereas, TKO-ND and TKO-HFD groups had persistently lower FPBG levels compared to WT-ND group. These results indicate that in our model, HFD resulted only in inducing insulin resistance and pre-diabetes in WT-HFD mice, without progressing into severely higher FPBG levels or frank type 2 diabetes, whereas, TKO-HFD mice were relatively protected to a greater extent against the HFD pre-diabetic and insulin resistant effect, due to their higher basal insulin sensitivity. Our findings are in line with previously published reports that TKO-mice are inherently more insulin sensitive and have higher basal levels of plasma triglycerides [36] and that, TXNIP deletion preserves insulin sensitivity without affecting obesity or weight gain in both HFD diet-induced and genetic obesity models [44, 45].

4.4.2 Deletion of TXNIP abrogates HFD-induced NLRP3-inflammasome activation in the retina.

As shown in Fig.4.2, HFD induced retinal NLRP3-inflammasome activation in WT group, evidenced by increased expression of the receptor; NLRP3, the downstream active effector enzyme; cleaved Caspase-1 and active cleaved IL-1β by 1.7, 2.3 and 2.4-fold, respectively compared to WT-ND. In contrast, TKO-ND and TKO-HFD groups showed either no change in both NLRP3 and cleaved IL-β expression and significantly lower levels of cleaved caspase-1 levels by 0.5 and 0.3-fold, respectively, relative to WT-ND group.

4.4.3 Overexpression of TXNIP activates NLRP3-inflammasome in human ECs.

In order to demonstrate the direct causal relationship between TXNIP and EC-mediated NLRP3 inflammasome activation, stable overexpression of TXNIP was achieved using human plasmid (TXNIP⁺⁺) in ECs treated with or without IL-1 β receptor antagonist. As shown in (Fig. 4.3), TXNIP overexpression in ECs (TXNIP⁺⁺) induced the activation of the NLRP3 inflammasome, evidenced by the upregulation of NLRP3, cleaved caspase-1 and cleaved IL-1 β expression by 2.5, 3 and 2.5-fold respectively, compared to the empty vector tagged with GFP (EV-GFP) control group. In parallel, the expression of TNF α , another potent pro-inflammatory cytokine was also higher by 1.8-fold receptively in TXNIP⁺⁺ compared to the EV-GFP control group. Treatment of TXNIP-overexpressing ECs with 100ng/ml of IL-1RA (TXNIP⁺⁺ + IL-1RA) was able to suppress the effect of TXNIP overexpression on inflammasome activation and TNF α expression, highlighting an essential role of IL-1 β in mediating endothelial inflammation in an autocrine fashion.

4.4.4 Deletion of TXNIP prevents HFD-induced retinal microvascular inflammation and leukostasis.

Increased retinal leukostasis is positively correlated with expression of adhesion molecules in dysfunctional endothelium and can result in vascular injury in the diabetic retina [10, 11]. Nevertheless, the impact of HFD on retinal vascular injury remains unexplored. As shown in Fig. 4.4a-b, HFD resulted in increased levels of retinal intercellular adhesion molule-1 (ICAM-1) expression by 1.6-fold in WT-HFD group compared to WT-ND group, whereas the TKO mice groups showed no change in response to HFD. In parallel, HFD also induced a significant increase in the number of adherent leukocytes per retina in the WT-HFD group by 1.5-fold but had no significant effect on the TKO-HFD group relative to the WT-ND group (Fig. 4.4c). These results highlight the effect of HFD on inducing retinal microvascular inflammation

and leukostasis in WT mice, and the protective effect of TXNIP deletion against HFD in TKO mice.

4.4.5 Silencing TXNIP or blocking IL-1 β receptor prevents adhesion molecule expression in human ECs.

We have recently published that TXNIP is required for palmitate-induced NLRP3inflammasome activation in ECs [18]. Hence, we tested the hypothesis that TXNIP is also required for palmitate-induced adhesion molecule expression in ECs under the same conditions. As shown in Fig. 4.5a, incubating ECs with 400µmol/l Pal-BSA (Pal-BSA) resulted in significant increases in ICAM-1 and platelet endothelial cell adhesion molecule (PECAM-1) by 1.7 and 1.4-fold for PAL-BSA, respectively, relative to BSA-controls in the scrambled-siRNA group (Fig. 4.5a-c). Silencing TXNIP expression using siRNA abolished such responses. In order to test the direct causal relationship between TXNIP-mediated NLRP3 inflammasome activation axis and induction of adhesion molecule expression in ECs, we tested the hypothesis that blocking the IL-1 β effect using IL-1 β receptor antagonist (IL-1RA), would overcome the effect of TXNIP overexpression in ECs. TXNIP overexpression induced expression of adhesion molecules; ICAM-1 and PECAM-1 by 1.9 and 1.8-fold respectively compared to the EV-GFP control group (Fig.4.5d-f). Treatment of TXNIP-overexpressing ECs with 100ng/ml of IL-1RA (TXNIP⁺⁺ + IL-1RA) was able to suppress the effect of TXNIP overexpression on ICAM-1 and PECAM-1 expression, highlighting an essential role of IL-1β in mediating endothelial inflammation and adhesion molecule upregulation in an autocrine fashion.

4.4.6 Deletion of TXNIP in leukocytes prevents leukostasis and endothelial cell death.

The above results were generated from global TKO mice. In order to dissect the role of leukocyte-TXNIP in retinal leukostasis, peripheral blood mononuclear cells (PBMNCs) were isolated from all animal groups and incubated with immortalized mouse retinal endothelial

(MRE) cells in culture for both 2-hours for an in-vitro leukostasis and or 24 hours cell death assessment assay, respectively. Isolated PBMCs from WT-HFD group showed 2-fold increase in number of adherent labeled PBMCs compared to WT-ND (Fig.4.6a) as well 1.8-fold in EC death evident by TUNEL positive nuclei compared to the WT-ND control group (Fig. 4.6b&e). Whereas, both TKO-ND and TKO-HFD groups showed no significant changes versus WT-ND control group.

4.4.7 Activated leukocytes from obese non-diabetic subjects mediate EC death in culture.

PBMCs were also isolated from both obese non-diabetic (OB) and control lean healthy subjects (LN) and were incubated with ECs in culture for both 2-hours or 24 hours for a similar in-vitro leukostasis and cell death assessment assay, respectively. Similar to the animal model results, PBMCs from OB subjects showed increased numbers of adherent labeled PBMNCs and TUNEL positive nuclei after 2-and 24 hours by 1.6 and 1.4 -fold, respectively, compared to the LN control group.

4.4.8 HFD induces retinal BRB breakdown and microvascular degeneration via TXNIP.

We next evaluated the effects of HFD on inducing retinal vascular injury assessed by BRB function after 8-weeks and microvascular degeneration after 18-weeks of HFD. As shown in Fig.4.7a., HFD induced BRB breakdown assessed by 2.4-fold extravasation of BSA-Fluorescence into the retina tissue; whereas, both TKO-ND and TKO-HFD groups had lower levels of BSA-Fluorescence extravasation by 0.5 and 0.75 -fold respectively, relative to the WT-ND group (Fig.4.7a). We next examined the effect of HFD on retinal cell death and development of degenerate acellular capillaries, a hall mark of retinal ischemia in trypsin digests after 18-weeks. HFD resulted in upregulation of the pro-apoptotic protein PARP expression by 1.4-fold in WT-HFD group versus WT-ND control group, whereas TKO-ND was significantly less by 0.7-fold and TKO-HFD group showed no change. Similarly, cleaved PARP expression has a

trend towards significance (P-value=0.09) in WT-HFD group compared to WT-ND control group and Both TKO groups showed no significant differences (Fig.4.7b&c). In addition, HFD also resulted in a 1.5-fold increase in acellular capillary formation in WT-HFD compared to WT-ND, whereas, both TKO-ND and TKO-HFD groups showed significantly lower counts of acellular capillaries by 0.7 and 0.6 -fold, respectively (Fig.4.7d&e).

4.4.9 HFD induces retinal microvascular changes in WT but not in TKO mice.

Furthermore, in parallel to the increase in retinal capillaries drop out in WT-HFD mice that was reversed in TKO mice, we have also observed that WT mice tend to have decreased branching density in response to HFD versus WT-ND control group. Whereas, TKO mice had comparable levels compared to WT-ND that did not change in response to HFD (Fig.4.8). Together, these results highlight the effect of HFD on inducing retinal microvascular inflammation, leukostasis and increased microvascular permeability on the short term, which can be manifested into increased total retinal cell death, microvascular degeneration and morphological changes in WT mice on the long term and the protective effect of TXNIP deletion against HFD in TKO mice.

4.5 Discussion

Clinical and experimental evidence signifies sterile inflammation characterized by upregulation of the caspase-1 activation/IL-β axis and increased retinal leukostasis as two major components in the pathophysiology of diabetic retinopathy [8, 9], [13-17]. Therefore, in this study, we attempted to decipher the underlying molecular mechanisms governing the interaction between these two detrimental events. Such information can provide insight whether this interaction can contribute to the early pathological manifestation of pre-diabetic retinopathy and retinal microvascular abnormalities observed in patients with obesity and metabolic syndrome independently or in addition to type 1 or type 2 diabetes [3, 4]. The major findings of our study can be summarized as follows: 1) HFD significantly induces retinal NLRP3-inflammasome activation, adhesion molecule upregulation, leukostasis and BRB breakdown, which are all dependent on TXNIP expression; 2) TXNIP is required for palmitate-induced adhesion molecule upregulation in endothelial cells in culture, and TXNIP-NLRP3 inflammasome axis mediates the process in an autotocrine positive feedback loop fashion; and 3) HFD can directly contribute to endothelial cell death through circulating leukocytes, and TXNIP deletion can protect against such effect.

Retinal microvascular cell death can occur either directly, due to different biochemical insults initiated within retinal endothelial cells themselves, or indirectly, secondary to the activation of other retinal cell types; including neurons and glial cells, or non-retinal cell types; mainly circulating or infiltrating leukocytes (reviewed in [10]). We have recently reported that HFD results in retinal TXNIP-NLRP3 interaction and inflammasome activation, which was associated by increased retinal microvascular degeneration in-vivo and that TXNIP-NLRP3 inflammasome axis, was required for direct palmitate-induced endothelial cell death in culture [18]. Previous reports have established retinal leukostasis as one of the indirect prerequisite events for inducing exacerbated endothelial cell death and BRB breakdown, and its inhibition can help to prevent retinal acellular capillaries formation [11, 12]. In the current study, our results showed that HFD-induced NLRP3 inflammasome activation was associated with parallel increases in retinal adhesion molecule (ICAM-1) expression, increased retinal leukostasis and BRB breakdown, which was all-dependent on retinal TXNIP protein expression. These results suggest a possible interplay between HFD-induced retinal TXNIP-NLRP3 inflammasome axis and increased leukostasis as one of the early contributing events for inducing retinal microvascular degeneration on the longer term.

Retinal leukostasis depends on the mutual interaction between both endothelial cells and circulating leukocytes via up-regulated adhesion molecules on the surface of endothelial cells [9, 10]. Therefore, we investigated the interaction between the TXNIP-NLRP3 inflammasome axis and endothelial adhesion molecule expression in-vitro. In parallel to our previous findings that TXNIP was required for Palmitate-induced NLRP3 inflammasome activation and its associated cell death in cultured ECs [18], our results elucidated that TXNIP inhibition also abolishes Palmitate-induced upregulation of adhesion molecules ICAM-1 and PAM-1 in ECs in-vitro. This establishes the role of TXNIP in upregulation of adhesion molecules in endothelial cells in culture, and the possible role of NLRP3 inflammasome in mediating this effect.

TXNIP is not only known as an inhibitor of the thioredoxin antioxidant protein system, but also as a member of the α-arrestin family of adaptor and scaf-folding proteins with a pivotal role in inducing pro-inflammatory signaling pathways [47, 48]. From which, TXNIP has been reported to activate the canonical NFxB and p38 MAPK pathways and downstream major proinflammatory cytokines and enzymes including IL-1β, ICAM-1, TNF-α, VEGF-A and Cox2, [24, 49-51]. Thus, it is important to dissect the relative contribution of the NLRP3 inflammasome activation through IL-1β in inducing endothelial cell inflammation and adhesion molecule expression versus other downstream pro-inflammatory mediators induced by TXNIP. Forced expression of TXNIP in ECs resulted in activation of the NLRP3 inflammasome evidenced by the upregulation of NLRP3, cleaved Caspase-1 and cleaved IL-β, along with TNFα and both adhesion molecules ICAM-1 and PAM-1 expression. Interestingly, blocking the effect of IL-1β by using the IL-1RA was able not only to suppress the induction of its own processing pathway of NLRP3 inflammasome, but also the expression of the other pro-inflammatory mediator TNFα and ICAM-1 and PECAM-1 adhesion molecules. These data establish a positive feedback loop mediated by Il-1β that stimulates its own activation and induction of endothelial

inflammation in an autocrine fashion. Our findings lend further credit to an earlier study which proposed the retinal endothelial tissue as an initial early source of increased IL-1 β production in response to another model of hyperglycemia, after which, increasing levels of IL-1 β are sustained via its own auto stimulation in endothelial and macroglia tissues (Müller cells and astrocytes) [52].

Increased retinal acellular capillaries formation as a result of retinal capillary nonperfusion, endothelial cell death and microvascular degeneration in addition to the associated BRB dysfunction and increased retinal thickness or edema are the hallmarks of the early initial vaso-regressive stage of non-proliferative diabetic retinopathy (NPDR). Such events are believed to comprise the founding stages for induction of cumulative focal ischemia, which is responsible for provoking the vaso-proliferative response of proliferative diabetic retinopathy (PDR) later in advanced stages of the disease [9, 53-55]. In our pre-diabetic HFD model, increased retinal acellular capillaries formation was indeed observed after 18-weeks of HFD alone in WT-HFD mice. Moreover, inhibition of the TXNIP-NLRP3 inflammasome axis was able to reverse it in TKO mice. Clinically, retinal microvascular capillary non-perfusion and degeneration can be evident as non-perfused areas in fluorescein-infusion retinal angiograms [9]. Similarly, in parallel to the increase in retinal capillaries drop out in WT-HFD mice, we have also observed that WT mice tend to have decreased branching density in response to HFD, whereas, TKO mice had a normal morphological appearance comparable levels to WT-ND that did not change in response to HFD. In line with our results, pharmacological inhibition of Caspase-1 or deletion of IL-1reptor was sufficient to inhibit IL-1β dependent increases of degenerated acellular capillaries formation in diabetic mice retinas [56]. These findings establish the detrimental long term impact of HFD on retinal microvascular degeneration and morphological abnormalities and highlight the protective effect of TXNIP deletion.

On the other hand, in further investigation of the role of leukocytes in mediating HFD-induced retinal microvascular cell death and degeneration, isolated PBMCs from the WT-HFD mice or obese non-diabetic subjects but not TKO-HFD mice or lean subjects resulted in increased leukostasis and apoptosis of both mouse and human endothelial cells respectively, after 2 and 24 hours respectively in co-culture. Together, these results highlight a novel role of circulating leukocytes in mediating endothelial cell death in models of HFD in an indirect way and further emphasize the potential clinical relevance of the role TXNIP plays in mediating HFD-induced microvascular inflammation and degeneration.

In summary, our experimental model depicts accelerated retinal acellular capillaries formation, microvascular morphological abnormalities and increased retinal leukostasis as pathological landmarks of HFD-induced obesity. In addition, our studies also establish the role of retinal microvascular leukostasis as one of the major contributing pathways for HFD-induced retinal microvascular degeneration. For the first time, we elucidate a novel intricate interplay between the TXNIP-NLRP3 inflammasome axis and induction of endothelial inflammation and leukostasis. In the era when obesity has been upgraded to an independent disease state rather than a mere risk factor, such paradigm proposes TXNIP-NLRP3 inflammasome axis as a promising therapeutic target for early treatment or prevention of obesity-associated microvascular diseases; benefiting more than 79-million obese Americans.

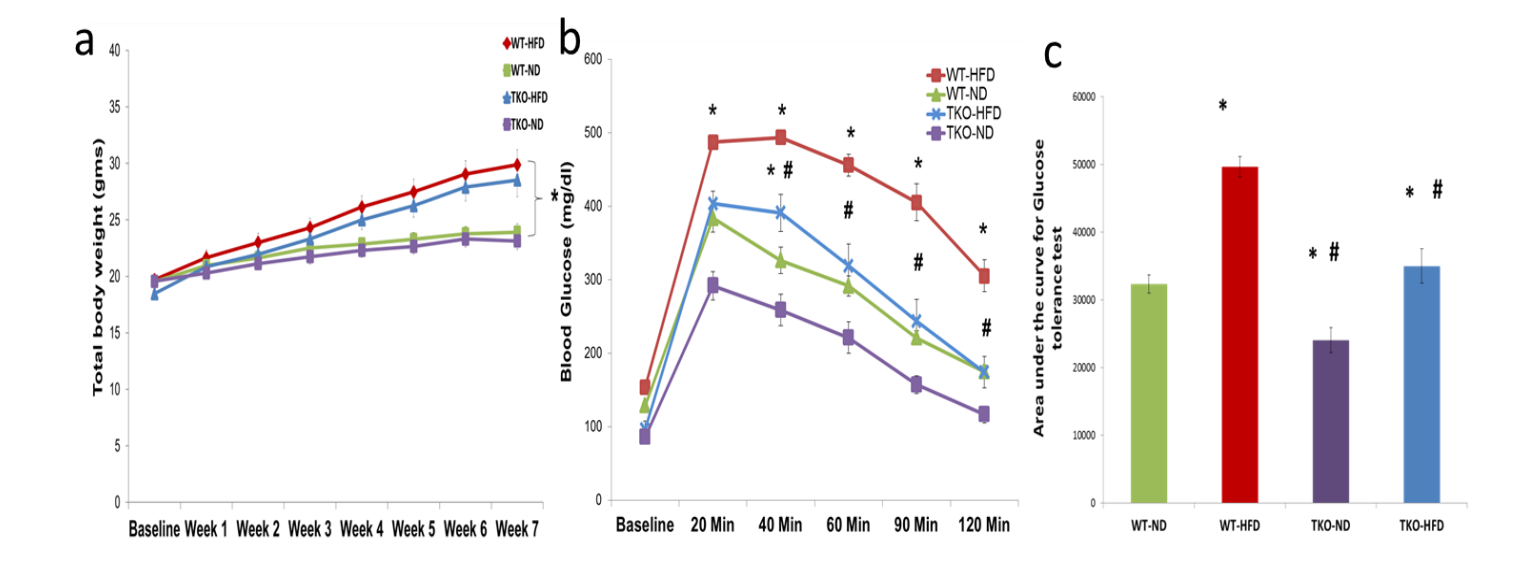
4.6 References

- 1. Wong, T.Y., et al., Associations between the metabolic syndrome and retinal microvascular signs: the Atherosclerosis Risk In Communities study. Invest Ophthalmol Vis Sci, 2004. **45**(9): p. 2949-54.
- 2. Kawasaki, R., et al., *The metabolic syndrome and retinal microvascular signs in a Japanese population: the Funagata study.* Br J Ophthalmol, 2008. **92**(2): p. 161-6.
- 3. Gopinath, B., et al., *Effect of obesity on retinal vascular structure in pre-adolescent children*. Int J Pediatr Obes, 2011. **6**(2-2): p. e353-9.
- 4. Nguyen, T.T. and T.Y. Wong, *Retinal vascular manifestations of metabolic disorders*. Trends Endocrinol Metab, 2006. **17**(7): p. 262-8.
- 5. Caballero, A.E., *Metabolic and vascular abnormalities in subjects at risk for type 2 diabetes: the early start of a dangerous situation.* Arch Med Res, 2005. **36**(3): p. 241-9.
- 6. Couillard, C., et al., Circulating levels of oxidative stress markers and endothelial adhesion molecules in men with abdominal obesity. J Clin Endocrinol Metab, 2005. **90**(12): p. 6454-9.
- 7. Hackman, A., et al., Levels of soluble cell adhesion molecules in patients with dyslipidemia. Circulation, 1996. **93**(7): p. 1334-8.
- 8. Kohner, E.M. and P. Henkind, *Correlation of fluorescein angiogram and retinal digest in diabetic retinopathy*. Am J Ophthalmol, 1970. **69**(3): p. 403-14.
- 9. Tang, J. and T.S. Kern, *Inflammation in diabetic retinopathy*. Prog Retin Eye Res, 2011. **30**(5): p. 343-58.
- 10. Kern, T.S., Contributions of inflammatory processes to the development of the early stages of diabetic retinopathy. Exp Diabetes Res, 2007. **2007**: p. 95103.
- 11. Adamis, A.P. and A.J. Berman, *Immunological mechanisms in the pathogenesis of diabetic retinopathy*. Semin Immunopathol, 2008. **30**(2): p. 65-84.
- 12. Joussen, A.M., et al., A central role for inflammation in the pathogenesis of diabetic retinopathy. FASEB J, 2004. **18**(12): p. 1450-2.
- 13. Demircan, N., et al., *Determination of vitreous interleukin-1 (IL-1) and tumour necrosis factor (TNF) levels in proliferative diabetic retinopathy.* Eye (Lond), 2006. **20**(12): p. 1366-9.
- 14. Dong, N., et al., Study of 27 aqueous humor cytokines in patients with type 2 diabetes with or without retinopathy. Mol Vis, 2013. **19**: p. 1734-46.
- 15. Koleva-Georgieva, D.N., N.P. Sivkova, and D. Terzieva, *Serum inflammatory cytokines IL-1beta, IL-6, TNF-alpha and VEGF have influence on the development of diabetic retinopathy.* Folia Med (Plovdiv), 2011. **53**(2): p. 44-50.
- 16. Kowluru, R.A. and S. Odenbach, *Role of interleukin-1beta in the development of retinopathy in rats: effect of antioxidants.* Invest Ophthalmol Vis Sci, 2004. **45**(11): p. 4161-6.
- 17. Kowluru, R.A. and S. Odenbach, *Role of interleukin-1beta in the pathogenesis of diabetic retinopathy*. Br J Ophthalmol, 2004. **88**(10): p. 1343-7.
- 18. Mohamed, I.N., et al., *Thioredoxin-interacting protein is required for endothelial NLRP3 inflammasome activation and cell death in a rat model of high-fat diet.* Diabetologia, 2014. **57**(2): p. 413-23.
- 19. Vandanmagsar, B., et al., *The NLRP3 inflammasome instigates obesity-induced inflammation and insulin resistance.* Nat Med, 2011. **17**(2): p. 179-88.

- 20. Stienstra, R., et al., *Inflammasome is a central player in the induction of obesity and insulin resistance*. Proc Natl Acad Sci U S A, 2011. **108**(37): p. 15324-9.
- 21. Schroder, K., R. Zhou, and J. Tschopp, *The NLRP3 inflammasome: a sensor for metabolic danger?* Science, 2010. **327**(5963): p. 296-300.
- 22. Chung, J.W., et al., *Vitamin D3 upregulated protein 1 (VDUP1) is a regulator for redox signaling and stress-mediated diseases.* J Dermatol, 2006. **33**(10): p. 662-9.
- 23. Junn, E., et al., *Vitamin D3 up-regulated protein 1 mediates oxidative stress via suppressing the thioredoxin function.* J Immunol, 2000. **164**(12): p. 6287-95.
- 24. Masutani, H., et al., *Thioredoxin binding protein (TBP)-2/Txnip and alpha-arrestin proteins in cancer and diabetes mellitus.* J Clin Biochem Nutr, 2012. **50**(1): p. 23-34.
- 25. Zhou, R., et al., *Thioredoxin-interacting protein links oxidative stress to inflammasome activation*. Nat Immunol, 2010. **11**(2): p. 136-40.
- 26. Zhou, R., et al., A role for mitochondria in NLRP3 inflammasome activation. Nature, 2011. **469**(7329): p. 221-5.
- 27. Lunov, O., et al., Amino-functionalized polystyrene nanoparticles activate the NLRP3 inflammasome in human macrophages. ACS Nano, 2011. **5**(12): p. 9648-57.
- 28. Park, Y.J., et al., TXNIP deficiency exacerbates endotoxic shock via the induction of excessive nitric oxide synthesis. PLoS Pathog, 2013. 9(10): p. e1003646.
- 29. Xiang, M., et al., *Hemorrhagic shock activation of NLRP3 inflammasome in lung endothelial cells.* J Immunol, 2011. **187**(9): p. 4809-17.
- 30. Oslowski, C.M., et al., *Thioredoxin-interacting protein mediates ER stress-induced beta cell death through initiation of the inflammasome*. Cell Metab, 2012. **16**(2): p. 265-73.
- 31. Lerner, A.G., et al., *IRE1alpha induces thioredoxin-interacting protein to activate the NLRP3 inflammasome and promote programmed cell death under irremediable ER stress.* Cell Metab, 2012. **16**(2): p. 250-64.
- 32. Knopp, R.H., et al., One-year effects of increasingly fat-restricted, carbohydrate-enriched diets on lipoprotein levels in free-living subjects. Proc Soc Exp Biol Med, 2000. **225**(3): p. 191-9.
- Wen, H., et al., *Fatty acid-induced NLRP3-ASC inflammasome activation interferes with insulin signaling*. Nat Immunol, 2011. **12**(5): p. 408-15.
- 34. Matsuzaka, T., et al., *Elovl6 promotes nonalcoholic steatohepatitis*. Hepatology, 2012. **56**(6): p. 2199-208.
- 35. Pejnovic, N.N., et al., Galectin-3 deficiency accelerates high-fat diet-induced obesity and amplifies inflammation in adipose tissue and pancreatic islets. Diabetes, 2013. **62**(6): p. 1932-44.
- 36. Hui, S.T., et al., *Txnip balances metabolic and growth signaling via PTEN disulfide reduction.* Proc Natl Acad Sci U S A, 2008. **105**(10): p. 3921-6.
- 37. Abdelsaid, M.A., S. Matragoon, and A.B. El-Remessy, *Thioredoxin-interacting protein expression is required for VEGF-mediated angiogenic signal in endothelial cells*. Antioxid Redox Signal, 2013. **19**(18): p. 2199-212.
- 38. Vu, V., et al., Delivery of adiponectin gene to skeletal muscle using ultrasound targeted microbubbles improves insulin sensitivity and whole body glucose homeostasis. Am J Physiol Endocrinol Metab, 2013. **304**(2): p. E168-75.
- 39. Ohshima, K., et al., *Direct angiotensin II type 2 receptor stimulation ameliorates insulin resistance in type 2 diabetes mice with PPARgamma activation.* PLoS One, 2012. **7**(11): p. e48387.

- 40. Mysona, B.A., et al., Modulation of p75(NTR) prevents diabetes- and proNGF-induced retinal inflammation and blood-retina barrier breakdown in mice and rats. Diabetologia, 2013. **56**(10): p. 2329-39.
- 41. Joussen, A.M., et al., *Leukocyte-mediated endothelial cell injury and death in the diabetic retina*. Am J Pathol, 2001. **158**(1): p. 147-52.
- 42. Rojas, M., et al., Requirement of NOX2 expression in both retina and bone marrow for diabetes-induced retinal vascular injury. PLoS One, 2013. **8**(12): p. e84357.
- 43. Tang, J., et al., MyD88-dependent pathways in leukocytes affect the retina in diabetes. PLoS One, 2013. **8**(7): p. e68871.
- 44. Al-Gayyar, M.M., et al., *Neurovascular protective effect of FeTPPs in N-methyl-D-aspartate model: similarities to diabetes.* Am J Pathol, 2010. **177**(3): p. 1187-97.
- 45. Chutkow, W.A., et al., *Deletion of the alpha-arrestin protein Txnip in mice promotes adiposity and adipogenesis while preserving insulin sensitivity.* Diabetes, 2010. **59**(6): p. 1424-34.
- 46. Yoshihara, E., et al., Disruption of TBP-2 ameliorates insulin sensitivity and secretion without affecting obesity. Nat Commun, 2010. 1: p. 127.
- 47. Spindel, O.N., C. World, and B.C. Berk, *Thioredoxin interacting protein: redox dependent and independent regulatory mechanisms*. Antioxid Redox Signal, 2012. **16**(6): p. 587-96.
- 48. Patwari, P. and R.T. Lee, *An expanded family of arrestins regulate metabolism*. Trends Endocrinol Metab, 2012. **23**(5): p. 216-22.
- 49. Perrone, L., et al., *Thioredoxin interacting protein (TXNIP) induces inflammation through chromatin modification in retinal capillary endothelial cells under diabetic conditions.* J Cell Physiol, 2009. **221**(1): p. 262-72.
- 50. Perrone, L., et al., *Inhibition of TXNIP expression in vivo blocks early pathologies of diabetic retinopathy*. Cell Death Dis, 2010. **1**: p. e65.
- 51. Al-Gayyar, M.M., et al., *Thioredoxin interacting protein is a novel mediator of retinal inflammation and neurotoxicity*. Br J Pharmacol, 2011. **164**(1): p. 170-80.
- 52. Liu, Y., M. Biarnes Costa, and C. Gerhardinger, *IL-1beta is upregulated in the diabetic retina and retinal vessels: cell-specific effect of high glucose and IL-1beta autostimulation.* PLoS One, 2012. **7**(5): p. e36949.
- 53. Frank, R.N., *Diabetic retinopathy*. N Engl J Med, 2004. **350**(1): p. 48-58.
- 54. Nunes, S., et al., Microaneurysm turnover is a biomarker for diabetic retinopathy progression to clinically significant macular edema: findings for type 2 diabetics with nonproliferative retinopathy. Ophthalmologica, 2009. **223**(5): p. 292-7.
- 55. Shimizu, K., Y. Kobayashi, and K. Muraoka, *Midperipheral fundus involvement in diabetic retinopathy*. Ophthalmology, 1981. **88**(7): p. 601-12.
- 56. Vincent, J.A. and S. Mohr, *Inhibition of caspase-1/interleukin-1beta signaling prevents degeneration of retinal capillaries in diabetes and galactosemia*. Diabetes, 2007. **56**(1): p. 224-30.

Fig.4.1



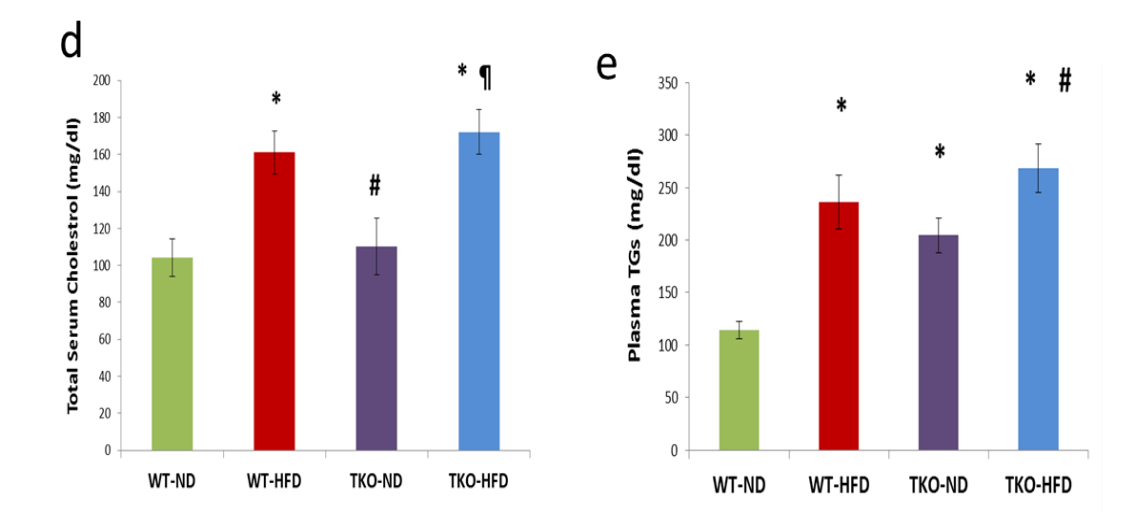


Fig. 4.1 HFD results in weight gain, impaired glucose tolerance and dyslipidemia in both WT and TKO mice. (a) Weekly total body weights (grams) records for all animal groups showing comparable weight gain between WT-HFD and TKO-HFD groups that were both significantly higher than both WT-ND and TKO-ND groups. (b) IPGTT showing peripheral blood glucose levels recorded over time after an IP bolus dose of 2 grams of glucose/kg mouse body weight. (c) AUC analyses showed 1.5-fold change in peripheral blood glucose response in WT-HFD group, versus 0.7-fold and no change in both TKO-ND and TKO-HFD groups, respectively, compared to WT-ND group. (n=13-23; * P-value <0.05 vs WT-ND and # vs WT-HFD). (d) & (e) Plasma total cholesterol and triglyceride levels showed higher levels in both WT-HFD and TKO-HFD groups by 1.5- and 1.7- fold for total cholesterol and 2.3- and 2.6-fold for triglycerides, respectively, compared to WT-ND. TKO-ND group showed no change in total cholesterol levels, but higher basal levels of triglycerides by 2-fold compared to WT-ND (n=8; * P-value <0.05 vs WT-ND, # vs WT-HFD and ¶ vs TKO-ND).

Fig.4.2

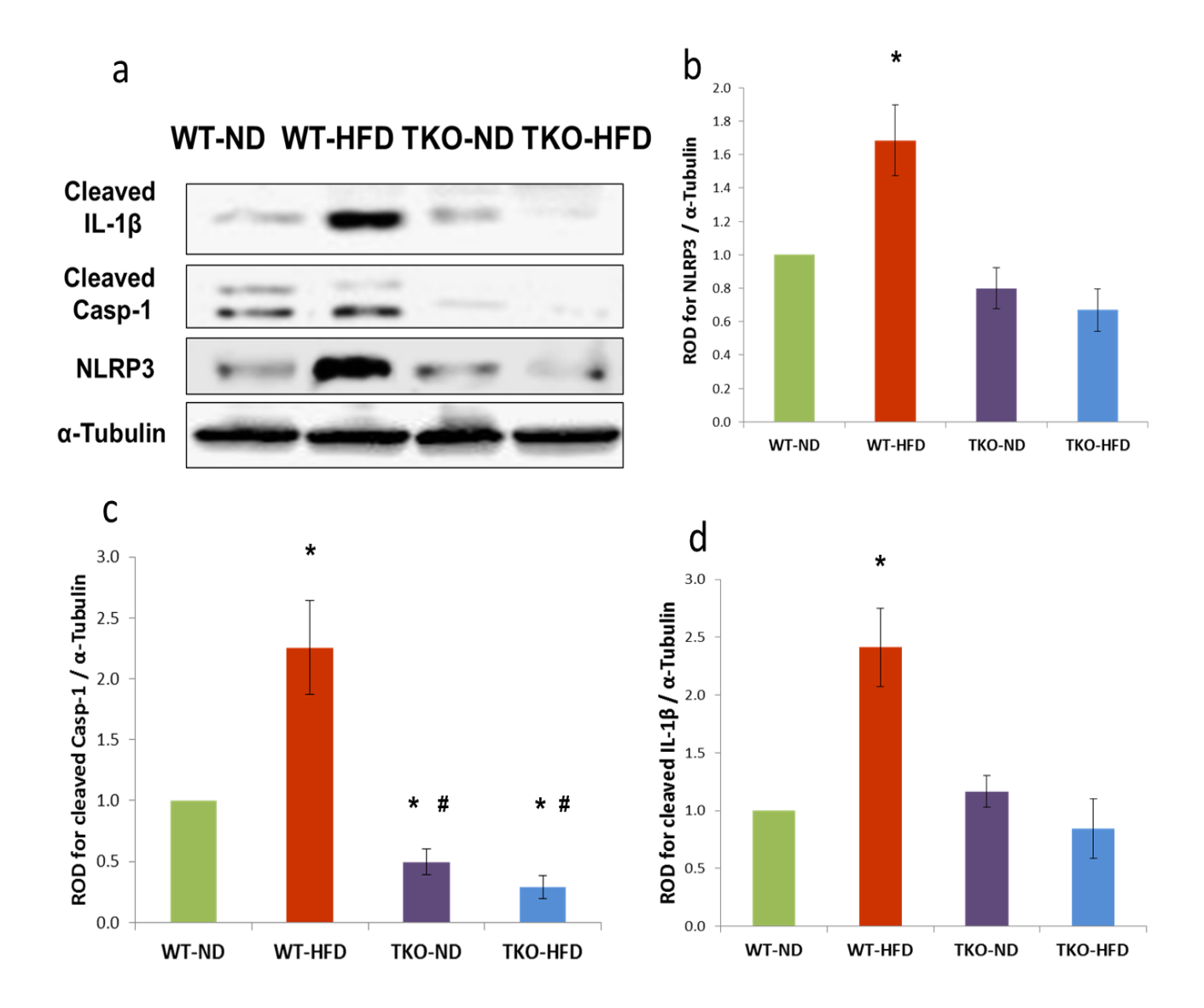


Fig.4.2 Deletion of TXNIP abrogates HFD-induced NLRP3-inflammasome activation in the retina. (a) Representative blots and WB analysis of retinal NLRP3 (b), cleaved Casp-1 (c) and cleaved IL-1β (d) protein expression showed higher levels by 1.7-, 2.3- and 2.4-fold, respectively in WT-HFD group compared to WT-ND. In contrast, TKO-ND and TKO-HFD groups showed either no change in both NLRP3 and cleaved IL-β expression and significantly lower levels of cleaved caspase-1 levels by 0.5- and 0.3-fold, respectively, relative to WT-ND group. Three-way ANOVA showed significant interaction between the type of diet and genotype on all NLRP3 inflammasome activation markers (n=8-11; * P-value <0.05 vs WT-ND and # vs WT-HFD).

Fig.4.3

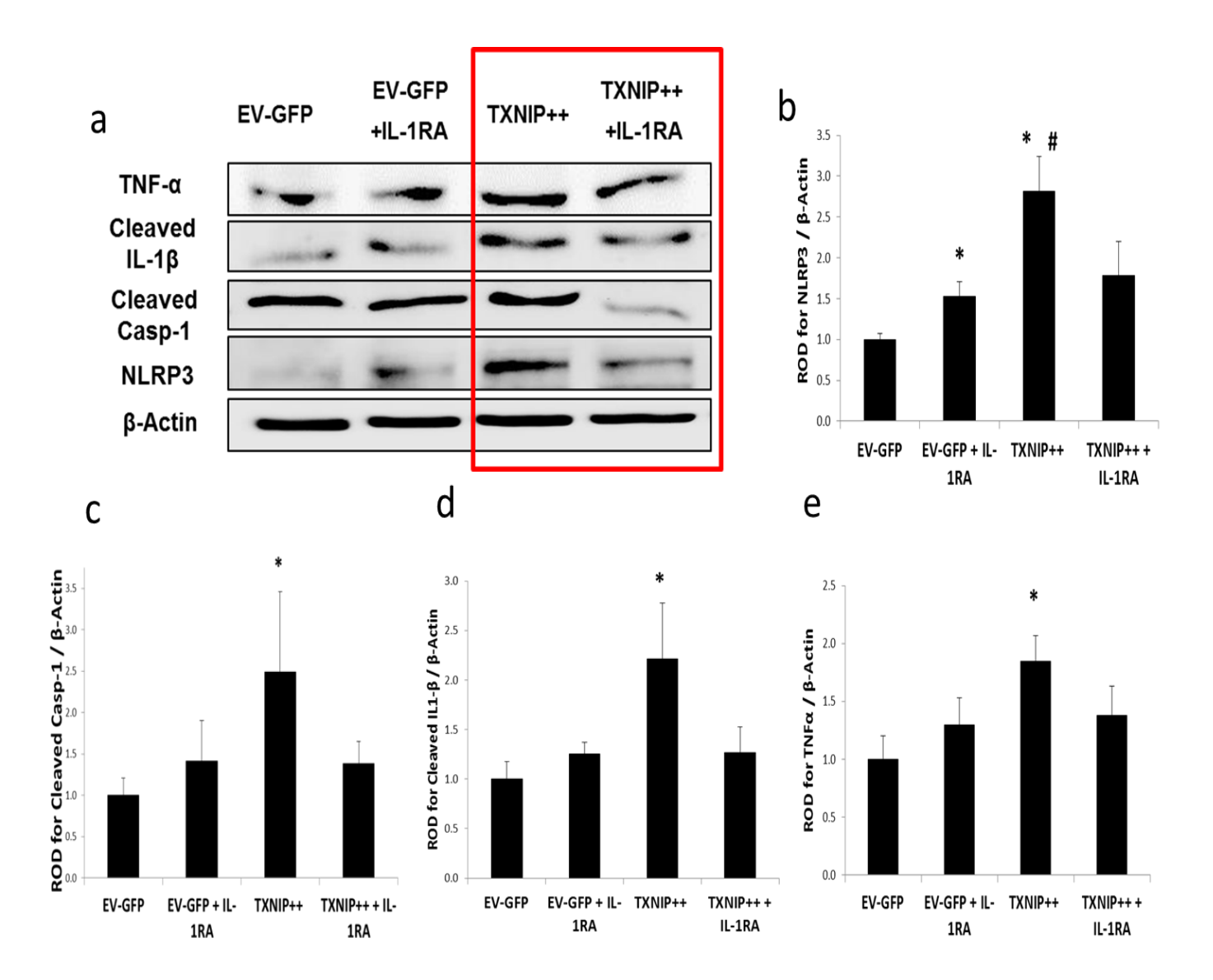


Fig.4.3 Overexpression of TXNIP activates NLRP3-inflammasome in human ECs. (a) Representative blots and WB analysis of NLRP3 (b), cleaved Casp-1 (c), cleaved IL-1β (d) and TNFα protein expression. NLRP3, cleaved caspase-1, cleaved IL-1β and TNFα expression was higher in the TXNIP⁺⁺ group by 2.5-, 3-, 2.5- and 1.8-fold receptively in TXNIP⁺⁺ compared to the EV-GFP control group. Treatment of TXNIP-overexpressing ECs with 100ng/ml of IL-1RA (TXNIP⁺⁺ + IL-1RA) was able to suppress the effect of TXNIP overexpression on inflammasome activation expression and TNFα. Two-way ANOVA showed significant interaction between IL-1RA and TXNIP overexpression (n=4-6; * P-value <0.05 vs EV-GFP and # vs EV-GFP + IL-1RA).

Fig.4.4

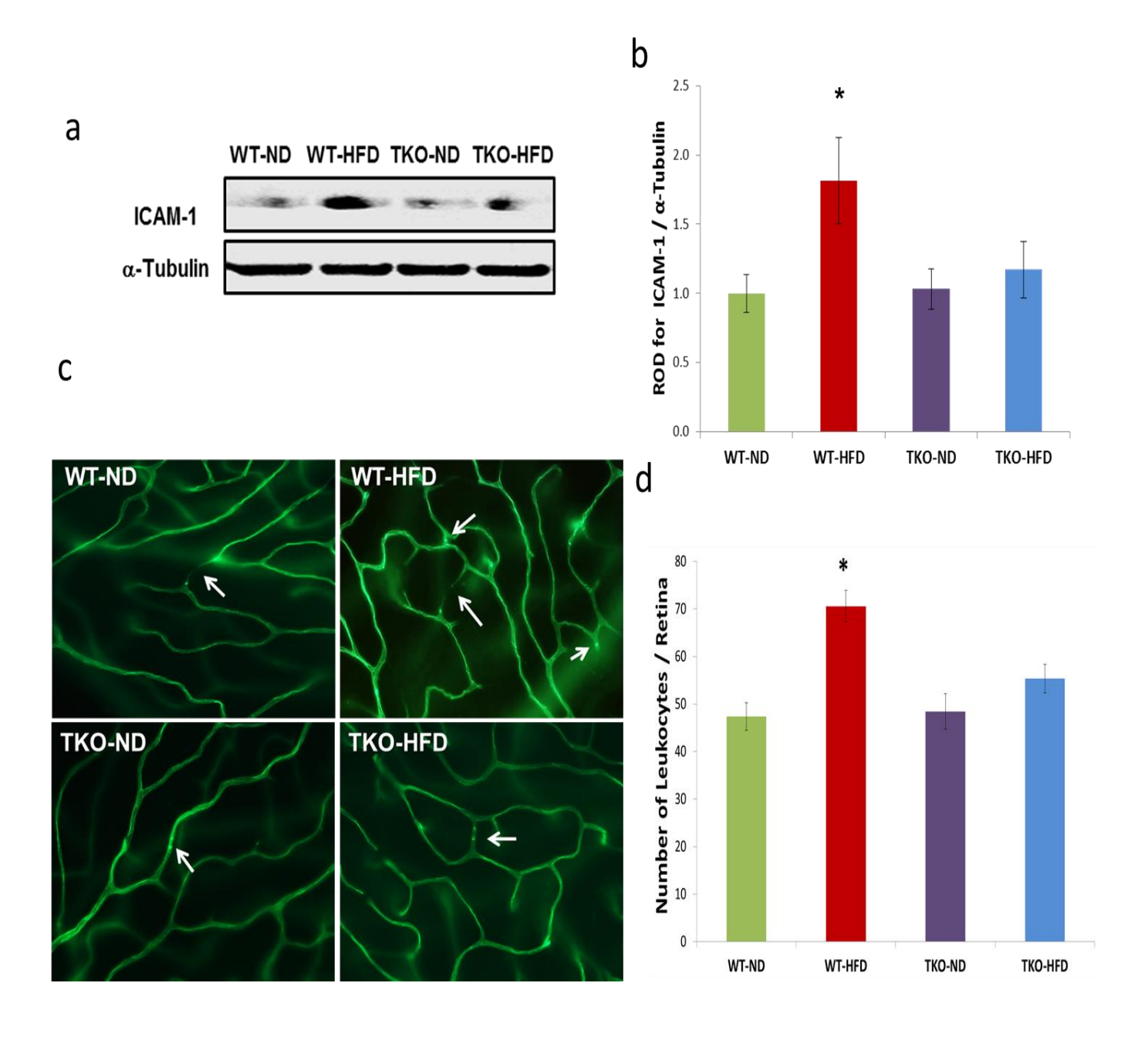


Fig.4.4 Deletion of TXNIP prevents HFD-induced retinal microvascular inflammation and leukostasis. (a) Representative blots and WB analyses (b) of ICAM-1 showed increased expression by 1.6-fold in WT-HFD group compared to WT-ND group, whereas the TKO mice groups showed no change in response to HFD (n=3-4; * P-value <0.05). (c) Representative pictures and quantification (d) of the number of adherent leukocytes per retina showed higher numbers in the WT-HFD group by 1.5-fold but had no significant effect on the TKO-HFD group relative to the WT-ND group. Three-way ANOVA showed significant interaction between the type of diet and genotype (n=10-17; * P-value <0.05).

Fig.4.5

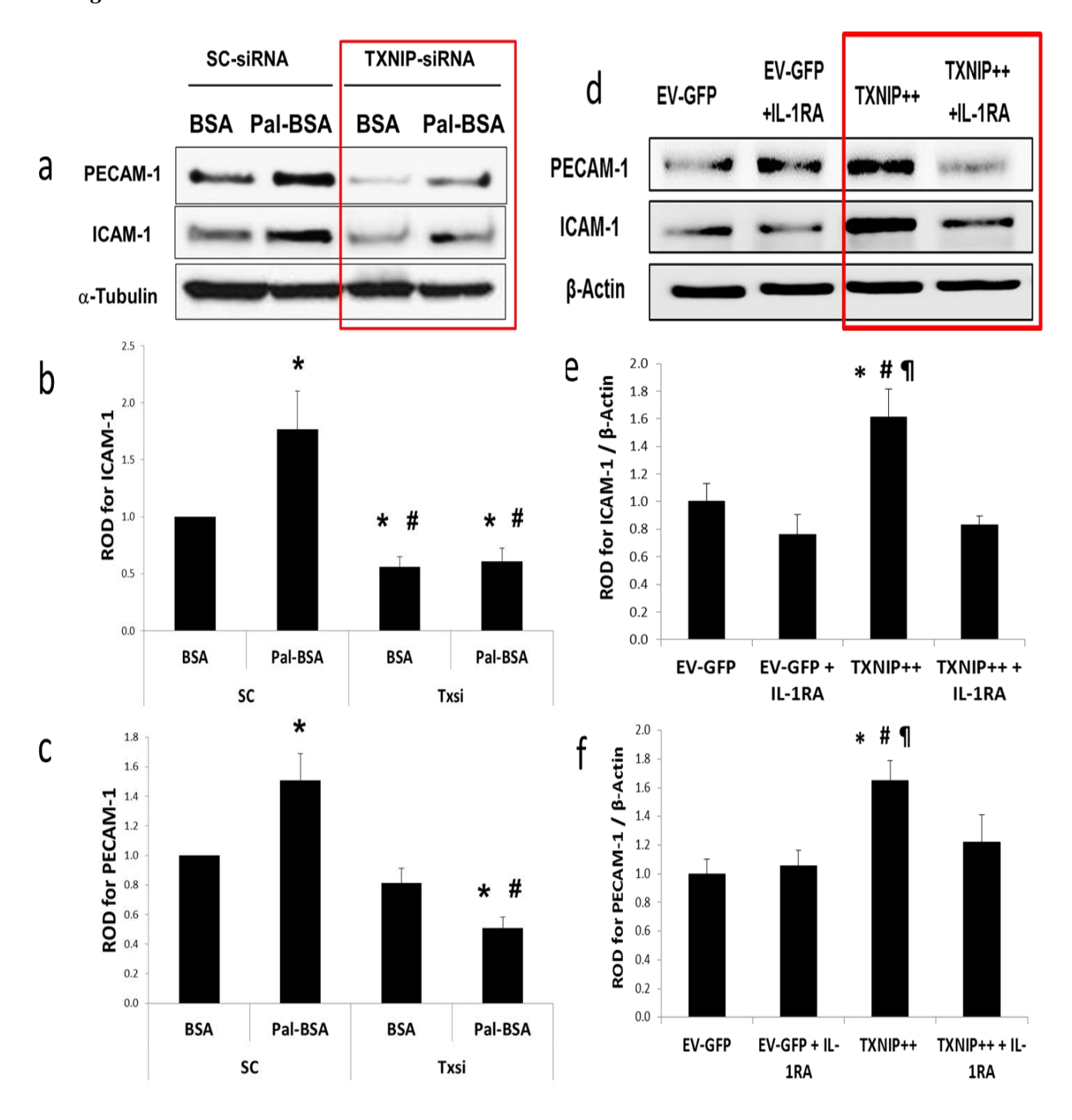


Fig.4.5 Silencing TXNIP or inhibiting IL-1 Receptor prevents adhesion molecule expression in human ECs. (a) Representative blots and WB analyses of ICAM-1(b) and PECAM-1 (c) showed increased expression by 1.7- and 1.4-fold for PAL-BSA, respectively, relative to BSA-controls in the scrambled-siRNA group. Silencing TXNIP expression using siRNA abolished such responses. Two-way ANOVA showed significant interaction between Pal-BSA and silencing TXNIP expression (n=3-4; * P-value <0.05 vs SC BSA, # vs SC Pal-BSA). (d) Representative blots and WB analysis of ICAM-1(e) and PECAM-1 (f) protein expression showed higher levels in the TXNIP⁺⁺ group by 1.9 and 1.8-fold respectively compared to the EV-GFP control group. Treatment of TXNIP-overexpressing ECs with 100ng/ml of IL-1RA (TXNIP⁺⁺ + IL-1RA) was able to suppress the effect of TXNIP overexpression on EC adhesion molecule expression. Two-way ANOVA showed significant interaction between IL-1RA and ¶vs TXNIP overexpression (n=4-6; * P-value <0.05 vs EV-GFP, # vs EV-GFP + IL-1RA and ¶vs TXNIP⁺⁺ + IL-1RA).

Fig.4.6

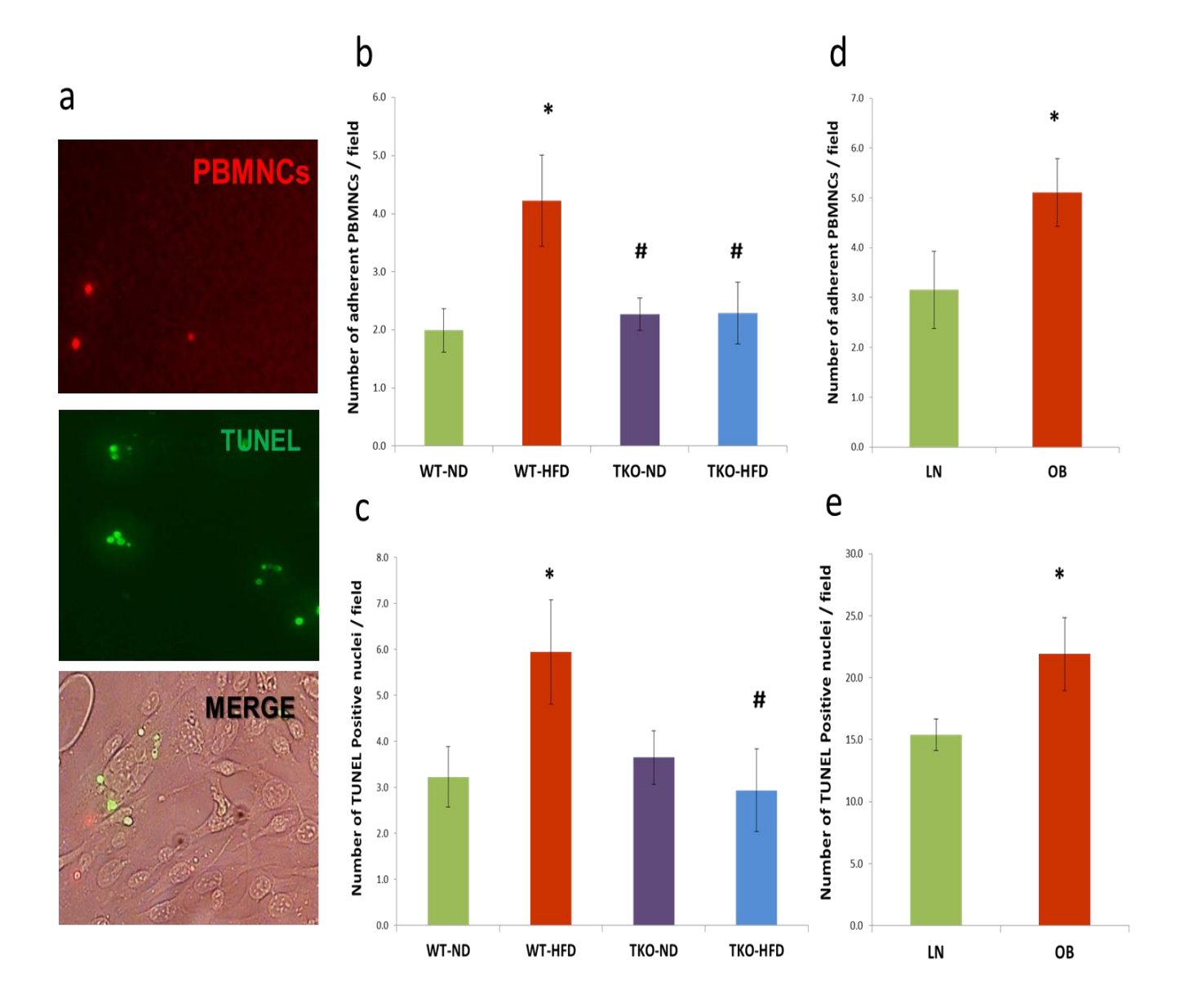


Fig.4.6 Deletion of TXNIP in leukocytes prevents leukostasis and endothelial cell death. Representative pictures (a) and quantification of the number of adherent PBMCs per field after 2-hours (b) and the number of TUNEL positive nuclei after 24-hours (c) showed higher numbers in the WT-HFD group by 2- and 1.8-fold respectively, compared to the WT-ND control group. Whereas, both TKO-ND and TKO-HFD groups showed no significant changes versus WT-ND control group. Three-way ANOVA showed significant interaction between the type of diet and genotype (n=4-6; * P-value <0.05 vs WT-ND and # vs WT-HFD). Quantification of the number of adherent PBMCs per field after 2-hours (d) and the number of TUNEL positive nuclei after 24-hours (e) showed higher numbers in the OB group by 1.6- and 1.4-fold respectively, compared to the LN control group. (n=4-5; * P-value <0.05 vs LN).

Fig.4.7

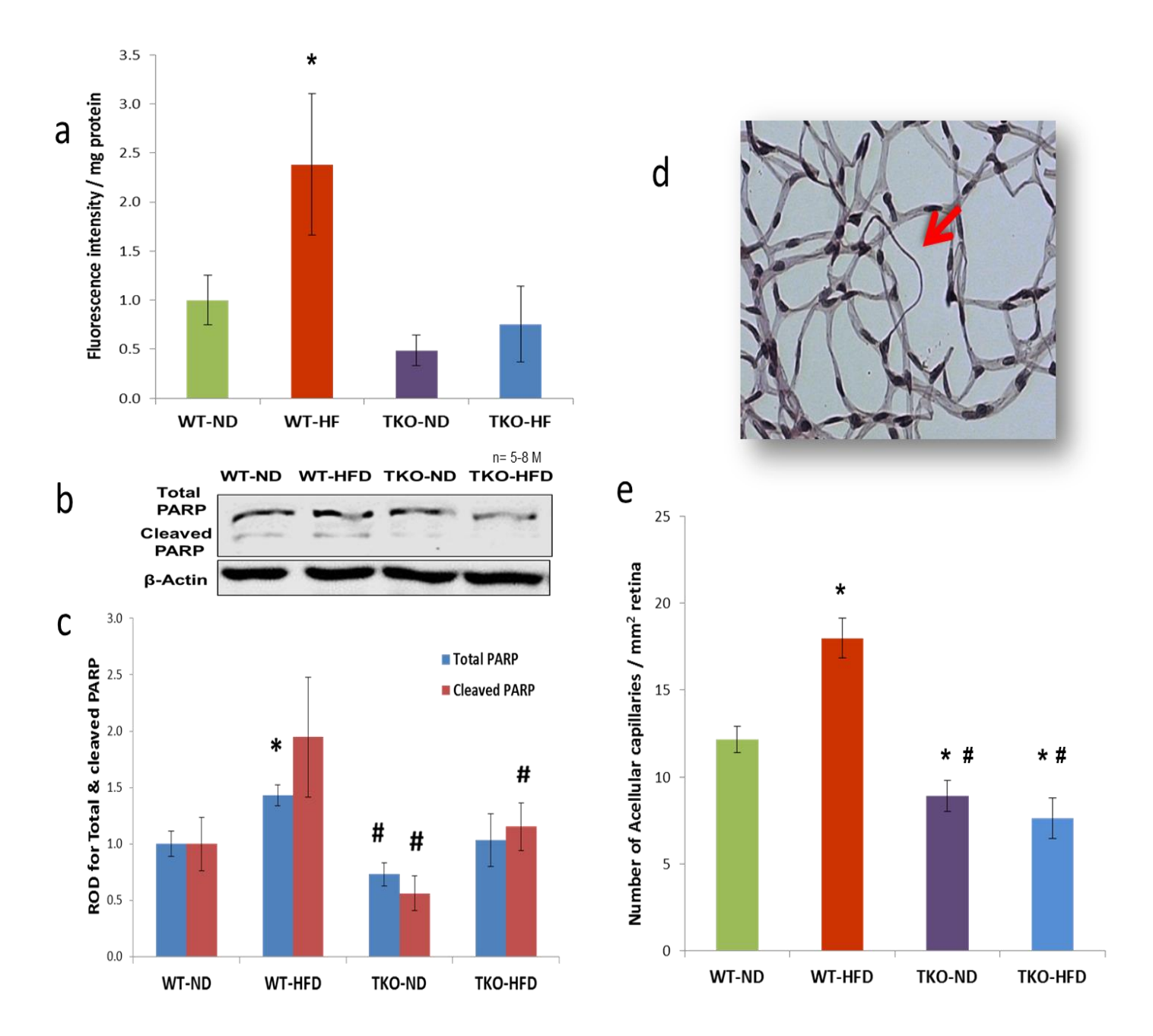


Fig.4.7 HFD induces retinal BRB breakdown and microvascular degeneration via TXNIP. (a) Extravasation of BSA-Fluorescence into the retina tissue was higher in the WT-HFD group by 2.4-fold; whereas, both TKO-ND and TKO-HFD groups had lower levels of BSA-Fluorescence extravasation by 0.5 and 0.75 -fold respectively, relative to the WT-ND group. Three-way ANOVA showed significant interaction between the type of diet and genotype (n=5-8; * P-value <0.05). (b) Representative blots and WB analyses (c) of total and cleaved PARP showed increased expression of the pro-apoptotic protein PARP expression by 1.4-fold and a trend towards significance in cleaved PARP expression in WT-HFD group versus WT-ND control group, whereas TKO-ND was significantly less by 0.7-fold in total PARP expression and TKO-HFD group showed no change. Representative picture (d) and quantification of the number of acellular capillaries per mm² (e) showed higher numbers in the WT-HFD group by 1.5-fold compared to WT-ND, whereas, both TKO-ND and TKO-HFD groups showed significantly lower counts of acellular capillaries by 0.7 and 0.6 -fold, respectively. Three-way ANOVA showed significant interaction between the type of diet and genotype (n=6; * P-value <0.05 vs WT-ND and # vs WT-HFD).

Fig.4.8

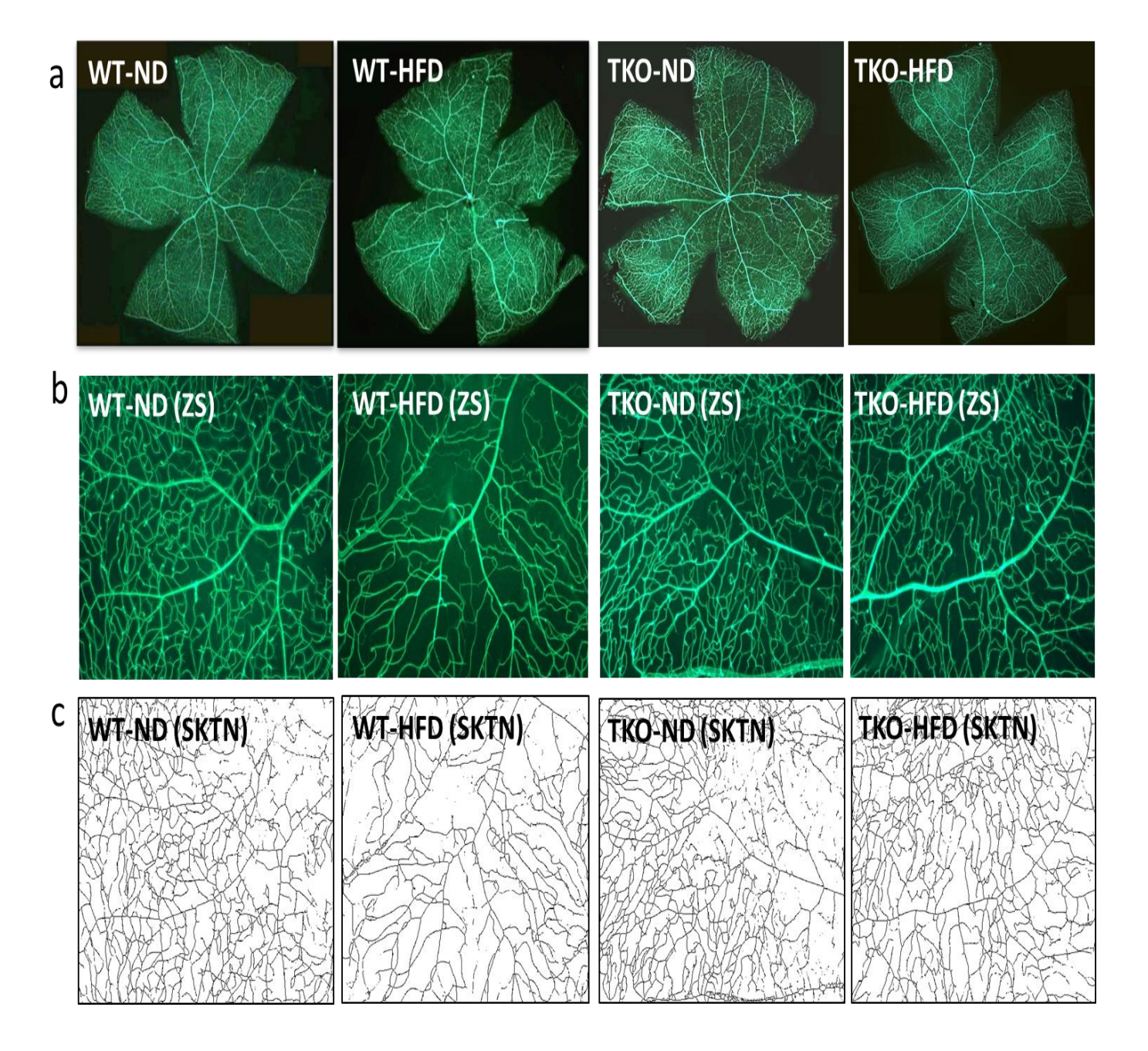
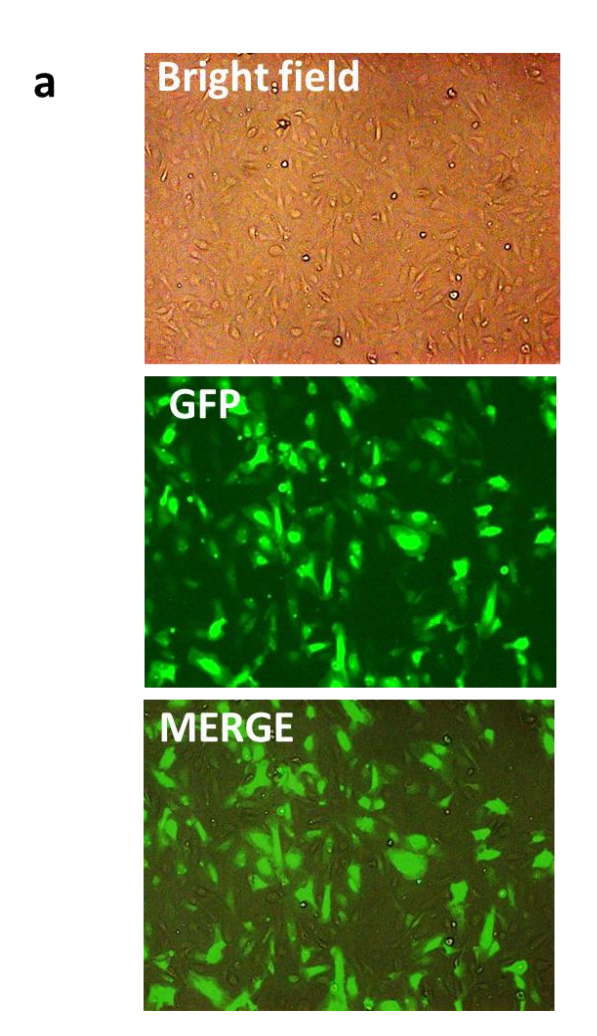
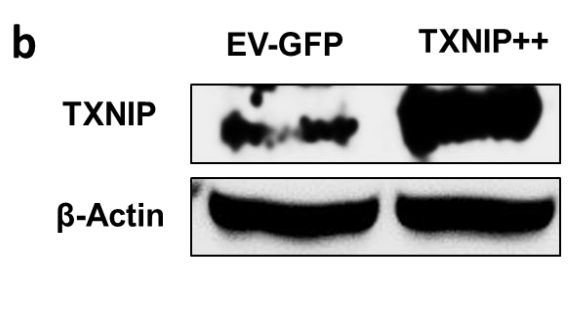
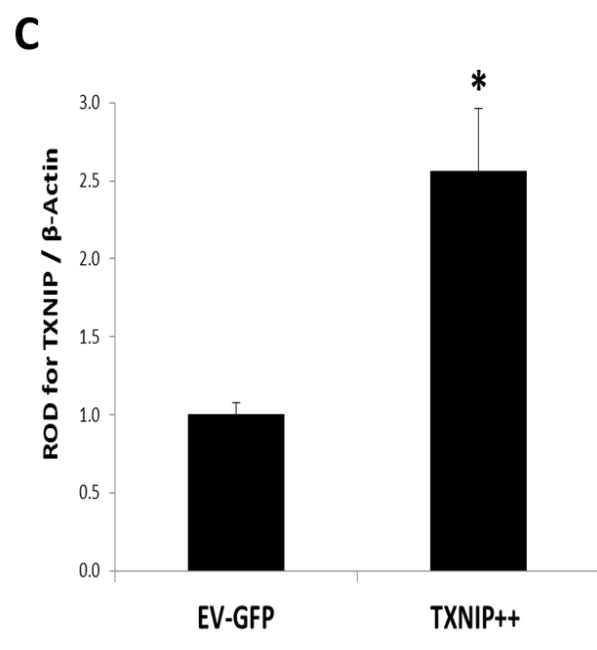


Fig.4.8 HFD induces retinal microvascular changes in WT but not in TKO mice. Representative images of (a) total retinal flat mounts, (b) Z-stack (ZS) and (c) Skeletonized (SKTN) compressed images of all animal groups showing a tendency for decreased branching density in WT-HFD group, compared to WT-ND group. TKO mice had comparable morphological appearance compared to WT-ND group (n=3-4/group).







Supplementary Fig.4.1 (a) Representative images for transfection efficiency (a), Western blot analyses (b) & (c) for the optimization experiments for overexpression of TXNIP in human EC cultures showing a transfection efficiency between 85 to 90% as indicated by number of GFP expressing cells and a 2.5-fold increase in TXNIP expression (n=4-6; * P-value <0.05 vs EV-GFP).

Table.4.1

Animal			
group	8-weeks	12-weeks	18-weeks
WT-ND	128.8 (± 7.95) mg/dl	126.91 (± 3.14) mg/dl	118.27 (± 5.07) mg/dl
WT-HFD	154.12* (± 6.61) mg/dl	130.71 (± 2.85) mg/dl	135.29 (± 5.84) mg/dl
TKO-ND	85.98*# (± 7.51) mg/dl	70.31*# (± 5.49) mg/dl	69.88*# (± 4.74) mg/dl
TKO-HFD	96.59*# (± 8.55) mg/dl	82.00*# (± 3.32) mg/dl	91.81*#¶ (± 3.93) mg/dl

Table.4.1 Summary of the FPBG levels of all animal groups throughout the study at 7, 12 and 18-weeks. (Data are represented as Mean \pm SEM, n=11-19 / animal group; * P-value <0.05 vs WT-ND, # vs WT-HFD and ¶ vs TKO-ND).

Table.4.2

Parameter	Lean (LN)	Obese (OB)
Age	18.2 (± 8.12) years	15.6^* (± 6.99) years
Height	174.3 (± 77.96) cm	174.2 (± 77.92) cm
Weight	62.6 (± 28.01) kg	$108.8^* (\pm 48.64) \text{ kg}$
ВМІ	$20.6 (\pm 9.19) \text{ kg/m}^2$	$35.7^* (\pm 15.95) \text{ kg/m}^2$
BMI Percentile	30.7 (± 13.72)	99.0* (± 44.25)
Systolic blood pressure	133.9 (± 59.86) mmHg	133.5 (± 59.68) mmHg
Diastolic blood pressure	74.7 (± 33.39) mmHg	76.3 (± 34.13) mmHg

Table.4.2 Summary of the physical and metabolic parameters of both lean and obese subjects enrolled for the isolation of their PBMCs and human in-vitro leukostasis experiments. (Data are represented as Mean \pm SEM, n=4-5 / group; * P-value <0.05 vs LN).

CHAPTER 5

INTEGRATED DISCUSSION

DR is the leading cause of blindness in US adults 20-75 years of age [1, 2], [3]. DR is a progressive neurovascular disease that is categorized based on the proliferative status of the retinal vasculature. It starts with an early initial vaso-regressive stage of non-proliferative diabetic retinopathy (NPDR), which cumulatively develops into a vaso- proliferative response of proliferative diabetic retinopathy (PDR) later in the disease. Nearly 79 million U.S. adults are obese (Over one-third) [4-6]. Obesity is now considered an established disease state, rather than just a mere risk stage for developing dyslipidemia, insulin resistance, culminating into the complex metabolic syndrome disorder, type 2 diabetes and associated cardiovascular complications [5], [7]. Although clinical evidence signifies obesity, hypertension and metabolic syndrome pre-diabetic stages for increasing the risk of retinopathy and retinal microvascular abnormalities independently from hyperglycemia [8, 9] or in addition to type 1 or type 2 diabetes [10], data from experimental models are lacking. Therefore, we attempted to model the detrimental elements of obesity and hypertension as major components of the metabolic syndrome and characterize their deleterious effects on the early development of retinal microvascular lesions in a series of two complementary studies. In the first study, we have observed that although HFD-induced obesity, hypertension or their combination showed early retinal microvascular lesions, significant increases in retinal TXNIP expression, oxidative stress

and inflammation, HFD selectively induced retinal TXNIP-NLRP3 interaction and inflammasome activation resulting in increased expression of cleaved caspase-1 and IL-1β. Moreover, retinal vasculature and surrounding macroglial tissue (astrocytes and Müller cell endfeet) were observed as the prominent sites for HFD-induced TXNIP up-regulation. Hence, in the second study, we sought to investigate the protective effect of TXNIP deletion against HFD-induced retinal NLRP3 inflammasome activation and its associated microvascular injury manifested as adhesion molecule upregulation, increased leukostasis and BRB breakdown and subsequent microvascular degeneration, acellular capillaries formation and morphological abnormalities, as pathological landmarks of early stage retinopathy. Furthermore, using molecular approaches in cultured endothelial cells, we have established the causal relationship between endothelial TXNIP expression and its direct role in induction of inflammation and cell death through NLRP3 inflammasome activation and its positive feedback interplay with leukostasis, as an indirect factor for mediating endothelial cell apoptosis.

Population studies have shown that subjects with various components of the metabolic syndrome including obesity, dyslipidemia and hypertension were more likely to have retinal microvascular abnormalities such as focal and generalized retinal arteriolar narrowing and venular dilatation [11, 12]. Systemic low grade inflammation, oxidative stress and its associated endothelial dysfunction/activation have been suggested as the most plausible reasons for such clinical observations [13-15]. We have previously reported that the combination of diabetes and hypertension can exacerbate retinal oxidative and inflammatory stress along with its associated retinal microvascular degeneration [16]. This supports the notion that combining commonly comorbid metabolic conditions can aggravate the pathophysiological development of retinal disease. In our first study, we attempted to model the essential components of the metabolic syndrome and their combination. Indeed, exposure to either HFD or hypertension alone or their

combination significantly triggered retinal oxidative stress evidenced by increased retinal lipid peroxides and nitrotyrosine levels (the foot-print of peroxynitrite formation implicating endothelial dysfunction), compared to control group, which was accompanied by parallel increases in retinal TXNIP expression (Fig.3.1 & 3.2). Increased lipid peroxidation and peroxynitrite generation and endothelial dysfunction were also reported in patients with hypertension-related microvascular changes [17, 18] and in retinas from BBZ rat, an obese and noninsulin-dependent model of diabetes [19] as well as coronary endothelial cells in response to HFD [20, 21]. Yet, this is the first report to demonstrate increases in retinal TXNIP expression in HFD, hypertension or their combination. TXNIP expression has been shown to be consistently elevated in the muscles of pre-diabetics and diabetics [22]. In addition, TXNIP has been traditionally known for its redox dependent signaling which involves the suppression of the antioxidant defense mechanism and increased unopposed levels of cellular reactive oxygen species (ROS) by limiting the availability of free sulfhydryl (thiol) group of TRX [23-25]. Moreover, as an oxidative stress sensor TXNIP was shown to couple increased oxidative stress levels to proinflammatory cytokine expression. Forced expression of TXNIP in isolated microvascular endothelial cells resulted in nuclear translocation and direct activation of the canonical NFκB pathway [26]. Knocking down TXNIP expression completely abolishes NF-kB binding to the cyclooxygenase-2 (Cox2) promoter, suggesting that TXNIP induces inflammatory gene expression by increasing transcription factor accessibility to gene promoters. The same study demonstrated evidence that the mechanism involves remodeling of histone H3 via activation of p38 MAPK. Later, studies demonstrated that TXNIP induces the expression of other proinflammatory cytokines and enzymes including IL-1β, ICAM-1, TNF-α, VEGF-A and Cox2, [26-28]. In agreement, our results have shown that HFD alone, hypertension alone or their combination significantly enhanced levels of NF κ B and downstream TNF- α expression (Fig.3.1).

In line with our findings, animals fed with a HFD or a high sucrose and cholesterol diet have increased expression of inflammation in isolated retinal vasculature and higher levels of retinal microaneurysms respectively [29, 30].

Lipotoxcicty or impaired tissue-homeostasis, occurs as a result of lipid-induced changes in intracellular signaling or increased lipid utilization [31, 32]. As a sensor for metabolic danger, NLRP3 inflammasome is known as one of the executional machineries responsible for the activation of caspase-1 and maturation of the pro-inflammatory cytokine IL-1β, and hence, instigating obesity-induced inflammation [33, 34]. The role of TXNIP as a redox sensitive switch that links between increased cellular oxidative stress levels and induction of the proinflammatory gene expression has been extended beyond the transcriptional factor level. Recent advances suggest the direct protein-protein interaction of TXNIP with the NLRP3-inflammasome. Nevertheless, the emerging role of TXNIP as a direct activator of the NLRP3-inflammasome has been quiet controversial. More importantly, the relationship between HFD-induced retinal and endothelial TXNIP expression and inflammasome activation in HFD-induced obesity has not been examined before. Here we show that HFD alone or in combination with hypertension selectively induced expression and interaction of TXNIP and NLRP3 resulting in cleaved caspase-1 and IL-1β expression independently from hypertension (NLRP3 inflammasome activation was not observed in hypertension alone group) (Fig.3.2 & 3.4). In addition, retinal microvasculature and surrounding macroglia (astrocytes and endfeet of Müller cells) were prominent sites for increased TXNIP expression (Fig.3.5). These results were further confirmed in the second study using wild type mice (WT) and TXNIP knock out (TKO) mice, where WT-HFD mice also showed increased activation of retinal NLRP3 inflammasome, evidenced with upregulation of NLRP3, cleaved caspase-1 and cleaved IL1-β levels compared to WT-ND control group; whereas, TXNIP deletion in both TKO-ND and TKO-HFD groups abrogated such

effect (Fig.4.2). Our results come in opposition to previously published reports questioning whether TXNIP or even increased oxidative stress is indeed required for NLRP3-inflammasome activation. These reports indicated that there was no difference in neither immune response nor IL-1β production in isolated macrophages from both TKO and Gp91phox knockout mice [35], and that TXNIP knockdown using siRNA did not affect caspase-1 activity under regular or increased glucose levels in cultured adipocytes [36]. However, our findings lend further support to an increasing body of literature advocating TXNIP as an essential molecule required for direct activation of the NLRP3-inflammasome in endothelial cells, macrophages and pancreatic beta cells in response to oxidative and endoplasmic reticulum stress, respectively (outlined in Fig. 5.1) [37-43]. This controversy might be in part explained by the differences in the nature/function of the cell types studied, where the function of TXNIP and the innate immune response machinery like NLRP3 inflammasome can differ greatly between professional and non-professional immune cells.

The initial vaso-regressive early stage of non-proliferative diabetic retinopathy (NPDR) is characterized with major pathophysiological hallmarks, including: increased retinal acellular capillaries formation as a result of retinal capillary non-perfusion, endothelial cell death and microvascular degeneration, in addition to the associated BRB dysfunction and increased retinal thickness or edema. Such events are believed to comprise the founding stages for induction of cumulative focal ischemia, which is responsible for provoking the vaso-proliferative response of proliferative diabetic retinopathy (PDR) later in advanced stages of the disease [44-47]. In our studies, HFD-induced obesity or hypertension alone demonstrated significant increases in retinal acellular capillaries formation that was further exacerbated upon their combination in SHR (SHR+F) rats as early as 10-weeks (Fig.3.1 & Supplementary Fig.3.1), that comes in line with a previous report of accelerated retinal capillary dropout, vascular tortuosity, and vascular leakage

in obese SHR rats starting at 12-weeks. [48]. The same observation of increased retinal acellular capillaries formation was also confirmed in the second study after 18-weeks of HFD alone in WT-HFD mice that was reversed in TKO mice (Fig.4.7). Clinically, retinal microvascular capillary non-perfusion and degeneration can be evident as non-perfused areas in fluorescein-infusion retinal angiograms [45]. Similarly, as we show in Fig.4.8, in parallel to the increase in retinal capillaries drop out in WT-HFD mice, we have also observed that WT mice tend to have decreased branching density in response to HFD. However, TKO mice had a comparable morphological appearance to WT-ND that did not change in response to HFD. These results establish the detrimental long term impact of HFD on retinal microvascular degeneration and morphological abnormalities and highlight the protective effect of TXNIP deletion.

Retinal microvascular cell death can occur either directly, due to different biochemical insults initiated within retinal endothelial cells themselves, or indirectly, secondary to the activation of other retinal cell types; including neurons and glial cells, or non-retinal cell types; mainly circulating or infiltrating leukocytes (reviewed in [49]). Moreover, previous reports have also established retinal leukostasis as one of the indirect prerequisite events for inducing exacerbated endothelial cell death and BRB breakdown, and its inhibition can help to prevent retinal acellular capillaries formation in advanced diabetic stages [50, 51]. In our current studies, our results showed that HFD was associated with parallel increases in retinal adhesion molecule (ICAM-1) expression, increased retinal leukostasis (Fig.4.4) and BRB breakdown (Fig.4.7) after 8-weeks of HFD only in WT-HFD mice. Furthermore, on the longer term; isolated PBMCs from obese WT-HFD mice after 18-weeks of HFD or obese non-diabetic subjects but not WT-ND or lean subjects resulted in increased leukostasis and apoptosis of both mouse and human endothelial cells after 2 and 24 hours in co-culture, respectively (Fig.4.6). Together, these results highlight the early impact of HFD in inducing retinal leukostasis and the novel role of circulating

leukocytes in mediating endothelial cell death in an indirect way in models of HFD. Further, it also emphasizes the potential clinical relevance of increased retinal leukostasis in mediating HFD-induced microvascular inflammation and degeneration.

TXNIP is well regarded as a stress sensor for induction of the pro-apoptotic protein ASK-1 and c-jun-N-terminal kinase (JNK) pathway(s) [23, 24, 28, 52] and its expression can be induced to a various number of exogenous and endogenous stimuli including inflammation, metabolic stress, changes in calcium levels, as well as changes in oxygen levels [26, 53-57]. On the other hand, TXNIP has been identified as a member of the alpha arrestin protein family, highlighting the other roles of TXNIP as a major metabolic sensor and a scaffold protein in a redox-dependent and independent ways inside and outside the retinal neurovascular unit (reviewed in [58-60]). TXNIP is known to be one of the master regulators of metabolism, a wellestablished inhibitor of glucose uptake, mediator of insulin resistance, and is primarily involved in proper fatty acid utilization. Glycolytic intermediates induce the binding of the transcription factor MondoA and Max-like protein X (MLX) (MondoA:MLX) to the carbohydrate response element (CRE) found within the TXNIP promoter [61-63]. TXNIP also acts on shutting down glucose uptake and facilitating insulin resistance. This can occur either directly; by mediating the internalization of glucose transporter (GLUT-1) from the plasma membrane in an AMP-activated protein kinase (AMPK) dependent manner [64], or indirectly; through induction of NLRP3 inflammasome and inflammation [65]. Our results have indicated that TKO mice are significantly more insulin sensitive and consistently had lower fasting blood glucose levels despite the comparable weight gain after HFD. Their metabolic profiling also showed comparable plasma cholesterol and triglycerides levels after HFD, but a higher basal level of plasma triglycerides on normal diet (in TKO-ND). These results are in line with previously published reports that TXNIP deletion preserves insulin sensitivity without affecting obesity or weight gain in both HFD diet-induced and genetic obesity models [66, 67]. TKO-mice are inherently more insulin sensitive and have higher basal levels of plasma triglycerides due to the altered redox status (a significant increase in the ratio of NADH to NAD⁺) which down-regulates the citric-acid cycle; sparing fatty acids for triglyceride and ketone body production [68-70]. Taken all together, it is unreasonable to exclude the contribution of other metabolic pathways outlined above (including lower blood glucose levels and increased insulin activity in TKO mice) that might be affected by TXNIP deletion and confine the protective effects observed against retinal microvascular inflammation and degeneration to HFD-induced TXNIP-NLRP3 inflammasome axis only. One certain advantage for the HFD-induced obesity model that it has the complex nature of different metabolic pathways like insulin resistance, dyslipidemia and associated inflammation acting together at the same time in a fashion that closely resembles what happens clinically in obese patients. However, the difficulty of pointing out a single major pathway involved might act also as a downside, which warrants further investigations to compensate for such limitation. Additionally, while the role of TXNIP expression was examined in retinal endothelial cells, our immunohistochemical analyses have shown that both retinal microvasculature and surrounding macroglia (astrocytes and endfeet of Müller cells) are prominent sites for increased TXNIP expression (Fig.3.5). These results do not exclude the contribution of other retina cell types in the pathological findings observed. However, the scope of the current study was to elucidate the impact of HFD and palmitate on retinal endothelial cells and the contribution of non-endothelial retina cell types is acknowledged and warrants further characterization.

High fat-high carbohydrate meals and elevated free fatty acid (FFA) plasma levels and can directly cause systemic inflammation, oxidative stress and endothelial dysfunction [71-73]. FFA plasma levels are relatively higher in obesity and are one of the major factors for inducing

obesity and metabolic syndrome-associated inflammation and insulin resistance [32, 74-76]. Previous reports have established palmitate, which is one of the most abundant circulating saturated fatty acid in plasma [77], as a direct activator of the NLRP3-inflammasome [78-80] and an inducer of the pro-inflammatory response in human coronary endothelial cells versus other unsaturated fatty acids [81, 82]. Therefore, to model the direct role of HFD in vitro, we examined the effects of saturated fatty acid palmitate alone or in combination with exogenous peroxynitrite in HRE cells. Indeed, silencing TXNIP abrogated palmitate-induced NLRP3 inflammasome activation and its associated increases in pro-apoptotic caspase-3 expression and reduced cell viability of HRE cells (Fig. 3.6-3.8 & Supplementary Fig.3.2). In addition, knocking down TXNIP abolished palmitate-induced upregulation of adhesion molecules ICAM-1 and PECAM-1 in HRE cells in-vitro (Fig.4.5). This establishes the role TXNIP plays in activation of NRLP3 inflammasome, upregulation of adhesion molecules and its contribution to increased cell death/apoptosis in a direct way within retinal endothelial cells themselves (Fig. 5.1). In line with our findings, pharmacological inhibition of caspase-1 or deletion of IL-1receptor suppressed IL-1β-dependent retinal acellular capillaries formation in diabetic animals [83, 84]. To the best of our knowledge, this is the first report of increased retinal TXNIP expression and activation of endothelial TXNIP-NLRP3 inflammasome in experimental models of HFD.

Since TXNIP and IL-1 β are both known for NF κ B pathway activation and induction of its downstream pro-inflammatory mediators including IL-1 β (its own self) and TNF- α and endothelial adhesion molecules as: ICAM-1, PECAM-1, E-selectin, VCAM-1 in-vivo and in isolated microvascular cells [26, 84-89]. Therefore, there is a need to determine the specific contribution of the NLRP3 inflammasome induced IL-1 β production in inducing endothelial cell inflammation and adhesion molecule expression, versus the pro-inflammatory upstream role mediated by TXNIP. Forced expression of TXNIP in HRE cells resulted in activation of the

NLRP3 inflammasome evidenced by the upregulation of NLRP3, cleaved Caspase-1 and cleaved IL- β , along with TNF α and both adhesion molecules ICAM-1 and PECAM-1 expression. Interestingly, blocking the effect of IL- 1β by using the IL-1RA was not only able to suppress the induction of its own processing pathway of NLRP3 inflammasome, but also the expression of the other pro-inflammatory mediator TNF α and ICAM-1 and PECAM-1 adhesion molecules. Hence, a positive feedback loop mediated by IL- 1β can stimulate its own activation and induction of endothelial inflammation in an autocrine fashion (Fig. 4.5). Together, these findings support the proposed link between TXNIP-NLRP3 inflammasome activation and accelerated retinal microvascular inflammation and degeneration (Fig. 5.1). In agreement, an earlier study proposed retinal endothelial tissue as an initial early source of increased IL- 1β production in response to another model of hyperglycemia, after which, increasing levels of IL- 1β are sustained via its own auto stimulation in endothelial and macroglia tissues (Müller cells and astrocytes) [90].

Our data suggest an inverse relationship between accumulation of intracellular cleavage/maturation of IL-1β and its release. Pal-BSA alone was able to induce both intracellular maturation and release of IL-1β in HRE cells which was mitigated by silencing TXNIP expression. On the other hand, exogenous PN alone resulted in a higher surge of IL-1β release that was independent of TXNIP inhibition, although it was not able to induce significant changes in its intracellular cleavage/maturation, suggesting accelerated activation and trafficking of IL-1β. Furthermore, this effect was quenched when exogenous PN was combined with Pal-BSA in presence of TXNIP, whereas TXNIP inhibition reversed this process and facilitated PN-induced IL-1β release despite its combination with Pal-BSA (Fig.3.7). This data indicate that, while TXNIP is required for palmitate-induced NLRP3 inflammasome activation and IL-1β maturation in HRE cells, it does not facilitate the maximum IL-1β release. Recent evidence suggests that caspase-1 activation/processing of pro-IL-1β by caspase-1 and the release of mature IL-1β from

human monocytes are distinct and separable events [91]. TXNIP has been shown to shuffle between different cellular compartments, including the nucleus, mitochondria [92] and plasma membrane [93]. A possible explanation for this intriguing observation might be due the nature of TXNIP as a member of the alpha arrestin scaffolding proteins, which are believed to play an important role in intracelleular cargo trafficking and/or internalization of different proteins [64, 93]. Hence, subcellular localization of TXNIP in response to different insults might reflect on enhancement or inhibition of mature IL-1β release.

In conclusion, as outlined in Fig. 5.1, our results in addition to others' establish the pivotal role TXNIP plays in mediating sterile metabolic inflammatory response in the retina in response to different metabolic insults. This role is not only attributed to the transcriptional factor activity of TXNIP, but also due to its nature as a scaffolding protein. Hence, it contributes to both; expression and direct protein interaction with executive pro-inflammatory machinery (NLRP3 inflammasome) responsible for maturation of IL-1 β , one of the potent pro-inflammaory cytokines in different retinal disease pathophysiology. Therefore, in conjunction with the fact that obesity has been upgraded from a mere risk factor to an independent disease-state [7], our studies highlight the early detrimental effect of obesity on the vasculature in general and the development of retinal microvascular lesions. Further, they point the attention that such events can occur even before reaching a state of significant hyperglycemia and frank diabetes. Similar to clinical observations, our experimental model depicts accelerated retinal acellular capillaries formation, microvascular morphological abnormalities and increased retinal leukostasis as pathological landmarks of HFD-induced obesity. We believe that our findings elucidate a novel intricate interplay between the TXNIP-NLRP3 inflammasome axis, induction of endothelial inflammation, cell death and leukostasis. In the era of scarce successful pharmacological therapies except for limited uses of anti-VEGF therapies and corticosteroids in advanced late

macular edema and PDR stages, such paradigm proposes TXNIP-NLRP3 inflammasome axis as a promising therapeutic target for earlier intervention or prevention of obesity and diabetes-induced retinal and general microvascular complications affecting millions of patients world-wide.

Fig. 5.1

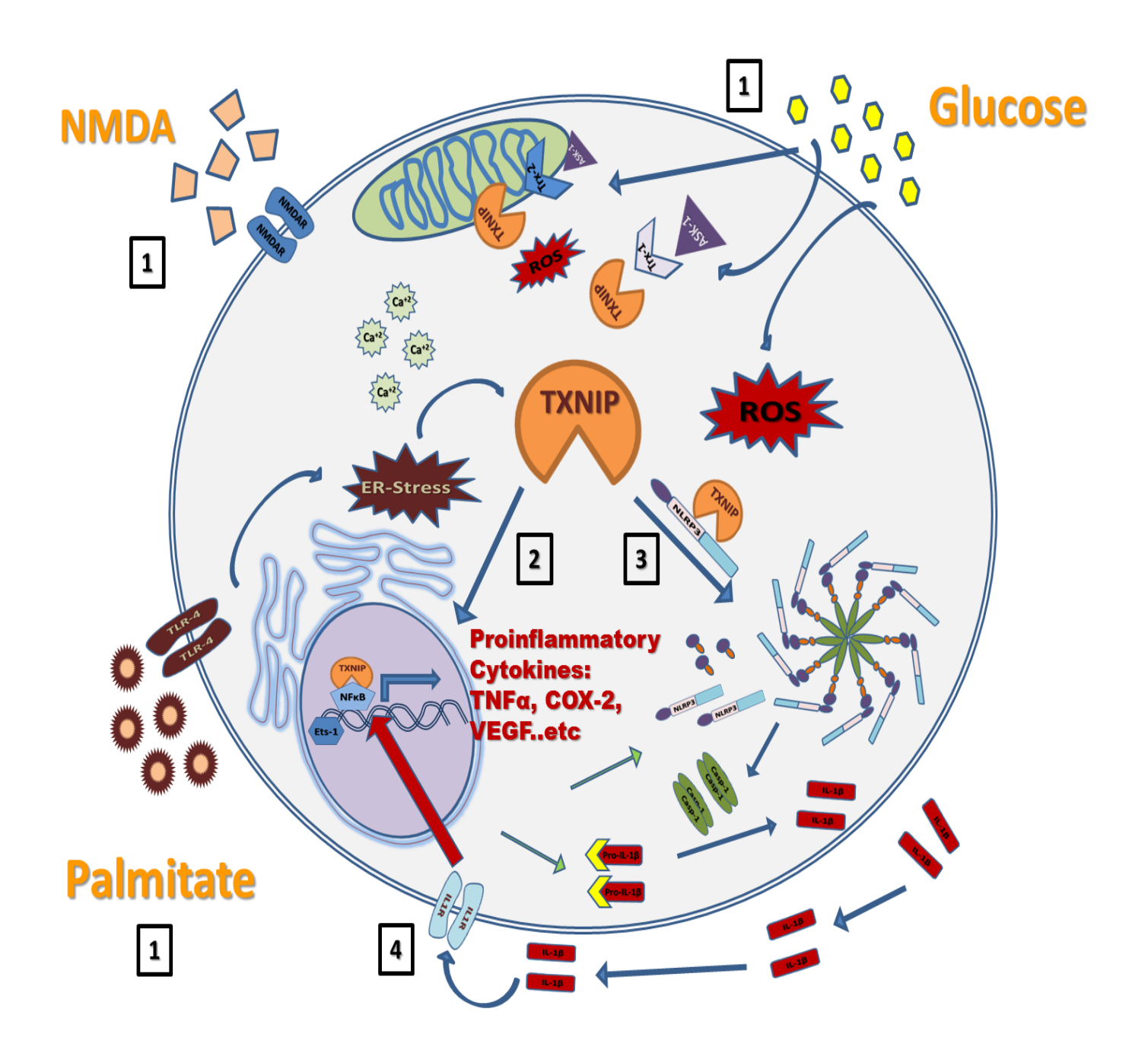


Fig. 5.1 Summary of the overall findings: 1) different metabolic danger signals including glucose, NMDA or palmitate converge on TXNIP upregulation. 2) TXNIP upregulation plays a role in induction of pro-inflammatory cytokine expression via NFκB pathway activation as transcription factor. 3) TXNIP mediates direct protein interaction with NLRP3 and inflammasome activation required for maturation and release of IL1-β. 4) IL-1β promotes inflammatory stress in an autocrine positive feedback loop manner.

5.1 References

- 1. Centers for Disease Control and Prevention, U.D.o.H.a.H.S., *National Diabetes Statistics Report: Estimates of Diabetes and Its Burden in the United States, 2014.* . 2014.
- 2. Association, A.D., Statistics About Diabetes. 2014.
- 3. Kempen, J.H., et al., *The prevalence of diabetic retinopathy among adults in the United States*. Arch Ophthalmol, 2004. **122**(4): p. 552-63.
- 4. Ogden, C.L., et al., *Prevalence of childhood and adult obesity in the United States*, 2011-2012. JAMA, 2014. **311**(8): p. 806-14.
- 5. Association, A.H. *Obesity Statistics*. 2012 May 5, 2011.; Available from: http://www.heart.org/HEARTORG/GettingHealthy/WeightManagement/Obesity/Obesity-Information_UCM_307908_Article.jsp#.Tx2sA4G8ioA.
- 6. Center for Disease Control and Prevention; Division of Nutrition, P.A., and Obesity (DNPAO), *Overweight and Obesity statistics*. 2014.
- 7. Association, A.M., American Medical Association's Council on Science and Public Health Report 4, Resolution: 420 (A-13). 2013.
- 8. Klein, R., et al., 15-year cumulative incidence and associated risk factors for retinopathy in nondiabetic persons. Arch Ophthalmol, 2010. **128**(12): p. 1568-75.
- 9. van Leiden, H.A., et al., *Risk factors for incident retinopathy in a diabetic and nondiabetic population: the Hoorn study.* Arch Ophthalmol, 2003. **121**(2): p. 245-51.
- 10. Nguyen, T.T. and T.Y. Wong, *Retinal vascular manifestations of metabolic disorders*. Trends Endocrinol Metab, 2006. **17**(7): p. 262-8.
- 11. Gopinath, B., et al., *Effect of obesity on retinal vascular structure in pre-adolescent children*. Int J Pediatr Obes, 2011. **6**(2-2): p. e353-9.
- 12. Kawasaki, R., et al., *The metabolic syndrome and retinal microvascular signs in a Japanese population: the Funagata study.* Br J Ophthalmol, 2008. **92**(2): p. 161-6.
- 13. Caballero, A.E., *Metabolic and vascular abnormalities in subjects at risk for type 2 diabetes: the early start of a dangerous situation.* Arch Med Res, 2005. **36**(3): p. 241-9.
- 14. Couillard, C., et al., Circulating levels of oxidative stress markers and endothelial adhesion molecules in men with abdominal obesity. J Clin Endocrinol Metab, 2005. **90**(12): p. 6454-9.
- 15. Hackman, A., et al., *Levels of soluble cell adhesion molecules in patients with dyslipidemia*. Circulation, 1996. **93**(7): p. 1334-8.
- 16. Mohamed, I.N., et al., *Diabetes exacerbates retinal oxidative stress, inflammation, and microvascular degeneration in spontaneously hypertensive rats.* Mol Vis, 2012. **18**: p. 1457-66.
- 17. Ferroni, P., et al., Endothelial dysfunction and oxidative stress in arterial hypertension. Nutr Metab Cardiovasc Dis, 2006. **16**(3): p. 222-33.
- 18. Coban, E., et al., *The association of low-grade systemic inflammation with hypertensive retinopathy*. Clin Exp Hypertens, 2010. **32**(8): p. 528-31.
- 19. Ellis, E.A., et al., *Increased NADH oxidase activity in the retina of the BBZ/Wor diabetic rat.* Free Radic Biol Med, 1998. **24**(1): p. 111-20.
- 20. Galili, O., et al., Early experimental obesity is associated with coronary endothelial dysfunction and oxidative stress. Am J Physiol Heart Circ Physiol, 2007. **292**(2): p. H904-11.

- 21. Jebelovszki, E., et al., *High-fat diet-induced obesity leads to increased NO sensitivity of rat coronary arterioles: role of soluble guanylate cyclase activation.* Am J Physiol Heart Circ Physiol, 2008. **294**(6): p. H2558-64.
- 22. Muoio, D.M., TXNIP links redox circuitry to glucose control. Cell Metab, 2007. **5**(6): p. 412-4.
- 23. Chung, J.W., et al., *Vitamin D3 upregulated protein 1 (VDUP1) is a regulator for redox signaling and stress-mediated diseases.* J Dermatol, 2006. **33**(10): p. 662-9.
- 24. Junn, E., et al., Vitamin D3 up-regulated protein 1 mediates oxidative stress via suppressing the thioredoxin function. J Immunol, 2000. **164**(12): p. 6287-95.
- 25. Nishiyama, A., et al., *Identification of thioredoxin-binding protein-2/vitamin D(3) up-regulated protein 1 as a negative regulator of thioredoxin function and expression.* J Biol Chem, 1999. **274**(31): p. 21645-50.
- 26. Perrone, L., et al., *Thioredoxin interacting protein (TXNIP) induces inflammation through chromatin modification in retinal capillary endothelial cells under diabetic conditions.* J Cell Physiol, 2009. **221**(1): p. 262-72.
- 27. Perrone, L., et al., *Inhibition of TXNIP expression in vivo blocks early pathologies of diabetic retinopathy*. Cell Death Dis, 2010. **1**: p. e65.
- 28. Al-Gayyar, M.M., et al., *Thioredoxin interacting protein is a novel mediator of retinal inflammation and neurotoxicity.* Br J Pharmacol, 2011. **164**(1): p. 170-80.
- 29. Gustavsson, C., et al., Vascular cellular adhesion molecule-1 (VCAM-1) expression in mice retinal vessels is affected by both hyperglycemia and hyperlipidemia. PLoS One, 2010. 5(9): p. e12699.
- 30. Helfenstein, T., et al., *Impaired glucose tolerance plus hyperlipidaemia induced by diet promotes retina microaneurysms in New Zealand rabbits*. Int J Exp Pathol. **92**(1): p. 40-9.
- 31. Symons, J.D. and E.D. Abel, *Lipotoxicity contributes to endothelial dysfunction: a focus on the contribution from ceramide*. Rev Endocr Metab Disord, 2013. **14**(1): p. 59-68.
- 32. Karpe, F., J.R. Dickmann, and K.N. Frayn, *Fatty acids, obesity, and insulin resistance:* time for a reevaluation. Diabetes, 2011. **60**(10): p. 2441-9.
- 33. Vandanmagsar, B., et al., *The NLRP3 inflammasome instigates obesity-induced inflammation and insulin resistance.* Nat Med. **17**(2): p. 179-88.
- 34. Stienstra, R., et al., *The inflammasome-mediated caspase-1 activation controls adipocyte differentiation and insulin sensitivity.* Cell Metab. **12**(6): p. 593-605.
- 35. Masters, S.L., et al., Activation of the NLRP3 inflammasome by islet amyloid polypeptide provides a mechanism for enhanced IL-1beta in type 2 diabetes. Nat Immunol, 2010. **11**(10): p. 897-904.
- 36. Koenen, T.B., et al., *Hyperglycemia activates caspase-1 and TXNIP-mediated IL-1beta transcription in human adipose tissue.* Diabetes, 2011. **60**(2): p. 517-24.
- 37. Zhou, R., et al., *Thioredoxin-interacting protein links oxidative stress to inflammasome activation.* Nat Immunol, 2010. **11**(2): p. 136-40.
- 38. Zhou, R., et al., *A role for mitochondria in NLRP3 inflammasome activation*. Nature, 2011. **469**(7329): p. 221-5.
- 39. Lunov, O., et al., Amino-functionalized polystyrene nanoparticles activate the NLRP3 inflammasome in human macrophages. ACS Nano, 2011. **5**(12): p. 9648-57.
- 40. Park, Y.J., et al., TXNIP deficiency exacerbates endotoxic shock via the induction of excessive nitric oxide synthesis. PLoS Pathog, 2013. 9(10): p. e1003646.

- 41. Xiang, M., et al., *Hemorrhagic shock activation of NLRP3 inflammasome in lung endothelial cells.* J Immunol, 2011. **187**(9): p. 4809-17.
- 42. Oslowski, C.M., et al., *Thioredoxin-interacting protein mediates ER stress-induced beta cell death through initiation of the inflammasome*. Cell Metab, 2012. **16**(2): p. 265-73.
- 43. Lerner, A.G., et al., *IRE1alpha induces thioredoxin-interacting protein to activate the NLRP3 inflammasome and promote programmed cell death under irremediable ER stress.* Cell Metab, 2012. **16**(2): p. 250-64.
- 44. Frank, R.N., *Diabetic retinopathy*. N Engl J Med, 2004. **350**(1): p. 48-58.
- 45. Tang, J. and T.S. Kern, *Inflammation in diabetic retinopathy*. Prog Retin Eye Res, 2011. **30**(5): p. 343-58.
- 46. Nunes, S., et al., Microaneurysm turnover is a biomarker for diabetic retinopathy progression to clinically significant macular edema: findings for type 2 diabetics with nonproliferative retinopathy. Ophthalmologica, 2009. **223**(5): p. 292-7.
- 47. Shimizu, K., Y. Kobayashi, and K. Muraoka, *Midperipheral fundus involvement in diabetic retinopathy*. Ophthalmology, 1981. **88**(7): p. 601-12.
- 48. Huang, S.S., et al., Characterization of retinal vascular abnormalities in lean and obese spontaneously hypertensive rats. Clin Exp Pharmacol Physiol Suppl, 1995. **22**(1): p. S129-31.
- 49. Kern, T.S., Contributions of inflammatory processes to the development of the early stages of diabetic retinopathy. Exp Diabetes Res, 2007. **2007**: p. 95103.
- 50. Adamis, A.P. and A.J. Berman, *Immunological mechanisms in the pathogenesis of diabetic retinopathy*. Semin Immunopathol, 2008. **30**(2): p. 65-84.
- 51. Joussen, A.M., et al., A central role for inflammation in the pathogenesis of diabetic retinopathy. FASEB J, 2004. **18**(12): p. 1450-2.
- 52. Al-Gayyar, M.M., et al., Neurovascular protective effect of FeTPPs in N-methyl-D-aspartate model: similarities to diabetes. Am J Pathol, 2010. 177(3): p. 1187-97.
- 53. El-Azab, M.F., et al., *Deletion of thioredoxin-interacting protein preserves retinal neuronal function by preventing inflammation and vascular injury*. Br J Pharmacol, 2014. **171**(5): p. 1299-313.
- 54. Dunn, L.L., et al., A critical role for thioredoxin-interacting protein in diabetes-related impairment of angiogenesis. Diabetes, 2014. **63**(2): p. 675-87.
- 55. Singh, L.P., *Thioredoxin Interacting Protein (TXNIP) and Pathogenesis of Diabetic Retinopathy.* J Clin Exp Ophthalmol, 2013. **4**.
- 56. Huang, C., et al., *Thioredoxin-interacting protein mediates dysfunction of tubular autophagy in diabetic kidneys through inhibiting autophagic flux.* Lab Invest, 2014. **94**(3): p. 309-20.
- 57. Chen, J., et al., Diabetes induces and calcium channel blockers prevent cardiac expression of proapoptotic thioredoxin-interacting protein. Am J Physiol Endocrinol Metab, 2009. **296**(5): p. E1133-9.
- 58. Spindel, O.N., C. World, and B.C. Berk, *Thioredoxin interacting protein: redox dependent and independent regulatory mechanisms*. Antioxid Redox Signal, 2012. **16**(6): p. 587-96.
- 59. Patwari, P. and R.T. Lee, *An expanded family of arrestins regulate metabolism*. Trends Endocrinol Metab, 2012. **23**(5): p. 216-22.
- 60. Polekhina, G., et al., *Crystallization and preliminary X-ray analysis of the N-terminal domain of human thioredoxin-interacting protein.* Acta Crystallogr Sect F Struct Biol Cryst Commun, 2011. **67**(Pt 5): p. 613-7.

- 61. Minn, A.H., C. Hafele, and A. Shalev, *Thioredoxin-interacting protein is stimulated by glucose through a carbohydrate response element and induces beta-cell apoptosis*. Endocrinology, 2005. **146**(5): p. 2397-405.
- 62. Stoltzman, C.A., et al., Glucose sensing by MondoA:Mlx complexes: a role for hexokinases and direct regulation of thioredoxin-interacting protein expression. Proc Natl Acad Sci U S A, 2008. **105**(19): p. 6912-7.
- 63. Yu, F.X., et al., *Thioredoxin-interacting protein (Txnip) gene expression: sensing oxidative phosphorylation status and glycolytic rate.* J Biol Chem, 2010. **285**(33): p. 25822-30.
- 64. Wu, N., et al., AMPK-dependent degradation of TXNIP upon energy stress leads to enhanced glucose uptake via GLUT1. Mol Cell, 2013. **49**(6): p. 1167-75.
- 65. Schroder, K., R. Zhou, and J. Tschopp, *The NLRP3 inflammasome: a sensor for metabolic danger?* Science, 2010. **327**(5963): p. 296-300.
- 66. Chutkow, W.A., et al., *Deletion of the alpha-arrestin protein Txnip in mice promotes adiposity and adipogenesis while preserving insulin sensitivity.* Diabetes, 2010. **59**(6): p. 1424-34.
- 67. Yoshihara, E., et al., *Disruption of TBP-2 ameliorates insulin sensitivity and secretion without affecting obesity*. Nat Commun, 2010. **1**: p. 127.
- 68. Hui, S.T., et al., *Txnip balances metabolic and growth signaling via PTEN disulfide reduction.* Proc Natl Acad Sci U S A, 2008. **105**(10): p. 3921-6.
- 69. Bodnar, J.S., et al., *Positional cloning of the combined hyperlipidemia gene Hyplip1*. Nat Genet, 2002. **30**(1): p. 110-6.
- 70. Sheth, S.S., et al., *Thioredoxin-interacting protein deficiency disrupts the fasting-feeding metabolic transition*. J Lipid Res, 2005. **46**(1): p. 123-34.
- 71. Tripathy, D., et al., *Elevation of free fatty acids induces inflammation and impairs vascular reactivity in healthy subjects.* Diabetes, 2003. **52**(12): p. 2882-7.
- 72. Ghanim, H., et al., *Increase in plasma endotoxin concentrations and the expression of Toll-like receptors and suppressor of cytokine signaling-3 in mononuclear cells after a high-fat, high-carbohydrate meal: implications for insulin resistance.* Diabetes Care, 2009. **32**(12): p. 2281-7.
- 73. Ghanim, H., et al., A resveratrol and polyphenol preparation suppresses oxidative and inflammatory stress response to a high-fat, high-carbohydrate meal. J Clin Endocrinol Metab, 2011. **96**(5): p. 1409-14.
- 74. Boden, G., *Interaction between free fatty acids and glucose metabolism*. Curr Opin Clin Nutr Metab Care, 2002. **5**(5): p. 545-9.
- 75. Boden, G., *Obesity, insulin resistance and free fatty acids*. Curr Opin Endocrinol Diabetes Obes, 2011. **18**(2): p. 139-43.
- 76. Eckel, R.H., S.M. Grundy, and P.Z. Zimmet, *The metabolic syndrome*. Lancet, 2005. **365**(9468): p. 1415-28.
- 77. Knopp, R.H., et al., One-year effects of increasingly fat-restricted, carbohydrate-enriched diets on lipoprotein levels in free-living subjects. Proc Soc Exp Biol Med, 2000. **225**(3): p. 191-9.
- 78. Wen, H., et al., Fatty acid-induced NLRP3-ASC inflammasome activation interferes with insulin signaling. Nat Immunol, 2011. **12**(5): p. 408-15.
- 79. Matsuzaka, T., et al., *Elovl6 promotes nonalcoholic steatohepatitis*. Hepatology, 2012. **56**(6): p. 2199-208.

- 80. Pejnovic, N.N., et al., Galectin-3 deficiency accelerates high-fat diet-induced obesity and amplifies inflammation in adipose tissue and pancreatic islets. Diabetes, 2013. **62**(6): p. 1932-44.
- 81. Krogmann, A., et al., *Inflammatory response of human coronary artery endothelial cells to saturated long-chain fatty acids.* Microvasc Res, 2011. **81**(1): p. 52-9.
- 82. Staiger, H., et al., *Palmitate-induced interleukin-6 expression in human coronary artery endothelial cells.* Diabetes, 2004. **53**(12): p. 3209-16.
- 83. Vincent, J.A. and S. Mohr, *Inhibition of caspase-1/interleukin-1beta signaling prevents degeneration of retinal capillaries in diabetes and galactosemia.* Diabetes, 2007. **56**(1): p. 224-30.
- 84. Kowluru, R.A. and S. Odenbach, *Role of interleukin-1beta in the development of retinopathy in rats: effect of antioxidants.* Invest Ophthalmol Vis Sci, 2004. **45**(11): p. 4161-6.
- 85. Al-Gayyar, M.M., et al., *Thioredoxin interacting protein is a novel mediator of retinal inflammation and neurotoxicity.* Br J Pharmacol. **164**(1): p. 170-80.
- 86. Perrone, L., et al., *Inhibition of TXNIP expression in vivo blocks early pathologies of diabetic retinopathy*. Cell Death Dis. 1: p. e65.
- 87. Kowluru, R.A. and S. Odenbach, *Role of interleukin-1beta in the pathogenesis of diabetic retinopathy*. Br J Ophthalmol, 2004. **88**(10): p. 1343-7.
- 88. Wang, J.G., et al., *Monocytic microparticles activate endothelial cells in an IL-1beta-dependent manner*. Blood, 2011. **118**(8): p. 2366-74.
- 89. Brown, G.T. and T.M. McIntyre, *Lipopolysaccharide signaling without a nucleus: kinase cascades stimulate platelet shedding of proinflammatory IL-1beta-rich microparticles.* J Immunol, 2011. **186**(9): p. 5489-96.
- 90. Liu, Y., M. Biarnes Costa, and C. Gerhardinger, *IL-1beta is upregulated in the diabetic retina and retinal vessels: cell-specific effect of high glucose and IL-1beta autostimulation*. PLoS One, 2012. **7**(5): p. e36949.
- 91. Galliher-Beckley, A.J., et al., *Caspase-1 activation and mature interleukin-1beta release are uncoupled events in monocytes.* World J Biol Chem, 2013. **4**(2): p. 30-4.
- 92. Lane, T., et al., TXNIP shuttling: missing link between oxidative stress and inflammasome activation. Front Physiol, 2013. **4**: p. 50.
- 93. Park, S.Y., et al., *Thioredoxin-interacting protein mediates sustained VEGFR2 signaling in endothelial cells required for angiogenesis*. Arterioscler Thromb Vasc Biol, 2013. **33**(4): p. 737-43.

APPENDICES

ARTICLE

Thioredoxin-interacting protein is required for endothelial NLRP3 inflammasome activation and cell death in a rat model of high-fat diet

Islam N. Mohamed • Sherif S. Hafez • Arwa Fairaq • Adviye Ergul • John D. Imig • Azza B. El-Remessy

Received: 23 May 2013 / Accepted: 9 October 2013 / Published online: 8 November 2013 © Springer-Verlag Berlin Heidelberg 2013

Abstract

Aims/hypothesis Obesity and hypertension, known proinflammatory states, are identified determinants for increased retinal microvascular abnormalities. However, the molecular link between inflammation and microvascular degeneration remains elusive. Thioredoxin-interacting protein (TXNIP) is recognised as an activator of the NOD-like receptor pyrin domain containing-3 (NLRP3) inflammasome. This study aims to examine TXNIP expression and elucidate its role in endothelial inflammasome activation and retinal lesions. Methods Spontaneously hypertensive (SHR) and control Wistar (W) rats were compared with groups fed a high-fat diet (HFD) (W+F and SHR+F) for 8–10 weeks.

Electronic supplementary material The online version of this article (doi:10.1007/s00125-013-3101-z) contains peer-reviewed but unedited supplementary material, which is available to authorised users.

I. N. Mohamed · S. S. Hafez · A. Fairaq · A. Ergul · A. B. El-Remessy (☒)

Program in Clinical and Experimental Therapeutics, College of Pharmacy, University of Georgia, 1120 15th Street, HM-1200, Augusta, GA 30912, USA e-mail: aelremessy@gru.edu

I. N. Mohamed A. B. El-Remessy Culver Vision Discovery Institute, Georgia Reagents University, Augusta, GA, USA

I. N. Mohamed • S. S. Hafez • A. Fairaq • A. Ergul • A. B. El-Remessy
Charlie Norwood Veterans Affairs Medical Center,
Augusta, GA, USA

A. Ergul

Department of Physiology, Georgia Reagents University, Augusta, GA, USA

J. D. Imig

Department of Pharmacology and Toxicology, Medical College of Wisconsin, Milwaukee, WI, USA Results Compared with W controls, HFD alone or in combination with hypertension significantly induced formation of acellular capillaries, a hallmark of retinal ischaemic lesions. These effects were accompanied by significant increases in lipid peroxidation, nitrotyrosine and expression of TXNIP, nuclear factor κB , TNF- α and IL-1 β . HFD significantly increased interaction of TXNIP-NLRP3 and expression of cleaved caspase-1 and cleaved IL-1β. Immunolocalisation studies identified TXNIP expression within astrocytes and Müller cells surrounding retinal endothelial cells. To model HFD in vitro, human retinal endothelial (HRE) cells were stimulated with 400 µmol/l palmitate coupled to BSA (Pal-BSA). Pal-BSA triggered expression of TXNIP and its interaction with NLRP3, resulting in activation of caspase-1 and IL-1β in HRE cells. Silencing Txnip expression in HRE cells abolished Pal-BSAmediated cleaved IL-1β release into medium and cell death, evident by decreases in cleaved caspase-3 expression and the proportion of live to dead cells.

Conclusions/interpretation These findings provide the first evidence for enhanced TXNIP expression in hypertension and HFD-induced retinal oxidative/inflammatory response and suggest that TXNIP is required for HFD-mediated activation of the NLRP3 inflammasome and the release of IL-1β in endothelial cells.

Keywords Caspase-1 · High-fat diet · Hypertension · IL-1 β · Inflammasome · Inflammation · NLRP3 · Obesity · Oxidative stress · Retinal acellular capillaries · TXNIP

Abbreviations

ARVO Association for Research in Vision and Ophthalmology

GCL Ganglion cell layer

GFAP Glial fibrillary acidic protein GFP Green fluorescent protein

